

1. Report No. FHWA/TX-91+1205-2		2. Government Accession No.		3. Recipient's Catalog No.	
4. Title and Subtitle DELAMINATION OF BONDED CONCRETE OVERLAYS AT EARLY AGES				5. Report Date January 1991	
				6. Performing Organization Code	
7. Author(s) James Ray Lundy, B. Frank McCullough, and David W. Fowler				8. Performing Organization Report No. Research Report 1205-2	
9. Performing Organization Name and Address Center for Transportation Research The University of Texas at Austin Austin, Texas 78712-1075				10. Work Unit No. (TRAIS)	
				11. Contract or Grant No. Rsch. Study 3/11-8-89/0-1205	
12. Sponsoring Agency Name and Address Texas Department of Transportation (formerly State Department of Highways and Public Transportation) P. O. Box 5051 Austin, Texas 78763-5051				13. Type of Report and Period Covered Interim	
				14. Sponsoring Agency Code	
15. Supplementary Notes Study conducted in cooperation with the U. S. Department of Transportation, Federal Highway Administration Research Study Title: "Finite-Element Analysis of Bonded Concrete Overlays"					
16. Abstract  A procedure is developed by which the likelihood of delamination of bonded concrete overlays on continuously reinforced concrete pavements is reduced. The procedure compares the early-age interface stress to the expected interface bond strength for a variety of environmental conditions. When the calculated stress exceeds the expected strength, it is recommended that overlay placement be curtailed until the possibility of debonding is reduced. A finite-element method program is used to determine the early-age stresses resulting from temperature and shrinkage-induced volume changes. Stresses were determined for a variety of environmental and material combinations and overlay thicknesses. Analyses show that a significant reduction in stress results from the use of overlay materials which have a lower modulus and thermal coefficient than those of the existing slab. The stresses for a given combination of materials and environmental conditions are compared to the interface bond strength at early ages. Early-age interface shear and tensile strengths are estimated from 7-day strength test results. The estimated strength, together with the variability of the interface strength, are used to calculate the likelihood of delamination for a given type of overlay and time of placement. This likelihood can be reduced through the selection of a different overlay material or time of placement.					
17. Key Words delamination, bonded concrete overlays, continuously reinforced concrete, early age, strength, stress, interface, temperature, shrinkage, variability			18. Distribution Statement No restrictions. This document is available to the public through the National Technical Information Service, Springfield, Virginia 22161.		
19. Security Classif. (of this report) Unclassified		20. Security Classif. (of this page) Unclassified		21. No. of Pages 94	22. Price



# **DELAMINATION OF BONDED CONCRETE OVERLAYS AT EARLY AGES**

by

James Ray Lundy  
B. Frank McCullough  
David W. Fowler

## **Research Report Number 1205-2**

Research Project 3/11-8-89/0-1205

Finite-Element Analysis of Bonded Concrete Overlays

conducted for

**Texas State Department of Highways  
and Public Transportation**

in cooperation with the

**U. S. Department of Transportation  
Federal Highway Administration**

by the

**CENTER FOR TRANSPORTATION RESEARCH**

Bureau of Engineering Research

THE UNIVERSITY OF TEXAS AT AUSTIN

January 1991

NOT INTENDED FOR CONSTRUCTION,  
PERMIT, OR BIDDING PURPOSES

B. Frank McCullough, P.E. (Texas No. 19914)  
David W. Fowler, P.E. (Texas No. 27859)

*Research Supervisors*

The contents of this report reflect the views of the authors, who are responsible for the facts and the accuracy of the data presented herein. The contents do not necessarily reflect the official views or policies of the Federal Highway Administration or the State Department of Highways and Public Transportation. This report does not constitute a standard, specification, or regulation.

## **PREFACE**

This report contains a historical review of much of the early development and trial uses of bonded concrete overlays. Also included is a detailed history of the use of bonded concrete pavement overlays performed by the State Department of Highways and Public Transportation (SDHPT) in Texas. Practically all the early-age failures in bonded concrete overlays are probably the direct result of delamination between the old existing pavement and the newer

overlay. Therefore, most of this report deals with the causes, consequences, and reduction of delamination in bonded concrete overlays. Delamination has been found to be an early-age phenomenon. Studies are directed toward an understanding of the mechanisms that initiate delamination, and then to construction and material combinations that reduce the chance of delamination during the early life of the pavement.

## **LIST OF REPORTS**

Research Report 1205-1, "An Empirical-Mechanistic Design Method Using Bonded Concrete Overlays for the Rehabilitation of Pavements," by Willem A. van Metzinger, B. Frank McCullough, and David W. Fowler, presents the background and techniques used in developing a design model for bonded concrete overlays. January 1991.

Research Report 1205-2, "Delamination of Bonded Concrete Overlays at Early Ages," by James Ray Lundy, B. Frank McCullough, and David W. Fowler, presents a study of the delamination phenomena in bonded concrete overlays and suggests construction and material techniques to reduce delamination. January 1991.

## **ABSTRACT**

A procedure is developed by which the likelihood of delamination of bonded concrete overlays on continuously reinforced concrete pavements is reduced. The procedure compares the early-age interface stress to the expected interface bond strength for a variety of environmental conditions. When the calculated stress exceeds the expected strength, it is recommended that overlay placement be curtailed until the possibility of debonding is reduced.

A finite-element method program is used to determine the early-age stresses resulting from temperature and shrinkage-induced volume changes. Stresses were determined for a variety of environmental and material combinations and overlay thicknesses. Analyses show that a significant reduction in

stress results from the use of overlay materials which have a lower modulus and thermal coefficient than those of the existing slab. The stresses for a given combination of materials and environmental conditions are compared to the interface bond strength at early ages.

Early-age interface shear and tensile strengths are estimated from 7-day strength test results. The estimated strength, together with the variability of the interface strength, are used to calculate the likelihood of delamination for a given type of overlay and time of placement. This likelihood can be reduced through the selection of a different overlay material or time of placement.

## SUMMARY

A viable rehabilitation procedure for continuously reinforced concrete pavement is the bonded concrete overlay. This rehabilitation procedure is especially attractive on heavily traveled urban freeways where long-life structures are needed and traffic delay for small preventative maintenance work becomes excessive for the user. Bonded concrete overlays have been found to perform well when properly designed and constructed; however, premature failures have been reported. These premature failures are most often associated with delamination between the existing pavement and the new overlay.

This report considers delamination by reviewing the history of previous bonded concrete overlay work and investigates the mechanisms which initiate delamination. The report also studies the interface stresses, studies the interface bond strengths, and uses a finite-element procedure to study the environmental and material effects.

These studies indicate that:

- (1) successful overlays have been placed in Texas at 2-, 3-, and 4-inch depths;
- (2) overlays can be placed successfully using welded wire fabric, steel fiber, or no reinforcement;
- (3) the modulus and thermal coefficient of the overlay material should be less than that of the existing slab;
- (4) shot-blasted and cold-milled surface preparation techniques can be used successfully, but a removal or texture depth should be specified;
- (5) overlays have been placed successfully with and without bonding agents; and
- (6) curing should be considered to reduce delamination, and the ACI evaporation rate of 0.2 lb/sq ft/hour is recommended.

## IMPLEMENTATION STATEMENT

Much of the information contained in this report is a result of close contact with State Department of Highways and Public Transportation district personnel in Houston and the close observation of construction and performance of projects placed in

that district. The results of these observations and studies have led to material, design, and construction recommendations as contained in this report. It is suggested that these recommendations be implemented in future bonded concrete overlay projects.

# TABLE OF CONTENTS

PREFACE.....	iii
LIST OF REPORTS.....	iii
ABSTRACT.....	iii
SUMMARY.....	iv
IMPLEMENTATION STATEMENT.....	iv
 CHAPTER 1. INTRODUCTION	
1.1 Background.....	1
1.2 Objective of Study.....	3
1.3 Scope of Study.....	3
 CHAPTER 2. PROBLEM DEVELOPMENT	
2.1 Historical Perspective of Bonded Concrete Overlays.....	4
2.1.1 Use in Highway and Airport Rehabilitation.....	4
2.1.2 Occurrence of Delamination.....	6
2.2 Consequences of Delamination.....	7
2.2.1 Bonded Overlay Design Procedures.....	7
2.2.2 Effect of Debonding.....	8
2.2.3 Reduction in Pavement Life.....	9
2.3 Causes of Delamination.....	11
2.3.1 Interstate Highway 80; Truckee, California.....	12
2.3.2 Loop Interstate Highway 610 North; Houston, Texas.....	13
2.3.3 Loop Interstate Highway 610 South; Houston, Texas.....	15
2.4 Summary.....	16
 CHAPTER 3. MODELING OF BONDED OVERLAY BEHAVIOR	
3.1 Modeling Techniques.....	17
3.1.1 Closed-Form Solutions.....	18
3.1.2 Finite-Element Method.....	22
3.2 Time-Dependent Characteristics of the Problem.....	23
3.2.1 Material Properties.....	23
3.2.2 Environmental Conditions.....	34
3.2.3 Interface Bond Strength.....	37
3.3 Summary.....	42
 CHAPTER 4. METHOD OF SOLUTION	
4.1 Evaluation of NSLIP.....	43
4.1.1 Closed-Form Solution Comparison.....	43
4.1.2 Finite-Element Comparison.....	45

4.2	Development of the Analysis Factorial.....	46
4.2.1	Environmental Conditions.....	46
4.2.2	Pavement Properties.....	47
4.3	Summary.....	56
<b>CHAPTER 5. ANALYSIS OF BONDED OVERLAYS</b>		
5.1	Typical Results.....	58
5.2	Edge Condition Analysis.....	62
5.3	Interior Condition Analysis.....	67
5.4	Summary.....	69
<b>CHAPTER 6. DESIGN AND CONSTRUCTION OF BONDED OVERLAYS</b>		
6.1	Design.....	71
6.1.1	Thickness.....	71
6.1.2	Reinforcement.....	72
6.2	Specification.....	73
6.2.1	Materials.....	73
6.2.2	Surface Preparation.....	74
6.3	Construction.....	75
6.3.1	Environmental Controls.....	75
6.3.2	Bonding Agents.....	77
6.3.3	Curing.....	78
6.4	Summary.....	78
<b>CHAPTER 7. CONCLUSIONS AND RECOMMENDATIONS</b>		
7.1	Conclusions.....	80
7.1.1	Case Studies.....	80
7.1.2	Modeling Techniques.....	80
7.1.3	Analysis Inputs.....	80
7.1.4	Analysis Results.....	81
7.2	Recommendations.....	81
7.2.1	Design, Specification, and Construction of Bonded Overlays.....	81
7.2.2	Further Research.....	81
<b>REFERENCES.....</b>		<b>83</b>

## CHAPTER 1. INTRODUCTION

Transportation plays a vital role in the economic well-being of any country and a significant role in the lives of its citizens. For example, in the United States, the transportation sector accounted for an estimated \$341 billion of personal consumption, or about 15 percent of all personal expenditures in 1987 (1). Transportation-related industries employ nearly 10 percent of the total civil work force, or 12 million persons (1). Although the rail, air, and water sectors play important roles in transportation in this country, nearly 88 percent of the passenger-miles logged by Americans are on highways and nearly 97 percent of these miles are in personal vehicles (1). Trucks carry nearly 30 percent of the total ton-miles of freight hauled in this country (2). Obviously, U. S. citizens rely heavily on highways for the transportation of persons and goods.

### 1.1 BACKGROUND

The U. S. highway system consists of roadways under the jurisdiction of local, state, and federal agencies totalling nearly 3.9 million miles. These facilities range in function from two-lane residential roads carrying tens of vehicles per day to multiple-lane controlled-access freeways serving tens of thousands of vehicles each day. Many of the high-volume facilities in this country are included in the National System of Interstate and Defense Highways, or Interstate System. Although this System constitutes only 1.1 percent of all road mileage, it carries roughly 20 percent of all motor vehicle traffic (3). Thus, the System is extremely important to the successful movement of persons and goods in this country.

The Interstate System was first authorized by the Federal-Aid Highway Act of 1944, which was adopted in 1947 (3). The selection of routes and development of design standards required approximately 8 years following the adoption of the Act. Studies were then initiated to develop preliminary cost estimates and plans for financing the system, culminating in the 1956 Federal-Aid Act, through which Congress made substantial funds available. The System was to have been completed by 1972 at a cost of about \$26 billion. Although not completed

on schedule, much of the System was constructed in the years between 1960 and 1970 at a cost of nearly \$120 billion. Thus, not only is the System vital to the movement of persons and goods; it also represents a significant capital investment in the infrastructure of this country.

In addition to the Interstate System, Congress established the Federal-Aid Primary System through a series of Federal Acts beginning in 1921. This aggregation of highways, the "A" System, now totals nearly 300,000 miles. In 1944, Congress authorized the creation of the Federal-Aid Secondary System. This System includes secondary state highways and county roads totalling 400,000 miles. A third Federal System was established to include approximately 125,000 miles of urban roads. Thus, through a series of Federal Acts spanning 50 years, Congress has authorized the creation of a vast system of highways totalling 825,000 miles. This network of roads is eligible for varying degrees of Federal aid to cover the cost of construction and rehabilitation. Although no exact dollar figure can be attached to these highways, the estimated cost to reconstruct this System exceeds one trillion dollars (4).

As noted above, the years between 1947 and 1956 were used, in part, to develop design standards for the Interstate System. A design life of 20 years was selected for the facilities. Simple arithmetic shows that much of the original Interstate System pavement is between 20 and 30 years old. Many roads in the Federal-Aid System are more than 50 years old. As the roadway approaches the end of its design life, several problems develop which directly impact the travelling public and therefore are the concern of the transportation engineer.

From the perspective of the public, as a roadway ages it simply fails to fulfill its purpose, that is, to provide a smooth, comfortable, and safe ride. The need for highway engineers to quantify this perception of the public resulted in the development of the serviceability-performance concept by Carey and Irick (5). Stated simply, the serviceability-performance concept relates certain physical characteristics of highways to the user's perception of comfort and convenience. The AASHO Road Test

validated the serviceability-performance concept put forth by Carey and Irick. Furthermore, the Road Test showed that roughness is the physical characteristic most representative of the public's perception of comfort (6).

A graphic representation of the serviceability-performance concept is shown in Figure 1.1. This conceptual figure demonstrates that, as a roadway nears the end of the intended design life, the serviceability level drops or the roughness increases. This increase in roughness causes increased dissatisfaction among the travelling public. Increased roughness also escalates vehicle maintenance costs and accident rates and accelerates the loss of serviceability. Although complete reconstruction is an option, the construction of a six-lane freeway in Texas costs approximately \$5 million per mile (4). The need for reducing roughness at an acceptable cost has led owner-agencies to perform maintenance and rehabilitation as funds allow.

The justification for expenditures of agencies' monies to maintain and rehabilitate highways is based on the idea that these agencies exist to provide a service to the public. This service is the provision of a safe, comfortable, convenient roadway for use by the travelling public. Furthermore, it is the goal of the agency to provide these services at the lowest cost. Generally this goal of lowest cost can be met through timely maintenance and rehabilitation. To this end, virtually all the Interstate and Federal-Aid System highways receive some form of ongoing maintenance.

Several options are available to the highway agencies as a means of reducing roughness or restoring structural integrity of the existing pavement. Deciding which type of rehabilitation is most appropriate for a given highway is a complicated matter: often the personal experiences and biases of the individual in charge determine the type of rehabilitation chosen. The intended scope of this investigation does not include a thorough investigation of all

the attributes of each rehabilitation option. However, some discussion of the options currently in use is appropriate, particularly when they pertain to the use of bonded overlays.

Rehabilitation of pavements often includes the application of an overlay to the existing pavement. Both rigid and flexible overlays are used to reduce roughness, correct structural or safety deficiencies, and extend the life of existing facilities. The term flexible is used herein as a generic term for paving materials made from bituminous materials. Flexible overlays are the most common type of rehabilitation used today, being used on both rigid and flexible pavement (7). Flexible overlays may be placed in layers less than 1 inch thick or in multiple layers totalling several inches. Flexible overlays have given good service when placed on existing flexible pavements. When flexible overlays are placed on rigid pavements an intermediate layer consisting of a fabric or low stiffness material is sometimes placed to reduce the likelihood of reflective cracking. The performance of flexible overlays on rigid pavements is more varied than that of flexible overlays on existing flexible pavements, particularly when the pavements are subjected to heavy traffic.

Rigid overlays have also been placed on flexible and rigid pavements, although the most common application is on existing rigid pavements. Rigid overlay designs may use either (1) continuously reinforced, (2) jointed reinforced, or (3) plain designs. These overlays are further categorized into three types, depending on the design bond condition. The interface between the overlay and the existing pavement may be fully bonded, partially bonded, or unbonded. Flexible overlays on rigid pavements are the most common rehabilitation type due to their low initial cost and the minimal traffic disruption which results from the quick-setting properties of asphalt (8).

Although flexible overlays are the most widely used rehabilitation procedure, some problems have arisen from their use, particularly in very heavy traffic areas where the existing pavement was rigid. In these cases, the overlays failed earlier than expected, by rutting and loss of bond to the existing pavement (9). These premature failures led to the early placement of a second overlay, resulting in unexpected costs to the agency and added delay costs to the users. In areas of heavy traffic, some agencies have suggested that money could be saved if less frequent rehabilitation could be performed as a result of using materials which have a longer life expectancy and, thereby, require less maintenance.

When properly designed and constructed, rigid overlays provide a suitable alternative to flexible overlays on existing rigid pavements. Rigid overlays

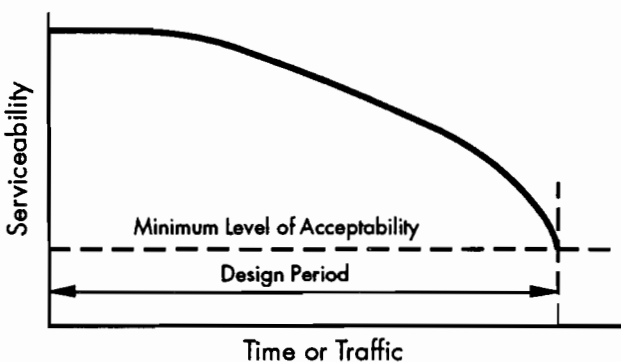


**Figure 1.1** The serviceability-performance concept as developed by Carey and Irick (5)

of existing rigid pavement have been used for some time and are performing well in most cases. However, in some instances, premature failures have been reported. These costly failures have been attributed to the delamination of the overlay from the existing pavement (10). The intent of this investigation is to develop a procedure which will reduce the likelihood of delamination.

### **1.2 OBJECTIVE OF STUDY**

If the rehabilitation of existing rigid pavements using bonded overlays is to be considered a viable alternative to complete reconstruction or flexible overlays, then every effort should be made to ensure complete bonding. To that end, the objectives of this study were to investigate the mechanisms which

initiate delamination of bonded overlays and, based on an evaluation of these mechanisms, develop recommendations for construction procedures, specifications, and materials combinations that will ensure more complete bonding.

### **1.3 SCOPE OF STUDY**

The majority of the investigation was directed toward the study of bonded overlays on existing continuously reinforced concrete (CRC) pavement. However, where applicable, the analysis and evaluation were extended to bonded overlays of jointed pavements. Furthermore, the investigation was directed toward the characterization of overlays at early ages, that is, before the overlay was subjected to traffic.

## CHAPTER 2. PROBLEM DEVELOPMENT

The technique of resurfacing concrete with concrete was attempted as early as 1910 (11). This project developed bond strength that provided 30 years of service. Despite the success of this early project, and many others that followed, some rehabilitation projects using bonded concrete overlays have been categorized as failures due to delamination at the interface. In this chapter, several bonded overlay projects are described. Both successful and unsuccessful projects are discussed; however, emphasis is given to those projects where delamination occurred, in order to provide insight into the mechanisms that initiate debonding. The consequences and possible causes of debonding are discussed. Finally, a hypothesis is presented which forms the basis of the subsequent research, analysis, and evaluation.

### 2.1 HISTORICAL PERSPECTIVE OF BONDED CONCRETE OVERLAYS

Although bonded concrete overlays have been used for many years as a means of rehabilitating existing portland cement concrete pavements, a literature review indicates there has been no nationally organized effort to document the performance of this overlay technique. Furthermore, no uniformly recognized design technique or construction procedure has been developed or implemented. The lack of consistency in design and construction among agencies carries over into the reporting activities of each agency. Each report, documenting what is commonly an experimental project, places emphasis on different aspects of the rehabilitation work. As a result, if delamination occurred, detailed analyses and comparisons between projects are difficult to perform. Further compounding the problem is the fact that most bonded overlays placed to date were used to rehabilitate jointed concrete pavements, which are not the primary focus of this investigation. Nevertheless, a review of several publications documenting highway and airport rehabilitation projects provides insight into the possible causes of delamination and the types of construction techniques that tend to reduce the chance of debonding.

#### 2.1.1 Use in Highway and Airport Rehabilitation

In 1932, and again in 1956 and 1964, Portland Cement Association (PCA) engineers prepared reports documenting the performance of concrete overlays throughout the United States (11, 12, 13). These reports cover overlay projects dating back to 1909. The first of these reports summarizes surveys of concrete resurfacing projects in various parts of the country (12). The very early concrete resurfacings (placed before 1912) consisted of 1 to 2 inches of concrete placed directly on the existing pavement. While some of these overlays gave very good service, few details of the condition of the existing pavements prior to overlay placement or the construction operation survive. Thus, little can be learned from these early projects. However, in the early 1930's several state highway departments placed experimental concrete resurfacing projects for which more complete information is available.

Projects constructed in Missouri, Maryland, and Illinois did attempt to establish bond between the two layers through various means. In these projects, the surface was cleaned by wet or dry brushing which was followed by the application of a neat cement paste or water on the pavement immediately before overlay placement. Fleming concluded that these special measures were not justified and that the removal of oil or asphalt was not necessary to secure a bond except in the case of very thin resurfacings (12). When a bond was desired, the author recommended a thorough washing using brooms and water, followed by a coating of cement mortar immediately before overlay placement. These are the first recommendations made on the construction of bonded concrete overlays.

Reports published by the Highway Research Board in 1956 and 1964 focus more specifically on bonded concrete overlays (11, 13). Felt, in 1956, used laboratory bond tests, experimental field projects, and surveys of existing projects to develop recommended practices for future bonded overlay placement (13). Laboratory tests were conducted on overlay specimens prepared on newly-constructed

base slabs and on slabs cut from 25 year-old pavements. The factors evaluated in this study included smooth and rough surfaces, damp and dry surfaces, cement-sand and neat cement grouts, concrete overlay mix design, and overlay placement technique. Direct shear tests were used to assess the bond strength of laboratory prepared overlay specimens. Although considerable variability in shear strength results was noted, as exemplified by a coefficient of variation in excess of 35 percent, several conclusions were reached: better bond strengths were developed when the base slab was dry than when the base slab was saturated-surface dry, and the use of grout increased the bond strength, while surface roughness did not seem to have a great or consistent influence on bond strength. The author determined that adequate bond strengths could be developed with any typical concrete mix design using any normal placement technique.

Four experimental sections were constructed between 1951 and 1954 as part of the investigation by Felt, one on the Rhode Island State Airport runway and the others on city streets in Wisconsin, Illinois, and Minnesota. Although details of the experimental sections are not of interest here, two results from the follow-up surveys are noteworthy. First, three of the four projects showed some delamination. The delamination was always adjacent to cracks or joints and represented a very small percentage of the total area. Second, on one project the effectiveness of sand-cement grout in increasing bond strength was investigated. The average strength of 10 cores taken from the grouted area was 275 psi, whereas the average of 8 cores taken from the ungrouted area was 197 psi.

Felt also surveyed bonded concrete overlay projects in nine states in the Upper Midwest and

Northeast constructed between 1912 and 1953 for his study (13). The results of bond strength tests run on cores taken from these projects are shown in Table 2.1. These data demonstrate what has been shown by several other researchers, namely that bond strength test results display a high degree of variability within any given project (14, 15, 16, 17).

Using information from laboratory and field experimentation, as well as in-service projects, Felt concluded that bonded overlays were a reliable rehabilitation option provided the following fundamental factors were observed during placement. First, proper surface preparation was necessary; he advised using hydrochloric acid when the existing surface was sound or mechanical scarification where unsound concrete was present. Second, he said that grout should be applied as a bonding agent following careful cleaning of the surface and that, after the placement of quality concrete, curing with wet burlap covered with vaporproof paper should continue for a period of at least three days, preferably one week.

Gillette also added to the existing body of knowledge by surveying 15 projects constructed between 1954 and 1963 (11). The majority of the projects were constructed on U. S. Military Air Fields and were surveyed in 1964. Details of the surveys are not significant to this study; however, several conclusions reached as a result of the surveys are noteworthy. Gillette determined that a bond strength of 200 psi is adequate and that wherever loss of bond occurred it probably developed soon after construction. Furthermore, Gillette concluded that little or no growth in the debonded area occurred over time or under traffic loading. At least one project constructed since 1977 has shown that, although delamination may indeed develop soon after overlay

**Table 2.1 Bond strengths from projects surveyed in the 1950's (13)**

Project Name	Date	Resurfacing	Bond Strength (psi)
		Thickness (in.)	
Ilene St, Detroit, MI	1950	1/2	256
Tennant Co, Minneapolis, MN	1952	1	316, 424, 596
Themis St, Cape Girardeau, MO	1922	5	0, 291
Market St, Savannah, MO	1914	3	0, 86, 208
First St, Hastings, NE	1948	4	0, 308, 348
Seventh St, Hastings, NE	1948	4	0, 186
South St, Hastings, NE	1949	4	0, 168
Bus Stop, Rochester, NY	1942	4	444, 480
Meadowbrook Rd, Rochester, NY	1942	1-1/2	0, 120, 396, 520
U.S. 27, Suffolk Co, NY	1947	6	500, 594, 524
Dublin Bridge, OH	1945	1	448
Stratford Bridge, OH	1949	3	210, 356, 416
Warsaw St, Toledo, OH	1913	1-1/2	188, 320, 484
U.S. 322, Clearfield Co, PA	1938	2	348, 364, 500
Rt. 44, Providence, RI	1936	2	484, 640

placement, the amount of debonding developed at early ages does not necessarily represent the terminal condition (18).

### 2.1.2 Occurrence of Delamination

Varying degrees of delamination have been reported on several overlay projects throughout the United States, and it might be found that it exists on most bonded overlay projects if one were willing to perform a thorough investigation. Three rehabilitation projects in which delamination was found are discussed here, and one case resulted in the project's being overlaid three months after construction. A fourth overlay project, in Texas, is investigated in considerable detail for clues to the cause of delamination.

The Iowa Department of Transportation undertook a research project in 1977 which placed 1.3 miles of a variety of concrete overlays in Clayton County. Details of the experimental sections may be found elsewhere (19, 20, 21). The experiment investigated three main factors: (1) surface preparation (cold milling, sand and water blasting), (2) reinforcement (none and wire fabric), and (3) overlay thickness (2, 3, 4, and 5 inches). Delamination was discovered in the bonded overlays in two areas. In the first, water blasting had been used to prepare the surface. In the other area the delamination was associated with secondary joint cracking (20).

Secondary joint cracking in this context is taken to mean cracks that form immediately adjacent to sawn transverse or longitudinal joints in the overlay. Darter and Barenberg have hypothesized that either the cracking initiates before saw cuts are made or that the secondary crack propagates from a spalled region near the joint in the existing pavement (22). A schematic of each condition is shown in Figure 2.1. The concrete between the secondary crack and the sawn joints tends to work loose with time. This secondary cracking was more common in the thinner sections (2 and 3 inches) than in the 4- and 5-inch overlay sections in the Clayton County, Iowa, study (20).

Delamination was also reported by the Louisiana Department of Transportation in a 4-inch overlay constructed on a 9-inch-thick jointed plain concrete pavement. When it was surveyed in 1986, five years after construction, debonding was noted along transverse joints and the pavement edge (23). Approximately 36 percent of the joints experienced some form of delamination.

Another rehabilitation project that reported delamination is a thin bonded overlay constructed by the California Department of Transportation, CALTRANS, beginning in June 1981. The 3-inch bonded overlay was placed on a 1.5-mile section of Interstate 80 near Truckee. This section, which is at

a high elevation, is subjected to frequent freeze-thaw cycling and had considerable tire chain wear. Details of the site preparation and construction are available elsewhere (10). Debonding of the overlay was noted shortly after placement, and, in some sections, nearly 90 percent of the overlay separated from the underlying slab. The entire project was overlaid with asphalt concrete in October 1981. Details of an investigation by CALTRANS are discussed later.

The Texas State Department of Highways and Public Transportation (SDHPT) began using bonded concrete overlays to rehabilitate continuously reinforced concrete pavements in 1983 with the construction of a 4-lane-wide, 1,000-foot-long experimental section. This section, constructed on Loop IH 610 South in Houston, consisted of five test areas each approximately 200 feet long. The factors investigated are shown in Table 2.2. A short section (20 feet long by 4 lanes wide) was placed without grout. All other sections used portland cement grout as the bonding agent. Surface preparation consisted of cold-milling followed by sandblasting. Details of the construction and early monitoring may be found elsewhere (24).

These test sections have been in service for seven years, carrying approximately 150,000 vehicles per day. Sounding surveys conducted in February and March 1990 show that some debonding has occurred. The results of the sounding survey are shown in Table 2.3. The majority of the delamination was found near the longitudinal construction

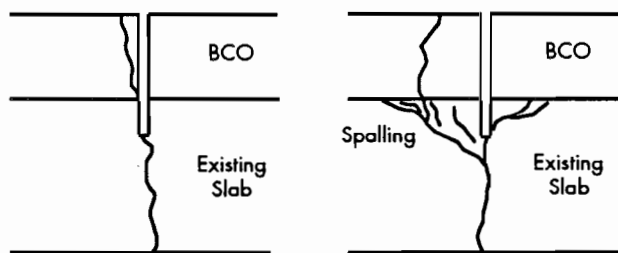


Figure 2.1 Possible modes for the formation of secondary joint cracking in bonded concrete overlays (22)

Table 2.2 Main factors investigated in the Loop IH 610 South experimental bonded concrete overlay test sections

Reinforcement Type	Thickness (2 in.)	Thickness (3 in.)
Plain	X	-
Wire Mesh	X	X
Steel Fibers	X	X

joint at the center of the 48-foot-wide pavement. It is not known if this delamination occurred shortly after construction or developed over time, because no record can be found of soundings prior to February 1990.

The Texas SDHPT constructed a large-scale bonded overlay project in Houston consisting of approximately 25 lane-miles. This project has about 0.6 percent delamination overall, but a few station-lanes have more than 15 percent of the total area debonded. All delamination areas were found adjacent to either longitudinal or transverse cracks or joints. A detailed investigation of the causes of delamination is included in a subsequent section.

A third overlay project is currently (1990) under construction in Houston. To date, only one experimental area, which used a latex bonding agent, has delaminated. One month after placement, about 30 percent of the total experimental area had delaminated. The area was removed and replaced using the normal overlay for this project. The failure is examined in considerable detail later in this report.

It has been shown that many bonded concrete overlays have some delamination. In addition, it can be said that delamination occurs adjacent to uncontrolled cracks or construction joints. Also, an examination of the available literature indicated that delamination might be found at very early ages if a specific effort were made to locate debonding. Thus, given that debonding will occur to a greater or lesser extent in virtually all bonded overlays, it might seem prudent to attempt to prevent this distress. However, if the effect of the delamination of the overlay on the long-term performance of the pavement is minimal, then there is no need to undertake measures to prevent the debonding.

## 2.2 CONSEQUENCES OF DELAMINATION

As noted in the previous section, many BCO projects have delamination, and considerable effort and expense are directed toward preventing its occurrence. However, it could be argued that if the

consequences of debonding do not significantly alter the long-term performance of the overlay then there is no need to work toward a complete bond. It is therefore prudent to examine (1) the assumptions used in preparing bonded overlay thickness designs, (2) how debonding represents a violation of these assumptions, and (3) what effect, if any, debonding has on the long-term performance of overlays.

### 2.2.1 Bonded Overlay Design Procedures

Several overlay thickness design procedures are in use throughout the world and, although there are differences in implementation, most have a common conceptual basis. All bonded overlay design procedures attempt to provide a pavement structure after rehabilitation that will perform in a manner equivalent to that of a new pavement designed for the prevailing conditions (25). A generic form of a common thickness design equation used by many agencies is shown below:

$$D_o^A = D_n^A - CD_e^A \quad (1)$$

where

$D_o$  = overlay thickness,

$D_n$  = new pavement thickness adequate for anticipated conditions,

$D_e$  = existing pavement thickness,

$A$  = exponent used to reflect the degree of bonding expected between layers, and

$C$  = coefficient used to reflect the condition of the existing pavement.

The new pavement design thickness,  $D_n$ , is determined using any of the current rigid pavement design procedures (20, 26, 27). Agency experience and preference play a large role in the selection of the design procedure. The strategy used to determine the value of the coefficient,  $C$ , is also determined to a large degree by the experience of the agency. This coefficient indicates the structural capacity or remaining life of the existing pavement. Visual inspection,

**Table 2.3 Delamination in the Loop IH 610 South experimental sections as of March 1990**

Test Section Identification	Thickness (in.)	Reinforcement Type	Section Length (ft)	Percent of Total Area Delaminated <sup>2</sup>
A	2	None	160	0.0
B <sup>1</sup>	2	Welded Wire Fabric	200	0.01
C	3	Welded Wire Fabric	180	0.6
D	3	Steel Fiber	180	0.01
E	2	Steel Fiber	160	0.0

<sup>1</sup>Section B includes a 20-foot length of overlay placed without grout.

This no-grout area contains the delamination in the section.

<sup>2</sup>Includes all four lanes.

agency experience, and deflection measurements are commonly used to establish the coefficient value. A complete description of the various methods available for determining  $D_n$  and  $C$  is beyond the scope of this investigation. Additional information can be found in References 27 through 33.

After the thickness of a new pavement,  $D_n$ , and the coefficient,  $C$ , have been determined, the type of overlay interface must be chosen before the final overlay thickness can be determined. Work by the U. S. Army Corps of Engineers and others has broadly classified rigid overlays into three categories, based on the degree of bonding expected. The categories are (1) bonded, (2) partially bonded, and (3) unbonded. While this investigation is primarily directed to the bonded overlays, it is well to discuss the implied consequences of debonding as indicated by the thicknesses resulting from each of the three categories when other factors are held constant.

The exponent,  $A$ , in Eq 1 is included in the design equation to reflect the degree of bonding present between the existing slab and the rigid overlay. Values of  $A$  for each of the overlay categories are shown in Table 2.4.

**Table 2.4 Design equations for bonded, partially bonded, and unbonded overlays (33)**

<u>Rigid Overlay Interface Condition</u>	<u>Coefficient A</u>	<u>Resulting Design Equation</u>
Bonded	1.0	$D_o = D_n - CD_e$
Partially Bonded	1.4	$D_o^{1.4} = D_n^{1.4} - CD_e^{1.4}$
Unbonded	2.0	$D_o^2 = D_n^2 - CD_e^2$

A significant reduction in overlay design thickness results from the selection of the fully bonded condition. For example, if an 11-inch "new" pavement is required for a given set of circumstances and the  $CD_e$ -term is equal to 8 inches, then the required bonded overlay thickness is 3 inches. However, when the design is for a partially- or non-bonded overlay, 5.3 and 7.5 inches would be necessary, respectively. This increase in design thickness for the non-bonded cases reflects the information gathered from the field studies conducted by the U. S. Army Corps of Engineers (34). Although the equations developed by the U. S. Army Corps are empirically based, the increase in thickness indirectly recognizes the stress increase which results as the extent of delamination increases.

### 2.2.2 Effect of Debonding

The simple example presented above indicates the importance of maintaining the interface bond throughout the life of an overlay designed as a

bonded overlay, if the resulting pavement is to perform as intended. Although the analysis of stress in rigid pavements is the subject of considerable research, relatively few studies have undertaken to determine the change in stress resulting from delamination of a previously bonded overlay. Still fewer studies have attempted to apply these results to estimate the resulting reduction in pavement life. One study sponsored by the Federal Aviation Administration investigated the effect of debonding on airfield pavement performance. The results, presented by van Dam et al, are discussed below (35).

Their study analyzed combined aircraft and temperature loadings on typical airfield pavement which had been overlaid. Aircraft loadings were analyzed using a finite-element program, ILLI-SLAB, and temperature induced stresses were calculated using the Westergaard-Bradbury equations. This study concluded that the maximum tensile stress and deflection caused by aircraft loadings increases as the loss of bond increases. The aircraft-load induced stresses calculated from each of the conditions investigated are shown in Table 2.5.

Thermally-induced stress proved to be a much more difficult analysis problem. The investigators attempted to apply the Westergaard-Bradbury equations to the unbonded condition in order to calculate temperature stresses. However, as the authors point out, the equations are not directly applicable to the unbonded condition because the original assumptions of Westergaard precluded the analysis of two layer systems. The existing slab was modeled as an extremely stiff support layer to circumvent this problem.

Westergaard assumed that full contact between the slab and the underlying slab was maintained throughout the analysis. The assumption of complete contact between two slabs subjected to thermal

**Table 2.5 Maximum tensile stresses in the overlay from wheel loads in 8-inch slabs with bonded and unbonded overlays (35)**

<u>Slab Size (ft)</u>	<u>Overlay</u>		<u>Bonding Condition</u>	
	<u>Thickness (in.)</u>	<u>k (pci)</u>	<u>Bonded</u>	<u>Unbonded</u>
12.5 x 15.0	3	200	-	428
	6	200	-	668
	9	200	24	652
	3	500	-	338
	6	500	-	538
	9	500	21	536
20.0 x 20.0	3	200	-	426
	6	200	-	665
	9	200	24	654
	3	500	-	337
	6	500	-	536
	9	500	21	538

loading was investigated by Lall and Lees (36). It was found that unbonded slabs separate at the interface when subjected to sufficient thermal gradients, as shown in Figure 2.2.

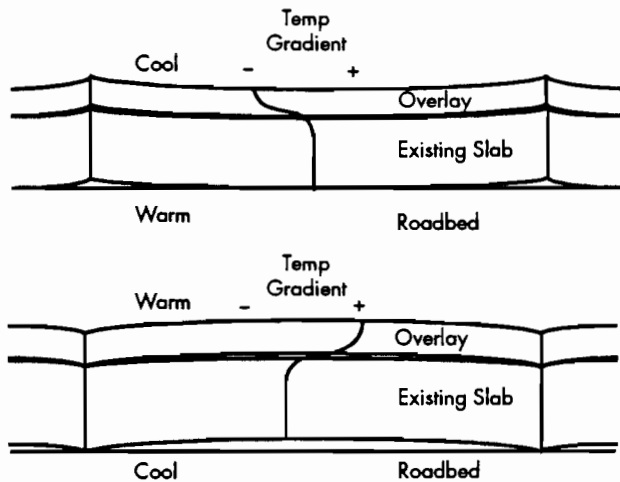


**Figure 2.2 Slab separation caused by differential curling of unbounded slab (36)**

The assumptions called for when using the Westergaard-Bradbury equations were not met in the calculation of temperature stresses shown in Table 2.6. A second approach using ILLI-SLAB and localized areas of very low support was undertaken in an attempt to model the zones of separation between the slabs. This phase of the investigation yielded unreasonably high stresses (in excess of 10,000 psi).

The results of the stress calculations shown in Table 2.6 also must be questioned as the result of the use of the principle of superposition. As pointed out by Korovesis and Ioannides, the validity of superposition depends on two conditions: (1) that only small deformations occur and (2) that the same boundary conditions apply for each of the calculations (37). While it may be accepted that the deformations are indeed small, the boundary conditions are probably different for wheel and temperature loadings, particularly in light of the study by Lall and

**Table 2.6 Total tensile stress in unbounded overlays from load and temperature (35)**

Slab Size (ft)	Overlay Thickness (in.)	k (pci)	Tensile Stress (psi)		
			ILLI-SLAB	Westergaard	Tot
12.5 x 15.0	3	200	428	116	54
	6	200	668	232	90
	9	200	652	348	1,00
	3	500	338	116	45
	6	500	538	232	77
20.0 x 20.0	9	500	536	348	88
	3	200	426	116	54
	6	200	665	232	89
	9	200	654	348	1,00
	3	500	337	116	45
	6	500	536	232	76
	9	500	538	348	88

Lees (36). Korovesis and Ioannides implemented a finite-element model proposed by Huang and Wang (38) and Chou (39) in the ILLI-SLAB program. This implementation allows for the presence of gaps under the slab and accommodates regaining of support under wheel loading. The results of a limited study are shown in Table 2.7.

A comparison of the results obtained using superposition and the ILLI-SLAB technique shows that superposition underestimates ILLI-SLAB results in the cases of interior and edge loading when the slab is under a positive gradient. Superposition will lead to a conservative estimate of the combined stress during nighttime conditions (negative temperature gradient). Only when conditions of a low gradient and soft subgrade are present will the two methods yield similar results.

### 2.2.3 Reduction in Pavement Life

The impact on long-term performance brought about by the increase in stress resulting from debonding can be assessed through the use of fatigue analysis. These equations normally define failure in terms of the amount of severe cracking or roughness present in a given area or length of highway. Regression analysis of field studies or road

**Table 2.7 Comparison of superposition and ILLI-SLAB stress results for three loading conditions (37)**

k (pci)	$\Delta T$ (°F)	Interior Load (psi)				Edge Load (psi)				Corner Load (psi)			
		L	C	TS	TI	L	C	TS	TI	L	C	TS	TI
200	-21	384	-64	320	293	658	-26	632	579	-482	-54	-536	-413
200	-42	384	-83	301	241	658	-32	626	511	-482	-62	-544	-418
200	21	384	70	454	484	658	40	698	753	-482	72	-410	-378
200	42	384	89	473	585	658	55	713	839	-482	97	-385	-322
500	-21	329	-84	245	212	579	-33	546	456	-415	-69	-484	-435
500	-42	329	-101	228	163	579	-36	543	387	-415	-77	-492	-449
500	21	329	88	417	509	579	59	638	744	-415	92	-323	-330
500	42	329	105	434	661	579	72	651	880	-415	113	-302	-268

tests relates the ratio of concrete tensile strength and tensile stress to the number of applications of load required to reach failure. Several researchers have analyzed the AASHO Road Test data or other field data to arrive at equations generally of the form shown below (27, 40, 41, 42, 43):

$$N = A \left( \frac{f_t}{\sigma} \right)^B \quad (2)$$

where

N = number of loads which induce stress,  $\sigma$ , which will yield a "failed" pavement,

$\sigma$  = tensile stress,

$f_t$  = tensile strength, and

A, B = regression coefficients.

While it may be intuitive that increased stress in pavements will shorten the life of the pavement, these regression analyses confirm the supposition.

The results of analyses by van Dam et al (35) indicate that delamination of overlays specifically designed to remain bonded throughout the design life will shorten the life of the facility. The airfield life was presented in terms of coverages. The average percent reduction in life for all the conditions studied was 88 percent. Although, the results presented were from an analysis of airfield pavement, analyses of highway pavements would yield similar results.

A limited study was performed to analyze the effect of debonding on pavement life. The overlaid pavement system was modeled using a multi-layered elastic computer program, BISAR (Bitumen Structures Analysis in Roads). This program allows variable slip between layers. Details of the assumptions and operational characteristics of the program can be found in Reference 44.

The parameters included in the computational analysis are shown in Table 2.8. Parameters identified as "variable" were determined to be the most important to the analysis. This should not be taken to imply that other factors are not important to an overall evaluation of bonded concrete overlay (BCO) failure mechanisms. Due to the limited nature of the investigation, some parameters were held constant or not included to reduce the problem to a manageable size. Specific values selected for use in the analysis were taken from Reference 45.

The equation derived by Taute et al was used to estimate the expected number of 18-kip equivalent single axle loads (ESAL) the pavement will carry before failure occurs (41). The fatigue equation is shown below using variables as defined in Eq 2:

$$N = 46,000 \left( \frac{f_t}{\sigma} \right)^{3.00} \quad (3)$$

The use of the fatigue equation presented above to define failure in continuously reinforced concrete (CRC) pavements requires that the maximum tensile stress in the concrete layer in question be determined. To that end, the pavement system shown in Figure 2.3 was analyzed using BISAR.

Stress results were determined at locations 1 through 4 for interface conditions of full friction and frictionless slip. Although only tensile stresses were of specific interest here, compressive stresses were also included in Table 2.9.

The fatigue equation from Taute et al allows the life of the pavement to be predicted. This equation does not take into account the remaining life of the existing slab prior to overlay. In order to make the results applicable to overlays placed on CRC pavement of various ages, Table 2.10 was developed. Flexural strength was varied from 500 to 1,000 psi for each stress condition in Table 2.9.

The number of repetitions to failure after overlay is controlled by the remaining life of the existing pavement prior to overlay. For example, if 75 percent of the life of the existing slab is consumed prior to overlay, then only 25 percent remains. The overlay reduces the stress in the existing slab, thus prolonging the life of the pavement. However, if the stress level is increased by delamination of the slab, the utility of the overlay is reduced. The results in Table 2.10 are plotted on page 12 in Figures 2.4 through 2.6 for remaining lives of 25, 50, and 75 percent.

The linearly elastic analysis of fully-bonded and delaminated concrete overlays of continuously reinforced concrete pavements shows the importance of a thoroughly bonded overlay in prolonging the life of CRC pavements. Stress increases of between 35 and 55 psi result when the overlay is debonded if

**Table 2.8 Factors included in analysis of effects of debonding using BISAR**

Parameter	Variable/Constant	Levels
Overlay Thickness	Variable	2, 3, 4 in.
Existing Slab Thickness	Constant	8 in.
Remaining Life	Variable	25, 50, 75 %
Concrete Modulus	Constant	3.6 (10 <sup>6</sup> ) psi
Flexural Strength	Variable	500, 750, 1,000 psi
Subbase Modulus	Constant	190 ksi
Roadbed Modulus	Constant	19 ksi
Loading	Constant	9,000 lbs, 6.0 in.
Percent Steel	Not Included	-
Steel Location	Not Included	-
Bonding Agent	Not Included	-
Environmental Stress	Not Included	-

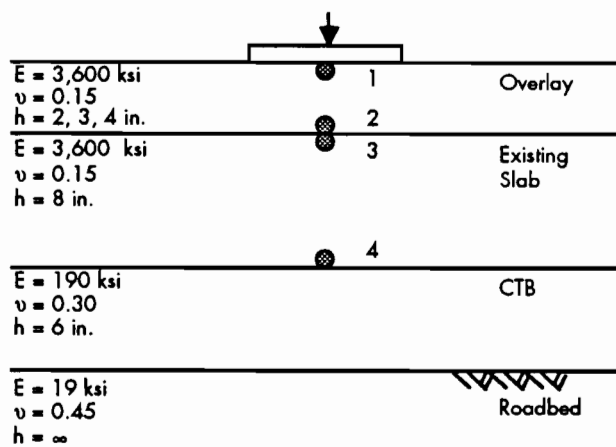


**Figure 2.3** Locations where stresses were determined using BISAR

the interface is assumed to be completely frictionless. In fact, some resistance to the relative movement between slabs would result even if the overlay is completely delaminated, and the stress would be lower.

The use of the fatigue equation from Taute et al (41) assumes that failure will occur in BCO pavements in the same manner as in the pavements in the Taute study. The actual mechanism by which BCO pavements fail is as yet unknown; however, a study by van Metzinger (46) provides considerable insight into the probable mode of failure. If the overlay remains fully bonded, then it could be conjectured that failure will follow patterns established in CRC pavements. However, as the overlay debonds, additional factors may control the mode of

**Table 2.9** Stress at analysis locations in bonded concrete overlays, in psi

Analysis Position	Fully Bonded			Complete Slip		
	2-in.	3-in.	4-in.	2-in.	3-in.	4-in.
1	119	108	100	50	76	92
2	63	39	23	-42	-67	-83
3	63	39	23	152	147	136
4	-89	-77	-67	-118	-112	-103

**Table 2.10** Expected repetitions to failure, in millions, for various combinations of thickness and remaining life

Remaining Life	Flexural Strength	Bonded			Unbonded		
		2-in.	3-in.	4-in.	2-in.	3-in.	4-in.
0.25	500	2.0	3.2	4.8	0.9	1.0	1.3
	750	6.9	10.6	16.1	2.9	3.45	4.4
	1,000	16.3	25.2	38.2	7.0	8.2	10.5
0.50	500	4.1	6.3	9.6	1.8	2.04	2.6
	750	13.8	21.3	32.3	5.9	6.9	8.9
	1,000	32.6	50.4	76.5	14.0	16.4	21.0
0.75	500	6.1	9.4	14.3	2.6	3.1	4.0
	750	20.6	31.9	48.4	8.8	10.4	13.3
	1,000	48.9	75.6	114.7	21.0	24.5	31.6

failure, such as wheel loading, thermal stresses, stress concentration due to steel position, and others. Therefore, these results should be used only as an indication of the relative importance of maintaining a bonded interface.

The studies by van Dam et al and by Korovesis and Ioannides, as well as the analysis described above, expose two important points regarding bonded overlays and the study of the effects of delamination. First, within the limits of the studies, debonding significantly increased the stress and deflection compared to a completely bonded situation. The increase in stress results in a reduction in pavement life. Therefore, if bonded concrete overlays are to remain an economically viable form of rehabilitation, then steps should be taken to determine the causes of delamination and the means of mitigating debonding. Second, these studies show that the modeling of delaminated overlays is extremely complex. Further discussion of this complexity is undertaken in a subsequent chapter, where the approach used in this investigation is developed.

### 2.3 CAUSES OF DELAMINATION

Potential causes of delamination have been examined by researchers for some time. In early projects debonding was common, in part because no genuine effort was made to obtain complete bonding. As greater effort was made to insure bonding, several hypotheses were advanced to explain the presence of delamination. Many failures on these early projects were attributed to inadequate surface preparation. On some projects constructed in the 1970's and 1980's, debonding was noted within two days after placement and again inadequate surface preparation was deemed to be the cause. However, as more sophisticated measurement and analysis techniques have been developed, research has been directed to more specific causes.

All of the potential causes identified by researchers thus far may be grouped into two categories. The distinguishing characteristics used to separate the factors are based on the history of the overlay itself. The first category, hereinafter called early-age characteristics, includes all factors influencing performance from the time the overlay is placed until it is first trafficked. The second category begins when the overlay is trafficked and continues until failure. Early-age characteristics of bonded overlays are the main focus of this investigation. The impetus for selection of this topic is based on an examination of both categories of potential causes in relation to the development of delamination in three overlay projects.

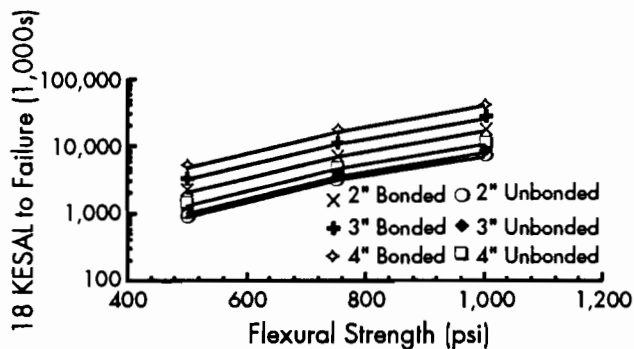


**Figure 2.4** Expected repetitions to failure when the existing slab has 25 percent remaining life

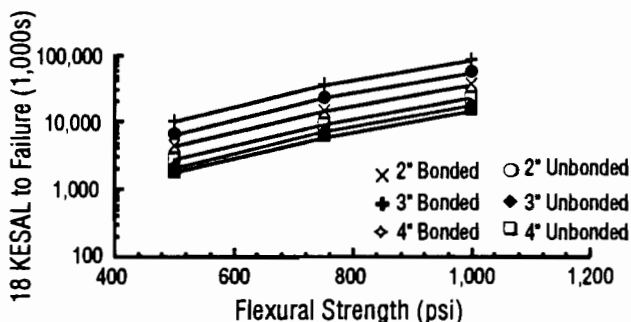


**Figure 2.5** Expected repetitions to failure when the existing slab has 50 percent remaining life

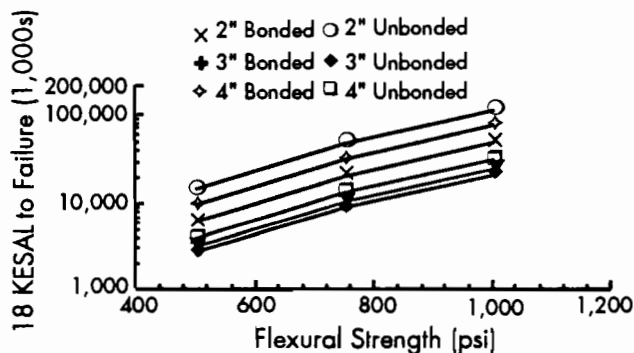


**Figure 2.6** Expected repetitions to failure when the existing slab has 75 percent remaining life

Failure of bonded overlays at early ages is thought to be initiated when the tensile or shear stress at the interface exceeds the available bond strength. These stresses develop when differential volume changes occur. Volume change can be initiated by temperature changes or shrinkage in the curing slab. The shear and tensile failure modes are shown schematically in Figure 2.7. Under normal circumstances these two failure modes work in combination to cause failure.

The most complete investigations of bonded overlay delamination and the mechanisms of

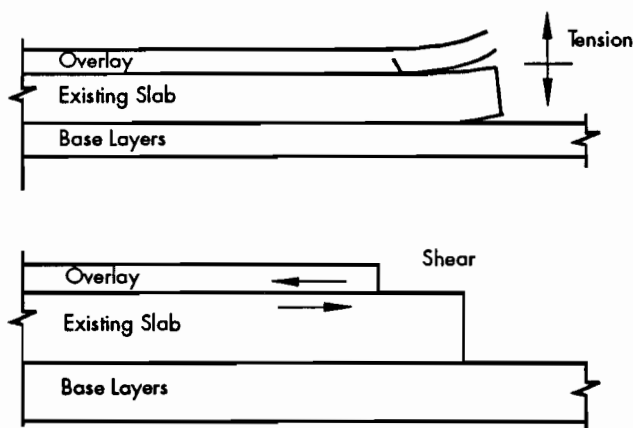


**Figure 2.7** Schematic representations of tensile and shear failure modes in bonded concrete overlays

debonding are available for three projects, one in California and two in Texas. These projects were described briefly earlier, but here they lead to the selection of early-age characteristics as the primary motivating force in the development of debonding.

### 2.3.1 Interstate Highway 80; Truckee, California

In June 1981, the California Department of Transportation, CALTRANS, began work on the placement of a 3-inch bonded overlay of a 1.5-mile section of Interstate 80 near Truckee. This section, which is at a high elevation, is subjected to frequent freeze-thaw cycling and has considerable tire chain wear. Details of the site preparation and construction are available elsewhere (10). Debonding of the overlay was noted shortly after placement, and in some sections nearly 90 percent of the overlay separated from the underlying slab. The entire project was overlaid with asphalt concrete in October 1981.

Following the discovery of debonding, an investigation to determine the reasons for the bond failure was undertaken. Field investigations of the project showed no clear trends, except that a definite correlation existed between the amount of aggregate exposed after the surface was prepared and the amount of delamination, i.e., there was less delamination with more aggregate exposed (10). Laboratory experiments were initiated to study the mechanics of the overlay failure. Grout thickness, temperature cycling, aggregate type, and surface roughness were included in the laboratory analysis. Some sections of the field overlay had been subjected to 50°F temperature differentials in the first night following placement. Therefore all laboratory slabs were subjected to large temperature differentials, in some cases as high as 60 degrees. In all

cases, delamination occurred within two weeks without traffic-like loadings.

These experiments and their field experience led California researchers to conclude that bond failure occurs in shear due to thermal stresses caused by high daily temperature fluctuations. Furthermore, they concluded that providing greater surface area on the existing slab (through the use of cold-milling) apparently allows the development of shear keys which are better able to resist bond failure. They also found that the abnormally high rates of cracking found in some areas were due to a high evaporation rate (0.3 lb per sq ft per hour) and high diurnal temperature differentials (greater than 50°F). They concluded that, for California conditions, thin bonded overlays using cement grout should not be used unless future studies indicated the debonding problem has been successfully addressed (10).

### 2.3.2 Loop Interstate Highway 610 North; Houston, Texas

A large-scale bonded overlay project was constructed in Houston on Loop IH 610 in 1985. This project, completed in 1986, consisted of approximately 28 lane-miles of 4-inch-thick bonded concrete overlay placed on an 8-inch CRC pavement. Surface preparation consisted of shot-blasting followed by air blasting immediately before the application of portland cement grout. The vast majority of the overlay was constructed using siliceous river gravel aggregate and welded wire fabric reinforcement, but some experimental sections were included. The main factors included in this project are shown in Table 2.11. Details of the construction can be found elsewhere (16, 47, 48).

Shortly after construction was completed, but after limited trafficking, delamination was discovered in some atypical areas placed in the vicinity of sign structures. The discovery of debonding in these long, narrow sections prompted the SDHPT to initiate an investigation to determine the location, extent, and cause of the delamination throughout the project. Details of the methods used to collect the data are available (49). A summary of the results from condition surveys conducted in March 1987 is presented in Table 2.12.

These data, along with results from condition surveys in 1988 and 1990, have shown the extent and location of debonded areas but do not address the third, and perhaps most important, issue—the cause of the delamination. It is through the investigation of this project, and a

**Table 2.11 Experimental factors investigated in the Loop IH 610 North bonded concrete overlay**

Aggregate Type	Reinforcement Type	Bonding Agent	Length of Section (Lane-Station)
Limestone	Welded Wire Fabric	PCC Grout	88
Siliceous River Gravel	Steel Fibers	PCC Grout	40
Siliceous River Gravel	Welded Wire Fabric	PCC Grout	1,440
Siliceous River Gravel	Welded Wire Fabric	None	16

companion project currently under construction, that early-age characteristics of overlays were identified as being important to the initiation of delamination.

Delamination was not discovered on the North Loop project until sometime after the overlay had been reopened to traffic. As a result, most of the study was conducted through a post-construction evaluation of paving reports, weather bureau records, and engineering diaries. After a review of available literature, several factors were identified as possibly having influence on the formation of debonded regions within the project:

- (1) Thermal properties of overlay and existing slab,
- (2) Temperature cycling in the first 24 hours,
- (3) Seasonal temperature cycling,
- (4) Moisture losses during the curing period, and
- (5) Condition of existing slab prior to overlay.

From available records, data were collected in the following areas for each station-lane on the entire project where delamination data were available (i.e., the two inner lanes):

- (1) Percent delamination,
- (2) Aggregate type,
- (3) Reinforcement type,
- (4) Concrete temperature at placement,
- (5) Air temperature at placement,
- (6) Bonding agent used,
- (7) Minimum daily temperature,
- (8) Maximum daily temperature,
- (9) Wind speed,
- (10) Relative humidity, and
- (11) Time, or traffic, since placement.

In addition to these data, information on concrete slump, flexural strength, alkali content of the cement, and air content were collected from Texas SDHPT

**Table 2.12 Percent delamination on the two inside lanes of Loop IH 610 North as of March 1987 (47)**

	Welded Wire Fabric Reinforcement			
	Steel Fiber Reinforcement		Welded Wire Fabric Reinforcement	
	Crushed Limestone	Siliceous River Gravel	Crushed Limestone	Siliceous River Gravel
PCC Grout	-	0.1	0.0	1.1
No Grout	-	-	-	1.6

records. Traffic loadings from the time of placement to the March 1987 survey were estimated from available data in terms of 18-kip ESALs for each lane. These data are summarized in Table 2.13. Beyond the obvious differences in the percent delamination between overlay types, no clear trends are apparent from the averages shown in the Table. It is noteworthy that surveys conducted in March 1988 and March 1990 show that there has not been any significant in delamination since the first survey in 1987.

When the same parameters are examined for differences between delaminated and non-delaminated areas, the importance of early-age influences may be seen. The data for the siliceous river gravel overlay only is shown in Table 2.14. One-factor analysis of variance (ANOVA) tests were run to determine if the differences between the parameter averages noted in Table 2.14 were statistically significant at the 5 percent level. All parameters were significant except those associated with construction quality control (i.e., slump, flexural strength, and air content) and time between overlay placement and the occurrence of the minimum temperature during curing.

Early-age characteristics of particular note include the magnitude of the differential temperature that occurred during the first 24 hours following placement. Non-delaminated sections had only a 15 degree differential while delaminated sections had a 20 degree differential. Also the evaporation rate, as calculated by the American Concrete Institute (ACI) recommended equation (50), was 40 percent higher for debonded sections than for sections that remained intact. The evaporation rate uses a combination of the concrete and air temperatures, wind speed, and relative humidity to estimate the loss of water from the fresh concrete. While these factors indicate that delamination may be initiated during the early stages of the curing, traffic appears to be a factor, because the delaminated areas have been exposed to more 18-kip equivalencies than the non-delaminated sections. Subsequent surveys in 1988 and 1990 have shown that the percent delamination is not increasing in the areas surveyed. Based on the results from four years of data in the Houston area, it would appear that traffic is not a factor in the propagation of delamination. Additional information

**Table 2.13 Values of various parameters identified as impacting the formation of delamination of Loop IH 610 North**

Parameter	SRG		Limestone		Steel Fibers	
	Average	Standard Deviation	Average	Standard Deviation	Average	Standard Deviation
Percent Delamination						
March 1987	1.1	4.2	0.0	0.0	0.1	0.5
March 1988	1.1	4.6	0.1	0.2	0.1	0.3
March 1990	1.1	4.6	0.1	0.2	0.1	0.3
Evaporation Rate (lb/ft <sup>2</sup> /hr)	0.11	0.04	0.12	0.04	0.11	0.02
Concrete Temperature (°F)	80	3.9	78	3.8	84	4.2
Wind Speed (knots)	7	1.7	10	0.3	7	0.5
Relative Humidity (%)	56	16.2	68	11.6	52	13.2
Placement Temperature (°F)	76	6.2	73	1.6	85	6.3
Average Temperature (°F)	71	4.8	71	4	81	2.9
Maximum Temperature (°F)	82	4.2	79	1.0	92	1.9
Minimum Temperature (°F)	60	7.2	53	0.5	68	2.1
Slump (in.)	2.8	0.4	2.5	-	2.7	0.0
Flexural Strength (psi)	940	50	880	-	-	-
Air Content (%)	4.9	0.7	5.3	-	4.1	0.2
Traffic to 3/87, 18 kip ESAL (10 <sup>5</sup> )	2.9	1.2	3.0	0.9	4.2	1.2
Differential Temperature in 1st 24 hours following placement	15	7.5	20	1.3	17	5.1
Time in hours to minimum temperature (1st 24 Hours)	18	3.0	18	4.6	17	2.8
Number of Station-lanes in sample	618	-	20	-	45	-

on the long-term performance of this project is contained in Reference 46.

### 2.3.3 Loop Interstate Highway 610 South; Houston, Texas

In 1989, the Texas SDHPT undertook the construction of a third bonded concrete overlay of an existing 8-inch CRC pavement. This project consists of approximately 40 lane-miles of 4-inch bonded overlay. Again, test sections were included in the project. The lengths of the various bonded overlay types are shown in Table 2.15.

Delamination was discovered within 18 hours after placement in the two test areas using latex-modified grout. This delamination had progressed in a period of six weeks to the extent that these two test sections were removed and replaced and no further use of latex-modified grout is planned. A detailed analysis of the cause and progression of the debonding follows.

Five of eight test sections and a control section were constructed on the inside lanes in July 1989. These test sections were to allow several surface preparation techniques to be evaluated. A plan view

**Table 2.14 Values of various parameters identified as impacting the formation of delamination of Loop IH 610 North—siliceous river gravel only**

Parameter	Non-Delaminated		Delaminated	
	Average	Standard Deviation	Average	Standard Deviation
Percent Delamination				
March 1987	0.0	0.0	1.1	4.2
Evaporation Rate (lb/ft <sup>2</sup> /hr)	0.10	0.06	0.14	0.04
Concrete Temperature (°F)	80	3.9	81	3.4
Wind Speed (knots)	7	2.2	8	2.0
Relative Humidity (%)	58	16.6	51	17.9
Placement Temperature (°F)	76	9.2	74	6.8
Average Temperature (°F)	72	9.1	68	5.5
Maximum Temperature (°F)	83	7.8	79	4.7
Minimum Temperature (°F)	61	10.7	57	7.2
Slump (in.)	2.8	0.4	2.5	0.3
Flexural Strength (psi)	940	50	880	60
Air Content (%)	4.9	0.7	5.3	0.6
Traffic to 3/87, 18 kip ESAL (10 <sup>5</sup> )	5.14	2.6	6.33	2.3
Differential Temperature in 1st 24 hours following placement	15	7.5	20	1.3
Time in hours to minimum temperature (1st 24 hours)	18	3.7	19	5.6
Number of Station-lanes in sample	443	-	175	-

**Table 2.15 Type and length of experimental test sections originally proposed for use on Loop IH 610 South**

Aggregate Type	Reinforcement Type	Bonding Agent	Surface Preparation	No. of Station-Lanes in Project
Limestone	Steel Fibers	PCC Grout	Cold Milled	16
Limestone	Welded Wire Fabric	No Grout	Cold Milled	16
Limestone	Welded Wire Fabric	PCC Grout	Cold Milled	16
Limestone	Welded Wire Fabric	Epoxy	Light Shot Blast	16
Limestone	Welded Wire Fabric	Latex-Modified Grout	Light Shot Blast	16
Limestone	Welded Wire Fabric	Latex-Modified Grout	Heavy Shot Blast	16
Limestone	Welded Wire Fabric	PCC Grout	Heavy Shot Blast	16
Limestone	Welded Wire Fabric	No Grout	Heavy Shot Blast	16
Limestone	Welded Wire Fabric	PCC Grout	Cold Milled	1952

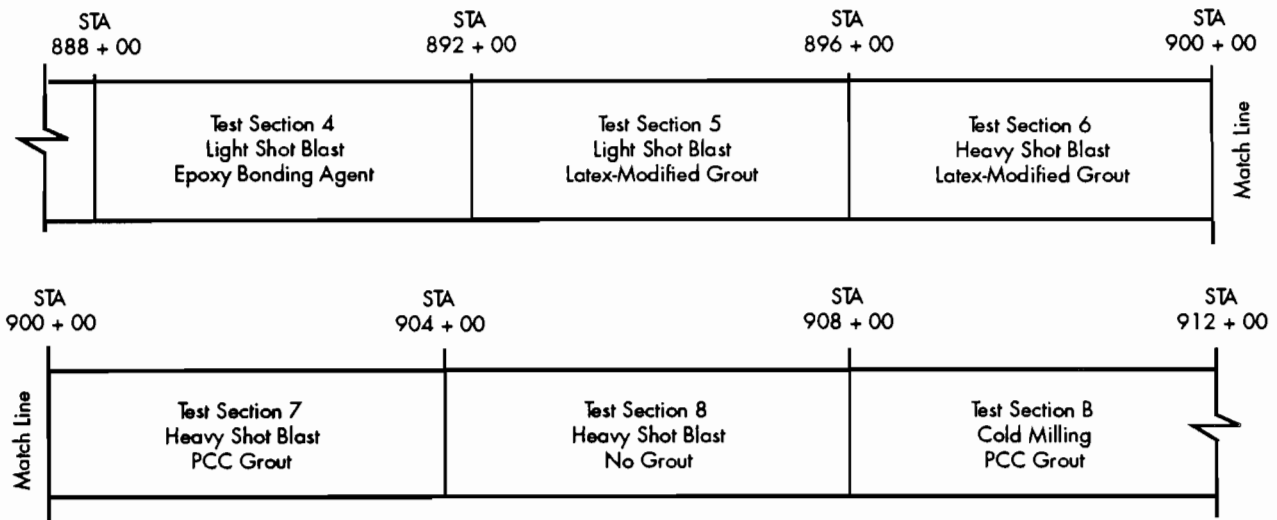


**Figure 2.8 Test section plan view for eastbound Loop IH 610 South, Houston**

of the test sections is shown in Figure 2.8. Delamination was found in the latex-modified grout sections (Test Sections 5 and 6) within 18 hours following placement and it continued to expand in area during the monitoring period of approximately 6 weeks. The progression of delamination can be seen in Figure 2.9. The progression of delamination for Section 5 is divided into parts (A and B) because the contractor placed this section on two successive days. It is noteworthy that adjacent sections placed under nearly identical circumstances did not debond. Also, no traffic was allowed on the overlay for a period of 7 days after placement, yet Section 5 had an average of 17 percent delamination. These two sections and about 100 feet of the adjacent section were removed and replaced with bonded overlay using PCC grout.

## 2.4 SUMMARY

There are benefits to be derived from the use of bonded concrete overlays for the rehabilitation of existing rigid pavements. These benefits can be realized through reduced facility maintenance and users delay costs. However, if these overlays delaminate, the resulting structure cannot function as planned. Felt (13) concluded portland cement grout increased bond strength, based on laboratory and field testing. He also concluded that increasing roughness of the surface beyond a general cleaning did not increase bond strength and that the dry surfaces yielded higher strengths than wet base slabs. While these measures may enhance the interface bond strength, some bonded overlays still delaminate.

Field experience has shown that bonded overlays do indeed debond, and some require complete replacement as a result. Limited work has been completed investigating the causes of delamination.

An investigation conducted by CALTRANS identified delamination as an early age problem with delamination occurring as a result of high interfacial shear stresses. They also identified the cause of excessive cracking as the high evaporation rate during and immediately after overlay placement. The fact that delamination is an early-age phenomenon was corroborated by field experience in Houston, Texas.

While the work by Felt and CALTRANS and the experience gained in Houston aid in the understanding of delamination, many questions remain unanswered. It is believed that through an understanding of the mechanisms that initiate delamination, construction procedures and material combinations that reduce the chance of delamination can be developed.

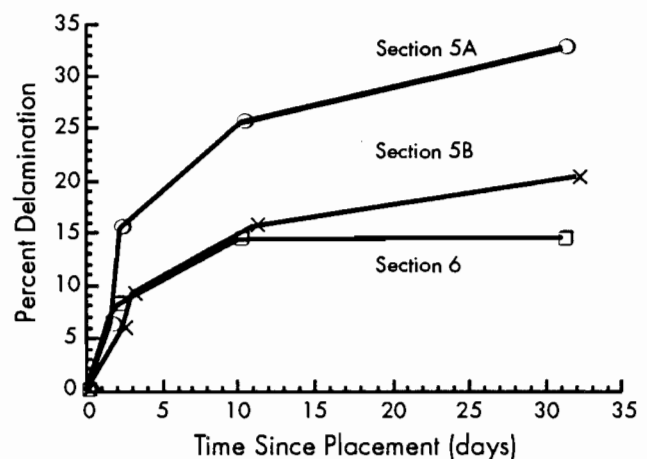


**Figure 2.9 Progression of delamination in test sections 5 and 6, Loop IH 610 South, Houston**

## CHAPTER 3. MODELING OF BONDED OVERLAY BEHAVIOR

The previous chapter has shown that bonded overlays are subjected to a variety of conditions in the first few days following placement which may cause debonding. Although it has not been demonstrated conclusively, many researchers have identified thermal stresses and adverse curing conditions (e.g., excessive moisture loss) as likely initiators of delamination (18, 22). It was also shown in the previous chapter that the analysis of a bonded concrete overlay-existing pavement system is a complex undertaking. This chapter develops the system to be modeled, describes several modeling techniques, and discusses the applicability of each technique to bonded overlays. Finally, several of the inputs required to effectively model the pavement system are described.

Before the various modeling techniques are discussed, it is appropriate to describe in some detail the system to be modeled. As noted in the section on scope (Chapter 1), only early-age characteristics of bonded overlays are investigated; therefore wheel loads, fatigue, and the eventual failure mechanisms are not included in the modeling scheme. Most delamination noted in bonded overlays has been associated with an edge, joint, or crack in the overlay. Figure 3.1 shows a plan view of a section of South Loop IH 610 in Houston that experienced delamination within 24 hours after placement. All the debonded areas discovered in this project are associated with the longitudinal construction joint or early-age transverse and longitudinal cracks. The association between cracks or joints and delamination has

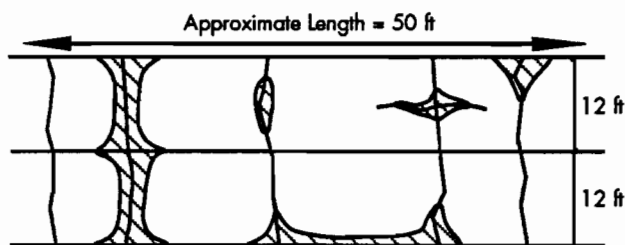


Figure 3.1 Plan view of bonded overlay section in Houston showing delaminated areas

also been noted in overlays placed in Iowa, California, and Louisiana (21, 23, 24). This association confirms the need to investigate the development of stresses in the vicinity of cracks or joints.

It has already been shown that delamination occurs without traffic loading; therefore, other causes of the stress at the interface between the two layers must be investigated, particularly that stress near joints and cracks. Thermal and early shrinkage stresses have been identified by other researchers as possible reasons for delamination (51, 52, 53). In order to investigate the development of thermal and shrinkage stresses at early ages, two cross sections were identified for modeling. These sections were selected by taking longitudinal and transverse cross sections of the pavement shown in Figure 3.2.

A transverse cross section of the pavement edge immediately after the placement of a bonded concrete overlay is shown in Figure 3.3. This figure does not include the reinforcement which, in the existing slab, would normally be located slightly above mid-depth. If the overlay contains reinforcement, it could be distributed (steel fibers) or located at or below mid-depth, depending on the thickness of the overlay (steel fabric). A longitudinal cross section is shown in Figure 3.4. Again, reinforcement is not shown, but transverse cracks are indicated in the existing slab.

Either of the two cross sections set forth above will allow the stresses of interest to be calculated provided an approach can be developed which will model the various constraints of the system. These constraints include (1) the physical boundaries of the existing pavement and the overlay, (2) the presence and location of reinforcement, (3) the existence of cracking in the original and overlay pavement, and (4) the changing physical properties of the overlay material. Several modeling techniques are examined and the most appropriate one is selected.

### 3.1 MODELING TECHNIQUES

Several different modeling techniques are available for the analysis of a bonded overlay. These techniques range from closed-form solutions

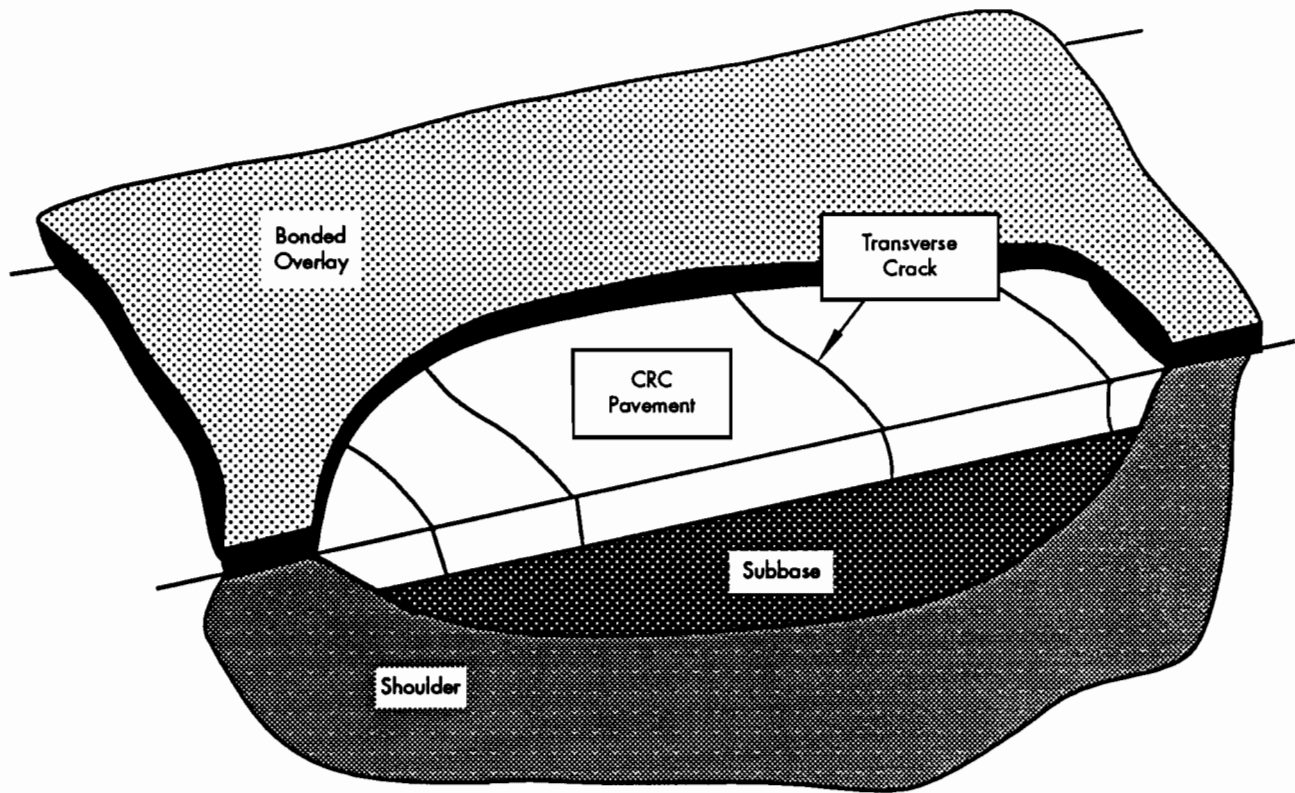


**Figure 3.2** Cut-away section of CRC pavement immediately after placement of the bonded overlay

of simplified pavement systems to three-dimensional finite-element analysis of pavement with overlays. As applied to the current problem, the most appropriate modeling technique must evaluate the stress regime at or near the interface between two dissimilar materials bonded together, with possible emphasis given to the stresses in the vicinity of the vertical discontinuities. Several methods are described below and the merits of each are discussed.

### 3.1.1 Closed-Form Solutions

A closed-form solution would, of course, provide the most accurate solution to the determination of the stress distribution near cracks in multi-layered pavement systems. However, for systems as complex as a pavement, very few closed-form solutions exist. All require the user to make several simplifying assumptions. Two early studies of thermal stresses in pavements or layered systems that are related to the present problem are the work of Westergaard and Timoshenko.

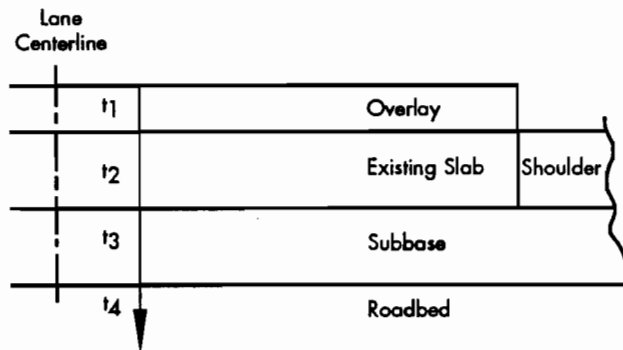


**Figure 3.3** Transverse cross section of the bonded-overlay and existing-pavement system immediately after overlay placement

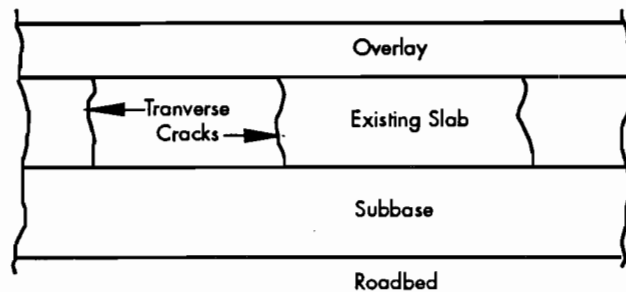


**Figure 3.4** Longitudinal cross section of the bonded-overlay and existing-pavement system

Some of the first work on the stress analysis of dissimilar materials subjected to changing thermal conditions was done by Timoshenko in 1925 (54). In this work, Timoshenko first derived equations for the stress in a simply supported beam composed of two dissimilar materials subjected to a uniform temperature change. He extended this analysis of bi-metal thermostats to other support conditions, including a fully restrained beam constructed of two different materials. Timoshenko assumed the following conditions during all the derivations contained in Reference 54: (1) the thermal coefficients remained constant during heating; (2) the width of the strip was very small compared to the length; and (3) the friction at the supports could be neglected. The derivation of Timoshenko, as summarized herein, is commonly referred to as the separate section method. While the derivation by Timoshenko does not directly address all the constraints of the bonded overlay problem, it is included because the solution provides an excellent base from which to judge the finite-element program discussed later.

The deflection in a narrow, simply supported bi-metal strip shown in Figure 3.5 is subjected to uniform heating. Timoshenko assumed that any cross section remains planar and perpendicular to the axis of the strip after bending. Consider an element far removed from the ends: if the thermal coefficient of Layer 2,  $a_2$ , is greater than the thermal coefficient of Layer 1,  $a_1$ , then the deflection will be convex down, as shown in Figure 3.5(c). The forces on Layer 1

can be represented by a tensile force,  $P_1$ , and a bending moment,  $M_1$ . For Layer 2,  $P_2$  will be compressive. All forces must be in equilibrium, so

$$P_1 = P_2 = P \quad (1)$$

$$Ph / 2 = M_1 + M_2 \quad (2)$$

Letting  $\rho$  = radius of curvature and

$E_1 I_1$  = the flexural rigidity of Layer 1 and

$E_2 I_2$  = the flexural rigidity of Layer 2,

then

$$M_1 = E_1 I_1 / \rho \text{ and}$$

$$M_2 = E_2 I_2 / \rho .$$

Substituting into Equation 2 yields

$$Ph / 2 = (E_1 I_1 + E_2 I_2) / \rho . \quad (3)$$

Considering the deformation of the strip, the unit deformation of Layer 1 at the interface must equal that of Layer 2; therefore

$$\alpha_1(t - t_0) + (P_1 / E_1 a_1) + (a_1 / 2\rho)$$

$$= \alpha_2(t - t_0) - (P_2 / E_2 a_2) - (a_2 / 2\rho)$$

Using (1) and (3)

$$\frac{h}{2\rho} = \frac{2(E_1 I_1 + E_2 I_2)}{h} \left\{ \frac{1}{E_1 a_1} + \frac{1}{E_2 a_2} \right\} = (\alpha_2 - \alpha_1)(t - t_0)$$

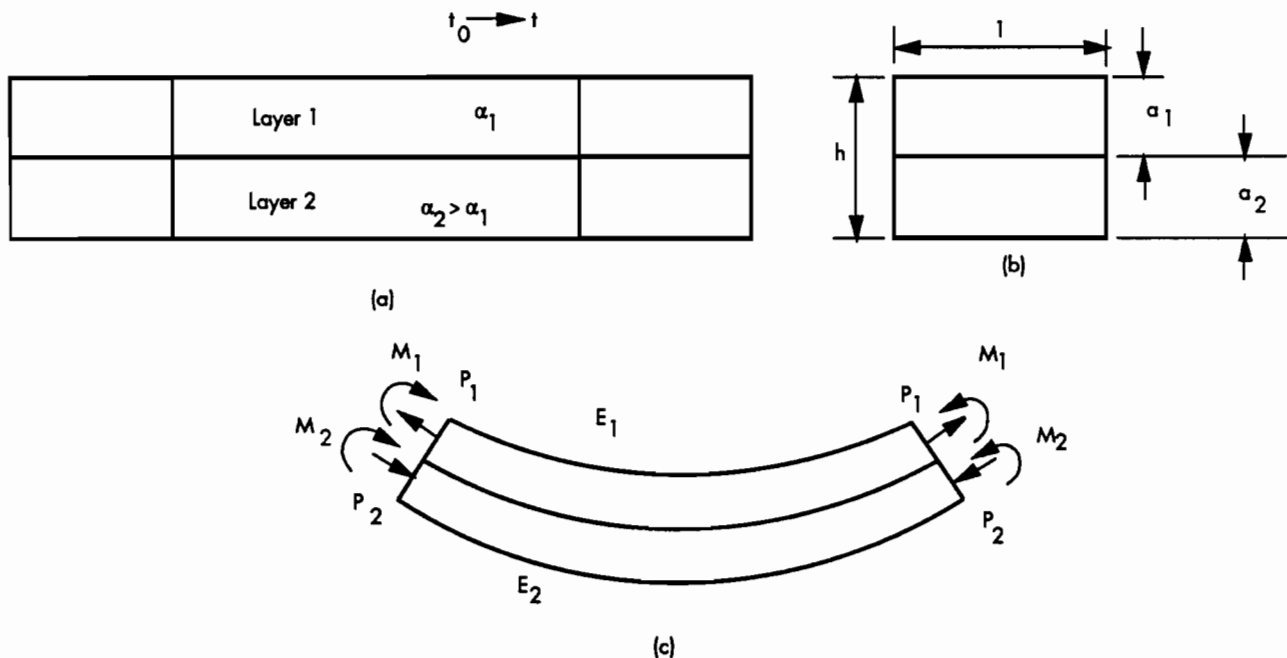


Figure 3.5 Deflection of a bi-metal strip while uniformly heated (54)

Simplifying, results in

$$\frac{h}{\rho} = \frac{(\alpha_2 - \alpha_1)(t - t_0)}{2(E_1 I_1 + E_2 I_2) \left\{ \frac{1}{E_1 a_1} + \frac{1}{E_2 a_2} \right\}}$$

Letting

$$\begin{aligned} a_1 / a_2 &= m, \\ E_1 / E_2 &= n, \\ I_1 &= a_1^3 / 12, \text{ and} \\ I_2 &= a_2^3 / 12, \end{aligned}$$

the following general equation for curvature results:

$$\frac{h}{\rho} = \frac{6(\alpha_2 - \alpha_1)(t - t_0)(1 - m)^2}{h \left[ 3(1 + m)^2 + (1 + mn) \left\{ m^2 + \frac{1}{mn} \right\} \right]} \quad (4)$$

The deflection,  $\delta$ , can be easily found by remembering that the deflection is small in comparison to the radius of curvature,

$$\delta = l^2 / 8\rho$$

Using elementary beam theory, Timoshenko developed equations to determine the internal stresses that result from heating the bi-metal strip. These stresses consist of two parts: (a) the stress due to the axial force and (b) the stress due to bending. For Layer 1 at some distance from the supports,

$$p_{\max} = (P / a_1) + (a_1 E_1 / 2\rho) \quad (5)$$

An examination of Equation 4 shows that, if the thermal coefficients of the layers are equal, there will be no differential movement. If there is no differential movement, then no bending and hence no stress will develop in the beam. Timoshenko assumed that the bending in the beam was caused by the different thermal coefficients of the layers. While this is certainly appropriate for an investigation of bi-metal thermostats, the concrete overlay and existing slab will have similar thermal coefficients if the same concrete aggregate is used in each layer. When materials with similar thermal coefficients are considered, curvature results if differential movements occur between the layers. Differential movements would occur if a temperature gradient exists in the beam. This gradient would cause the layer exposed to the higher temperature to move relative to the other layer. As will be discussed in the section on environmental conditions, a non-uniform temperature change is more representative of the conditions present in pavements.

A second problem associated with the use of the derivation by Timoshenko is particularly troublesome. As stated by Timoshenko, the shearing stress near the ends of the composite beam cannot

be determined using elementary beam theory. Timoshenko goes on to say that these stresses are of a "local" nature, concentrated near the ends of the beam, and that the stress decays to nearly zero along a distance equal to the thickness of the beam. Yet, from field experience with bonded overlay delamination, it is the area near the ends of the beam, or in pavement at cracks and joints, that is most susceptible to debonding. Other researchers have confirmed the concentration of shear stress near the ends of beams and several have attempted to analytically determine the magnitude of this end effect.

Hess (51) extended the results of Timoshenko by superimposing another stress field on that derived by Timoshenko so that the outer surfaces of the beams remain stress free. The details of the method by which Hess derived this stress field may be found in Reference 51. The results show that the solution by Timoshenko is valid everywhere except within a distance from each end equal to the total thickness, as predicted by the St. Venant's effect and stated by Timoshenko (54). The solution developed by Hess gives the correct shape of the interfacial stresses, but, as declared by Hess, the solution is not correct within a distance of the end equal to 0.05 times the thickness of the beam. As with the derivation given by Timoshenko, the system used in the derivation is a simply supported beam in which stress is induced by means of a uniform temperature change. In conclusion, Hess noted that the stress field near each end of the laminated strip includes transverse normal and shear stresses and that these stresses may be sufficient to induce delamination through adhesive failure or cracking (51).

Grimado used elementary beam theory to solve for the end stresses in a laminar system by considering the bond layer as a separate layer (55). Thus, the two-layer system examined by Timoshenko is transformed into a three-layer system. In the central portion of the beam, the normal stresses were similar to those calculated by Timoshenko. However, high shear stresses were found to exist near the ends of the beam. These stresses diminished to near zero at a distance approximately equal to the height of the beam, as suggested by Timoshenko. Chen et al (56) also considered the bond layer to be a separate layer in their analysis. They, and many others (57, 58, 59), have studied the behavior of adhesive-bonded joints analytically and experimentally. All these studies show stresses to be concentrated near the end of the beam or in the region of a joint.

Several other researchers have attempted to solve for the interfacial stresses near the end of a multi-layered beam using another approach. A method, termed the composite section method, was

developed separately by Branson and Roll (52, 53). In this method the shortening of one layer is restrained by the composite beam. Referring to Figure 3.6 and following the derivation of Birkland (60), the external force on the top layer due to a temperature change is

$$P = \Delta \epsilon A_1 E_1 \quad (6)$$

where

$$\Delta \epsilon = (\alpha_2 - \alpha_1) \Delta T .$$

This force, P, is of sufficient magnitude to cancel the differential movement and is applied at the centroid of the top layer. A compressive force of the same magnitude is applied on the top layer canceling the first applied force. The beam is then considered an eccentrically loaded column where the normal stresses are

$$\sigma = (P / A) \pm (M_c y / I_c) \quad (7)$$

where

$$M_c = P e_c .$$

The eccentricity,  $e_c$ , is measured from the centroid of the composite section, and the moment of inertia,  $I_c$ , is that of the transformed section. The stresses at the top and bottom of the overlay are

$$\sigma_1 = \left\{ \frac{P}{A_{1t}} - \frac{P}{A_c} - \frac{M_c y}{I_c} \right\} \frac{E_1}{E_2} \quad (8)$$

where

- $\sigma_1$  = stress in the overlay,
- $A_{1t}$  = transformed sectional area of Layer 1;  $A_1 (E_1 / E_2)$ ,
- $A_c$  = composite beam area;  $A_c = A_{1t} + A_2$ , and
- $y$  = distance from the composite beam centroid to the location where the results are desired.

The stresses at the top and bottom of Layer 2 are

$$\sigma_1 = \left\{ \frac{-P}{A_c} \pm \frac{M_c y}{I_c} \right\} \quad (9)$$

where P,  $A_c$ ,  $M_c$ ,  $y$ , and  $I_c$  are as previously defined.

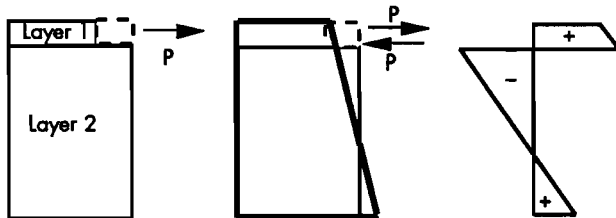


**Figure 3.6** Section used for the derivation of the composite section method of analysis (60)

Most of the analysis techniques discussed thus far are the result of research by materials engineers working with multi-layer laminates. These engineers have identified a phenomenon, frequently call the free-edge effect, which is considered to result from the presence and interactions of geometric discontinuities of the composite and material discontinuities through the laminate thickness (61). The high stresses that develop at the free edge have been observed to be responsible for the initiation and growth of delamination under static and cyclic fatigue loading (62, 63,64). Beginning in the 1920's, pavement engineers have also been investigating thermal stresses in materials.

In 1926, a paper by Westergaard was published which described a procedure for calculating the stresses in concrete pavements due to temperature variations (65). Westergaard investigated two cases: (1) a seasonal temperature change in which the temperature was assumed to be uniform throughout the depth of the pavement, and (2) a diurnal temperature variation in which a temperature gradient was assumed throughout the pavement, with the temperature unchanged at the mid-plane of the pavement. The seasonal variation of temperature is not considered herein; however, the daily temperature variation results are applicable to this problem. Details of the derivation and the assumptions made by Westergaard can be found in Reference 65. Westergaard presents the following equation for the deflection,  $z$ , at some distance,  $y$ , from the edge of an infinitely long slab of thickness,  $h$ , subjected to a temperature gradient,  $t$ :

$$z = -z_0 \sqrt{2} \cos \left( \frac{1}{1\sqrt{2}} \frac{y}{4} + \frac{P}{4} \right) e^{-\frac{y}{1\sqrt{2}}} \quad (10)$$

where

$$1 = \sqrt[4]{\frac{Eh^3}{12(1-\mu^2)k}} \quad z_0 = \left( \frac{(1+\mu)\epsilon_1 t}{h} \right) l^2$$

The derivation by Westergaard shows the edge, or corner, to be the critical stress location when the temperature of the top of the slab is lower than that of the bottom.

Each of the closed form solutions developed to analyze stresses in laminar beams predicts high interfacial stresses near the edge of the beam, as a result of the material differences between layers when the beam is subjected to a temperature change. Although most analyses were directed to temperature changes, the force causing the movement could just as well be drying shrinkage or any other mechanism which induces volume change. These high stresses may help to explain the occurrence of debonding at

or near edges and cracks in the overlay. The work of Westergaard shows that pavements are subjected to thermal gradients, which results in significant thermal stresses, again concentrated near the edge of the structure. These analyses demonstrate that curling of the overlay after debonding could be a factor in the propagation of delamination.

While these methods can estimate the maximum stress at the edge of the beam, they cannot predict stresses due to complex temperature distributions typically found in pavements. Moreover, pavements are continuously supported structures with cracks, not simply supported beams, as assumed in the interfacial stress analysis. Therefore, it was decided that the finite-element method would be used to analyze the bonded-overlay and existing-slab system, with the closed form solutions serving as a check on the reasonableness of the resulting solutions.

### 3.1.2 Finite-Element Method

The finite-element method was determined to be the most appropriate modeling technique because it is able to address the following issues in the overlay-original pavement system: (1) continuous support of the original pavement, (2) cracks in the original pavement or overlay, (3) development of variable interfacial shear stress as a result of differential material characteristics, (4) reinforcement in the pavement, and (5) complex temperature distributions in the pavement. No other method is capable of addressing all these needs simultaneously.

Ideally, the analysis of the stress state at the overlay-original pavement interface requires a three-dimensional modeling of the system shown in Figure 3.2. However, based on the work of other researchers and practical considerations, the system will be modeled as a two-dimensional, plane strain problem. Several researchers (66, 67) have used two-dimensional plane strain analysis to model thermal stresses in layered systems.

The finite-element method computer program used to analyze the overlay-existing pavement system was developed at Texas Tech University as part of a federally funded project to study the characteristics of bonded overlays. A general description of the finite-element method can be found elsewhere (68, 69, 70). The following description of the specific application of the finite-element method to the current problem is based on a report by the developers of the program (71).

A two-dimensional analysis finite-element computer program was adapted from existing computer code to analyze stresses and deformations in a concrete pavement system containing concrete overlays. Eight-noded isoparametric quadrilateral elements are used in the model. This program permits the addition of slip elements between, or within, the old

concrete and the overlay to allow the materials to displace relative to each other. These four-noded elements can be oriented between normal eight-noded elements on either horizontal or vertical planes. When the stress associated with the relative displacement of adjacent layers reaches a critical value, the limiting shear strength, a complete dislocation can occur. As noted earlier, failure may occur due to tension as well as shear near the edges of the overlay. This fact was taken into account by specifying a limiting tensile strength for these slip elements. Steel reinforcement can also be incorporated into the discretization through the use of a bar element located at any height within the eight-noded element. Bar elements cannot be located immediately adjacent to slip elements.

During the operation of the program, an iterative procedure allows the formation of vertical cracks or horizontal delaminations through the failure of the slip element in either tension or shear. The stress-deformation relationships for the vertical and horizontal slip elements are shown schematically in Figure 3.7. As can be seen, after the tensile strength limit has been exceeded, no tension is transmitted by the slip element to the adjacent element, while if the shear limit is exceeded that limiting shear continues to be transmitted. The reason for this formulation is that after a tensile failure the layers will be physically separated and therefore unable to transfer stress, while after a shear failure the layers will still be in contact, allowing shear to be transmitted between layers. This formulation allows the possible debonding mechanisms discussed earlier to be investigated by allowing the interfaces to fail progressively.

Several inputs and their importance to the solution must be discussed before proceeding with the

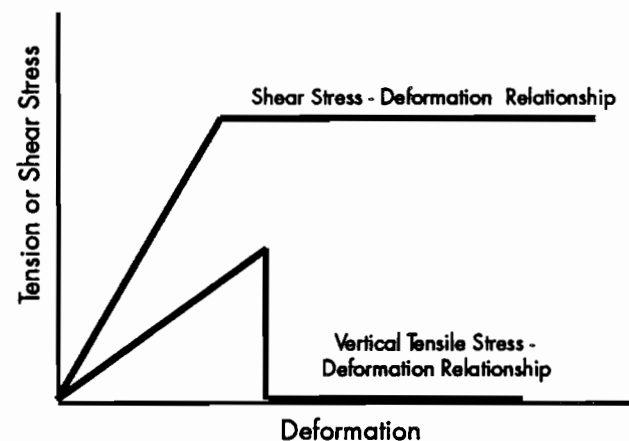


Figure 3.7 Relationships used in determining the tensile and shear stresses in slip elements

investigation. The required inputs to the finite-element program include: (1) steel and concrete moduli; (2) thermal coefficients of the overlay, existing slab, and steel; (3) ultimate shrinkage and the rate at which shrinkage accumulates; (4) temperature distribution in the overlay and slab before and for some time after placement; and (5) interfacial shear and tensile strength development rates. All these inputs depend in part on the season of placement and are influenced by the test methods used to obtain the values. The input values selected for analysis are discussed in the next chapter. Here, the intent is to describe briefly the nature and importance of each variable.

### 3.2 TIME-DEPENDENT CHARACTERISTICS OF THE PROBLEM

An investigation into the early-age characteristics of bonded concrete overlay implicitly requires consideration of the effects of time on the problem. The time of analysis certainly plays a role, given that delamination was discovered within the first 24 hours following overlay placement. Time plays an important role in the development of the problem for two additional reasons: (1) material properties of the overlay undergo substantial change during the first few days following placement, and (2) environmental conditions also change as the overlay cures and interfacial bonds form. Ideally, then, the problem solution would include a continuous time function which would allow the incorporation of the changing environmental conditions and material properties. However, from a practical standpoint this is not possible. It is therefore necessary to examine the nature of the changes for a variety of conditions and select critical times for further investigation. The time effects on the material properties of the overlay and the influence of the environment are discussed, particularly as they affect the inputs to the analysis program. The values which are used in subsequent analyses are described in Chapter 4.

#### 3.2.1 Material Properties

Four material properties of the concrete are of particular interest relative to the development of interfacial stresses at early ages in overlays. These are (1) concrete modulus, (2) coefficient of thermal expansion and contraction, (3) rate of and amount of ultimate shrinkage, and (4) temperature associated with the time at which the concrete begins to take stress, hereinafter referred to as the curing temperature. A fifth parameter, the rate of development of interfacial tensile and shear strength, is extremely important to the success of bonded overlays. Although this last factor cannot be defined properly as a material property, it nonetheless is

influenced by the material properties and therefore is included in the discussion that follows.

#### Modulus

The modulus of concrete is important in determining the stress regime at the interface between the overlay and the existing slab. The derivations of Timoshenko (54) and Grimado (55) show that differences in moduli between the layers have a significant influence on the thermally induced stresses. The modulus increases as the concrete hardens from a semi-fluid to a fully hardened state. Concurrently, the ratio of the overlay modulus to the base slab modulus undergoes considerable change. Factors influencing the ultimate modulus at later times and test methods used to determine the modulus are described before discussing the early-age modulus.

The factors influencing the modulus of concrete include essentially all the factors affecting strength: (1) water-cement (w/c) ratio, (2) aggregate type and gradation, (3) age at the time of testing, (4) curing conditions, (5) moisture content at the time of testing, (6) specimen size and shape, (7) rate of loading, (8) test method, (9) test apparatus, (10) operator, (11) specimen handling, (12) admixtures, and (13) temperature at the time of testing. It is beyond the scope of this investigation to thoroughly examine each of these factors in detail. However, it is known that for concrete mixes used in pavements and under standardized test conditions, the effect of many of these factors on bonded overlays will be minimal. When standardized test procedures are used the effect of specimen size and shape, rate of loading, test method, test apparatus, operator, and curing condition are minimized. Therefore, only aggregate type, water-cement ratio, and age are discussed further here.

The modulus of concrete is substantially affected by the type of aggregate used in the mixture. Aggregates typically constitute about 70 percent of the volume of the mix and may have widely varied physical properties, as shown in Table 3.1. The influence of aggregate on modulus of concrete can be seen in Figure 3.8 (72). It can be reasoned from Figure 3.8 and Table 3.1 that, the higher the modulus

**Table 3.1 Modulus of elasticity for cores taken from various rock types (73)**

Type of Rock	Modulus of Elasticity (psi)
Trap	13,300,000
Granite	8,660,000
Sandstone	7,400,000
Limestone	4,000,000

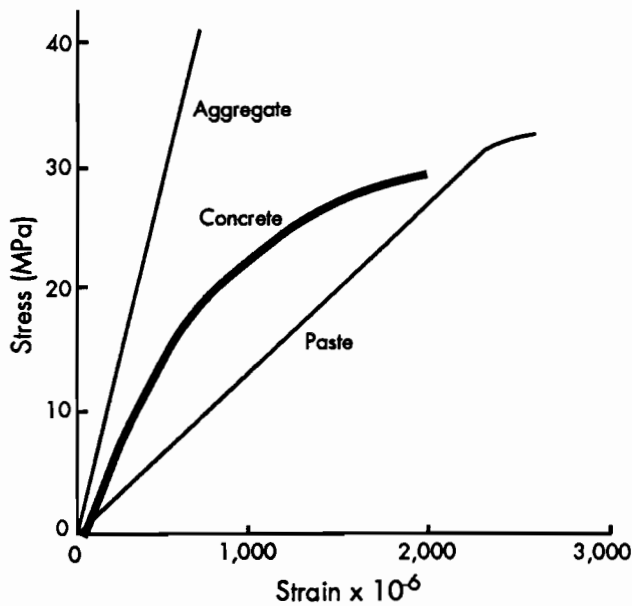


**Figure 3.8** Stress-strain relationships from cement paste, aggregate, and concrete (72)

of the aggregate, the higher the modulus of the concrete made using that aggregate.

An increase in modulus can also be expected from a decrease in the water-cement ratio. It is well known that, as the water-cement ratio decreases, the strength of the concrete mix increases. Several researchers have correlated concrete strength to modulus and, although a variety of regression equations exist, all relate an increase in strength with an increase in modulus. Noble (74) demonstrated the relationship between water-cement ratio and modulus for several different aggregate types (see Figure 3.9). It should be noted that the work by Noble also indicates that increasing the aggregate modulus results in an increased concrete modulus.

Modulus testing may be conducted using a variety of methods, but most standardized test methods require that the test specimens be held under specified curing conditions for a period of from 3 to 28 days. The rate of modulus gain with time is assumed normally to follow the form of the hyperbolic function shown in Figure 3.10. Modulus tests have been conducted on normal concrete mixtures after only one day of curing; however, these test results appear to be affected adversely by early handling and normally exhibit higher coefficients of variation than tests conducted after longer curing times (75). Therefore, if one is to obtain modulus data at times of less than 7 days, it is necessary to rely on the extrapolation of 7-, 14-, and 28-day measurements, as shown by the dashed line in Figure 3.10. It is common practice to extrapolate to longer ages since most of the change in modulus has already occurred.

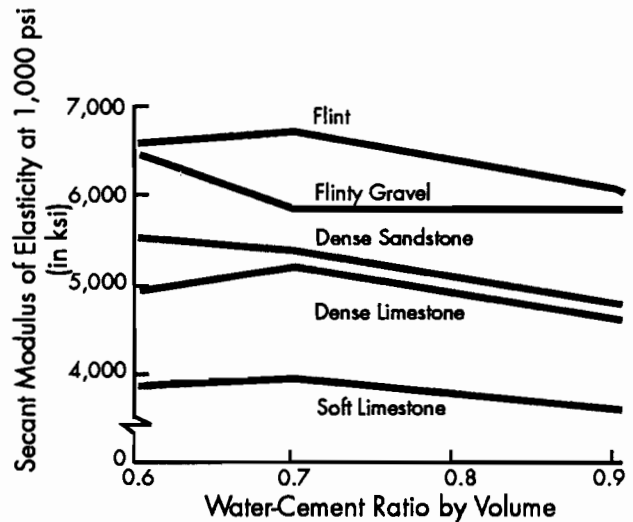


**Figure 3.9** Effect of water-cement ratio and type of aggregate upon modulus of elasticity. Mixes contained six sacks of cement per cubic yard. Age at test was 56 days (74)

Furthermore, data are available for concrete several years after placement. These data show the hyperbolic function is reasonably accurate at ages greater than 28 days.

The rates of modulus gain reported by several researchers (72, 73, 76) are averaged in Table 3.2. The average of these researchers places the one-day modulus at about 30 percent of the 28-day value. For a concrete with a 28-day modulus of 5,000,000 psi, the one-day modulus would be 1,500,000 psi. Similar percentages are found for the rate of compressive strength gain (72, 73, 76).

Another method of determining modulus at very early ages has been developed recently. This technique, adapted from geologic formation testing,

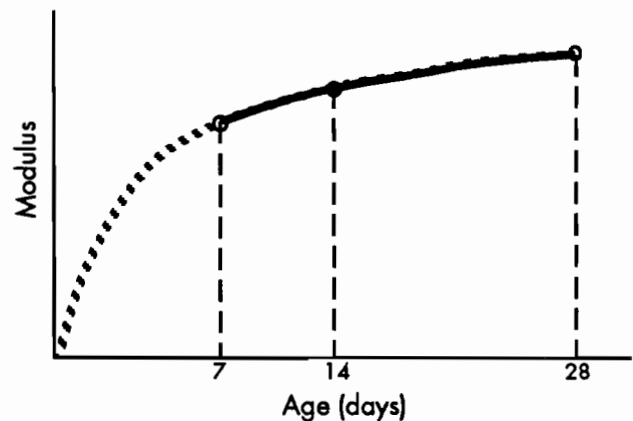


**Figure 3.10** Schematic of the relationship between concrete age and modulus

**Table. 3.2 Rate of modulus gain with time (72, 73, 76)**

Time (days)	Percent of 28-day Modulus
0.5	15
1	30
2	45
3	55
7	80
14	87
28	100

utilizes the capacity of continuous media to transmit seismic waves at velocities which can be related to the modulus of the material. This non-destructive method, termed spectral analysis of surface waves (SASW), analyzes the transmission times of surface waves over a known distance to back-calculate the shear wave velocity and, in turn, the shear and elastic moduli (77). Additional discussion of the theory and details of the test procedure can be found in Reference 77.

The SASW method allows modulus values to be calculated less than four hours after concrete placement. The rate of increase in modulus with time can be determined by repeated testing of the same location in the slab or on the same cylinder. Typical results from SASW testing are shown in Figure 3.11 (77).

A comparison of compression modulus results and those obtained from SASW shows fair agreement (77). As pointed out by Rix et al, the seismic test moduli were 13 percent higher than the compression

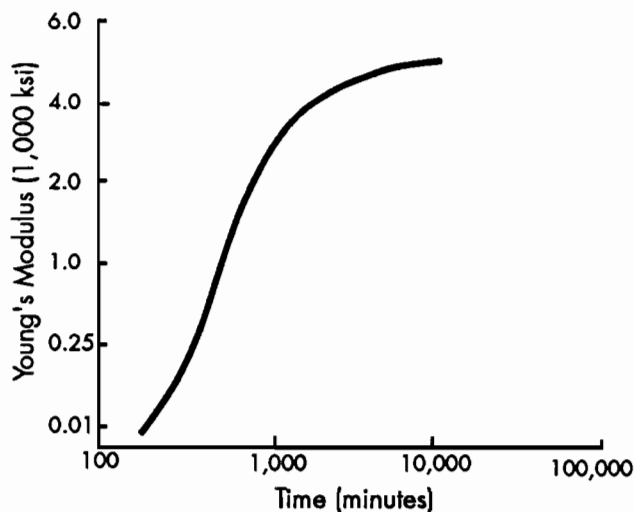


**Figure 3.11 Variation in surface wave velocity of the PCC layer during curing for pavement at El Paso, Texas (77)**

modulus results. The authors speculated that different cure rates for the cylinders and slab may contribute to differences between the methods. They also suggested that the differences may be attributed to the use of the initial tangent modulus in the SASW method (small strains) and the use of the secant modulus in compression testing. Unfortunately at this time only limited data are available from the SASW technique. The available data tend to support the use of the hyperbolic function to extrapolate from later test data to early ages, as suggested from compression testing. Therefore, modulus values used in this investigation are extrapolated from ASTM C39 compression test data, as shown in Table 3.2. Where appropriate, the influence of aggregate type is included.

#### *Coefficient of Thermal Expansion*

The coefficient of thermal expansion, also, is important to the successful determination of stresses in the bonded overlay system. Many of the same factors affecting modulus influence the coefficient of thermal expansion. However, research at The University of Texas at Austin (75) has shown that the age of the concrete is not an important factor. The type of aggregate used in the mixture does have a significant effect on the thermal coefficient. As explained by Troxell et al, the linear coefficient of thermal expansion for neat cement paste varies from 6 to 12 millionths per degree Fahrenheit (73). The normal range for air-cured concrete is 4 to 6 millionths, depending on the aggregate type. The reduction in the coefficient results from the restraining effect of the aggregate; as the paste tends to contract the aggregate is put into compression. This results in less total movement. Typical values are shown in Table 3.3 (72). Although values of the coefficient for limestones are commonly reported to be  $4(10^{-6})$  in./in./°F, Troxell noted that some limestones may have coefficients approaching 7 millionths, depending on the hardness of the limestone (73). Coefficient values are given for air-dried, water-cured, and mixed cured concrete to emphasize the influence of moist curing on the coefficient of thermal expansion.

Table 3.3 shows that for all aggregate types, the coefficient of linear expansion decreases with increasing exposure to moisture during curing. The influence of the moisture condition applies mainly to the paste because the total movement is made up of two components – kinetic movement and swelling pressure. Powers and Brownyard (79) reason that, as the temperature increases, the surface tension of the pore water decreases and swelling takes place. Obviously, the swelling pressure will not occur if the concrete is saturated or dry. Therefore for the paste shown in Figure 3.12, the “kinetic” coefficient of thermal expansion is about 6 millionths but the

**Table 3.3 Coefficient of thermal expansion of 1:6 concretes made with different aggregates (72)**

Type of Aggregate	Air-Cured Concrete 10 <sup>-6</sup> per °F	Water-Cured Concrete 10 <sup>-6</sup> per °F	Air-Cured and Wetted Concrete 10 <sup>-6</sup> per °F
Gravel	7.3	6.8	6.5
Granite	5.3	4.8	4.3
Quartzite	7.1	6.8	6.5
Dolerite	5.3	4.7	4.4
Sandstone	6.5	5.6	4.8
Limestone	4.1	3.4	3.3
Portland Stone	4.1	3.4	3.6
Blast Furnace Slag	5.9	5.1	4.9
Foamed Slag	6.7	5.1	4.7

measured coefficient at normal humidity would be almost 12 millionths. Figure 3.12 also shows that, as the paste ages, both the relative humidity at which the maximum thermal coefficient occurs and the maximum thermal coefficient are reduced. These decreases are due to the increase in crystalline structure of the older paste as additional hydration occurs (80).

The factors discussed above help explain the variability of coefficients for the different moisture conditions. However at early ages, if adequate curing has been provided, the relative humidity of the concrete will be near 100 percent. Therefore, the influence of moisture content on the thermal coefficient may be neglected.

Other factors also affect the thermal coefficient of the paste. However, Neville states that the chemical composition, fineness of the cement, and air void content do not affect the thermal coefficient (72).

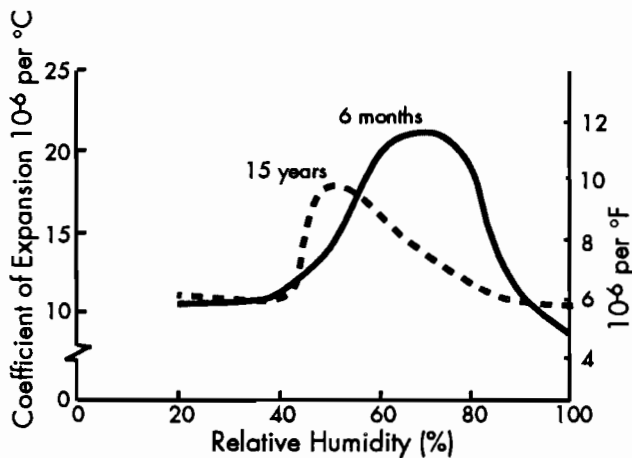


**Figure 3.12 The linear coefficient of thermal expansion of neat cement paste at different ages (80)**

The thermal coefficient is important because it is used to estimate the movement associated with a given change in temperature. The thermal strain,  $\epsilon$ , is defined by

$$\epsilon = \alpha \Delta T$$

where

$\alpha$  = the thermal coefficient, and

$\Delta T$  = the change in temperature from some reference condition.

The determination of the strain implies not only that the thermal coefficient and the temperature at the time in question are known, but that some reference temperature is known. This reference temperature is commonly referenced to a set or curing temperature. The curing temperature is essential to the calculation of the thermally-induced stresses. This curing temperature forms the reference point from which the temperature differential,  $\Delta T$ , is calculated.

#### Curing Temperature

The curing temperature has different meanings to different people. Structural engineers commonly define the curing temperature as the temperature at which concrete test specimens are held for the first 28 days following casting. While this temperature does not necessarily represent the temperature at which the structural concrete itself is held, in many cases the deviations are relatively small. Pavement engineers are confronted with a more difficult problem because concrete pavements are subjected to constantly changing conditions during the first few days. Intuitively, the curing temperature should be that temperature at which the concrete starts to act in an elastic way, or, in other words, when it is able to resist loads induced by shrinkage or changing temperatures. The curing temperature is often selected as the fresh concrete temperature at placement.

However, the temperature of the fresh concrete increases as the hydration of the cement proceeds and sometime during the first 24 hours following placement the concrete can be said to be cured. Therefore, the curing temperature is above the placement temperature in most cases. Several methods have been developed to determine the time at which the cure, or set, occurs.

Most test methods developed to monitor the progression of the hardening of concrete are used to assure that adequate time is available for placement and finishing. The curing temperature must be measured separately. Measurements of electrical resistance, consistency, wave velocity, bleeding characteristics, heat of hydration, volume change, and resistance to penetration have all been used to estimate the time to set. The technique used most commonly is ASTM C403 (81). This method uses the resistance to a series of plungers with different surface areas to determine the time of set. Two resistance levels, 500 psi and 4,000 psi, were chosen to represent initial and final set, respectively. The test is conducted on mortar sieved from the concrete mix. For normal concrete mixtures, initial set occurs between 2 and 4 hours after the addition of water while final set is from 5 to 8 hours after. Obviously, there is considerable variability in the temperature of the concrete during this time period due to hydration of the cement alone. Environmental conditions also play an important role in the temperature gain of the curing concrete. For example, on a 4-inch bonded concrete overlay placed in Houston, Texas during the summer, the concrete temperature increased from 85 to 106°F in the first 4 hours following placement. The same mix design placed in the winter varied from 60 to 66°F in the first 4 hours.

The time of placement also influences the temperature of the concrete. The effect of time of placement can be seen in Figures 3.13 and 3.14, which show the concrete and air temperatures in a 4-inch overlay placed in the morning and afternoon of May 5, 1990. Several features are noteworthy in these graphs. First, the maximum temperature rise in the overlay concrete was about 10 degrees higher for the morning placement than for the afternoon placement. If the curing temperature is assumed to be equal to this temperature, then, for a given temperature drop, the overlay placed in the morning will develop higher stresses. Second, the top of the overlay placed in the morning peaked at a temperature 5 degrees higher than that of the bottom of the overlay, while the temperature of the overlay placed in the afternoon remained constant with depth. This temperature gradient will further increase the stresses caused by temperatures of the type found in the pavements in the morning (i.e., lower surface temperatures). Finally, the temperatures in the over-

lay began to cycle with the air temperature approximately 24 hours after the overlay is placed. Some time within the first 24 hours, the concrete begins to take stress and therefore the curing temperature must be found within the first 24 hours. The question arises as to whether the initial or the final set is representative of the time, and hence temperature, at which the concrete begins to resist thermal and shrinkage movements.

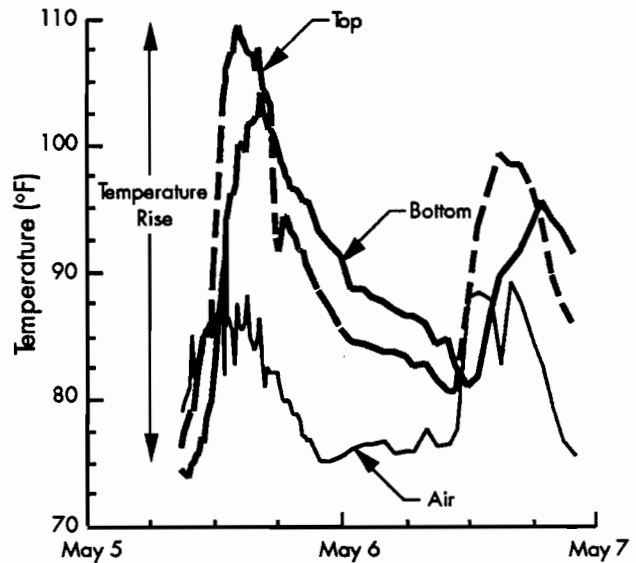


**Figure 3.13** Air and concrete temperatures in a 4-inch bonded overlay placed in the morning

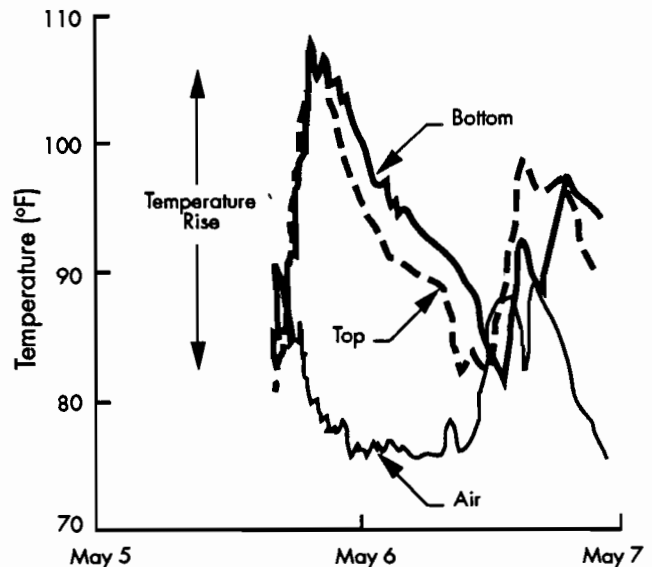


**Figure 3.14** Air and concrete temperatures in a 4-inch bonded overlay placed in the afternoon

Mindess and Young (76) define initial set as the indication that the paste is beginning to stiffen and final set as an indication that the cement has hardened to the point at which it can sustain load. Using these definitions, it would appear that the temperature corresponding to final set would be most indicative of the temperature from which thermal stresses should be determined. Again, referring to Figures 3.13 and 3.14 and assuming final set occurs from 5 to 8 hours after the addition of water, morning placements result in higher curing temperatures and therefore higher thermal movements for a given temperature drop.

Another approach has been suggested which would utilize the SASW technique described earlier in regard to modulus testing. Rix, Bay, and Stokoe (77) have attempted to correlate penetration-resistance values to early modulus values obtained from the SASW technique described above. As shown in Figure 3.15, the initial set occurs when the modulus is approximately 50,000 psi, while the final set occurs at a modulus of 4,000,000 psi. However, it must be remembered that the SASW induces very small strains and therefore overestimates the secant modulus normally used in analysis. The temperatures associated with the increase in modulus and penetration resistance were measured on a single slab (82). Strain measurements were also collected on the specimen, using embeddable strain measurements

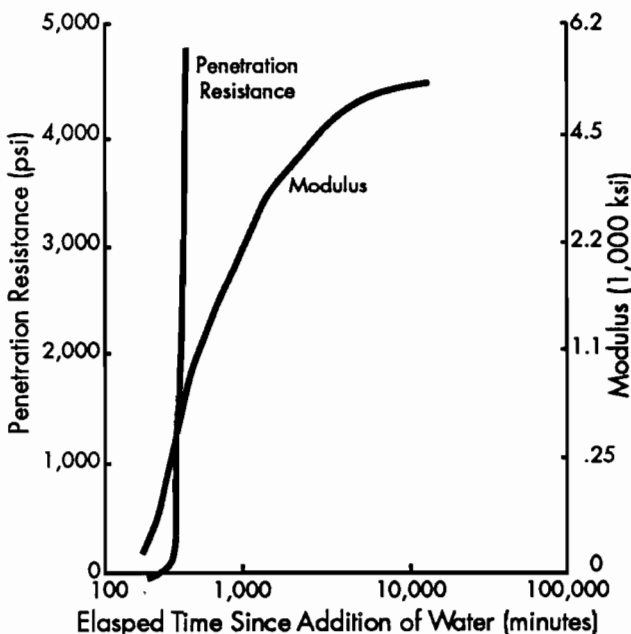


**Figure 3.15 Comparison of Young's modulus and penetration resistance measured during curing of the concrete slab at Balcones Research Center, Austin, Texas (77)**

devices. These results are case specific but indicate that the measurement of temperature, strain, and penetration resistance can be correlated to a modulus measured by the SASW technique. While it may be ultimately possible to correlate the onset of strain and stress to a temperature, current experience and the state-of-the-art do not allow more elaborate or exacting measurements than those provided by ASTM C403 (81).

### Shrinkage

Other material properties that affect the performance of bonded overlays at early ages are the ultimate shrinkage and the rate at which shrinkage occurs. Mindess and Young (76) define shrinkage as the volume changes that accompany a loss of moisture from either fresh or hardened concrete. Four categories of shrinkage are commonly identified: (1) drying, (2) plastic, (3) carbonation, and (4) autogeneous. Autogeneous shrinkage results from the self-desiccation of the concrete and is rare except in mass concrete placements (76). Carbonation shrinkage develops as the hardened cement paste reacts with atmospheric carbon dioxide. This phenomenon occurs very slowly under normal conditions and will not be considered further. Only drying and plastic shrinkage are considered here.

The main cause of drying shrinkage is the volume change in concrete due to moisture changes in the hardened paste. Plastic shrinkage, on the other hand, results from moisture losses in fresh concrete and, because of the early-age formation of debonding, is of particular concern in this analysis.

### Plastic Shrinkage

Plastic shrinkage is defined by Lerch (78) as volume change that occurs in the surface of fresh concrete within the first few hours after placement. This shrinkage is not objectionable in itself, provided the concrete is still plastic enough to accommodate the volume change without cracking. However, when the strains developed exceed the tensile capacity of the fresh concrete, then cracks develop at the surface. Although these cracks may extend to depths of 4 inches, most are shallow (less than 1 inch) and have little or no discernable pattern. Mindess and Young (76) report that cracks may develop from the lower surface of the fresh concrete if sufficient moisture is lost to formwork or subgrade materials. Shallow surface cracks are objectionable in normal concrete pavements because they allow the infiltration of water which can lead to surface deterioration and corrosion of the reinforcing steel. In addition to these concerns, bonded overlays are normally 2 to 4 inches thick, and, therefore, a 1-inch-deep crack may constitute 25 to 50 percent of the total thickness. This weakened zone may allow the propagation of the crack through the overlay to the existing slab.

This crack then becomes effectively another edge and a potential site of delamination. Thus, the prevention of plastic shrinkage cracking is important.

Laboratory and field studies have been conducted by many researchers to determine the cause of plastic shrinkage cracking (78, 83, 84, 85). Researchers disagree as to the mechanism of the volume change, but most agree that rapid evaporation of water from the surface is the chief cause of plastic shrinkage. One hypothesis is that the removal of water from the hardening paste causes negative capillary pressures which force the paste to contract. If the paste is still plastic, this strain can be accommodated without cracking; however if the paste has some degree of rigidity, but little strength, cracking will result.

The Portland Cement Association (PCA) reports that the nomograph shown in Figure 3.16 may be used to estimate the rate of evaporation from fresh concrete. An allowable upper limit of 0.2 lb/ft<sup>2</sup>/hr is recommended by the PCA to minimize plastic shrinkage cracking (86). Most modern construction of

pavement relies on liquid membrane-forming curing compounds to reduce the loss of moisture from the surface. Many pavements placed today receive one or two coatings of compound at a combined application rate of between 150 and 200 square feet per gallon (107). This coverage rate appears to be adequate to reduce the chance of plastic shrinkage cracking in all but the most severe conditions (107). In these cases, fogging or flooding of the slab is used to limit early age moisture losses. It would appear that, if cracking does not occur, then plastic shrinkage is of little consequence to the performance of the overlay.

Although plastic shrinkage may be severe enough to cause cracking, most investigators believe that drying shrinkage constitutes the largest portion of the early volume change in concrete (72, 73, 76). Neville defines drying shrinkage as the volume change associated with the loss of water from hardened concrete in unsaturated air (72). As shown in Figure 3.17, part of the initial volume change is irreversible and must be distinguished from the reversible portion resulting from alternating wet and dry conditions. The main focus in this investigation is on the causes and effects of the initial drying rather than on the mechanics of the reversible movements.

Several potential causes of and factors related to initial drying shrinkage have been identified. Although shrinkage is the volume change associated with the loss of moisture, it is not the loss of free water, or capillary water, that causes the volume change. Most researchers agree that the loss of the adsorbed water from the cement gel particles causes the change in volume (72). This has been shown by Powers (89) by adding increasing quantities of silica sand to cement pastes. The relationship between the weight of water lost and shrinkage is shown in Figure 3.18. For neat pastes, the shrinkage and loss of moisture are proportional to one another because no capillary water is present and only adsorbed water is removed. However, as the percentage of silica is increased, the water lost before appreciable volume change occurs increases. This moisture is associated with the water in the capillaries. Once the capillary water is lost, shrinkage begins at a rate approximately equal to the rate of neat paste.

In concrete specimens, the aggregate serves to restrain the total amount of shrinkage. The degree of restraint appears to be a function of the modulus and shrinkage characteristics of the aggregate. For example, aggregates with high moduli and characteristically low volume changes with varying moisture conditions generally produce low shrinkage concretes. Quartz aggregates are an example of these aggregates. Conversely, high shrinkage aggregates, such as sandstone, result in high shrinkage concrete. In Figure 3.19, the influence of

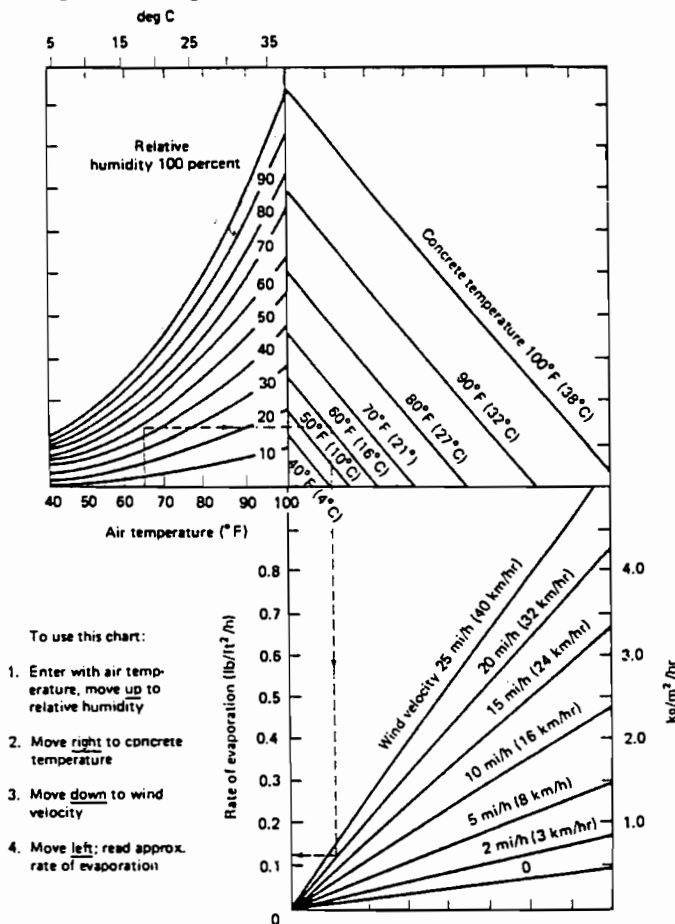


**Figure 3.16** Portland Cement Association nomograph for estimating the rate of moisture loss from fresh concrete due to the combined effects of wind, relative humidity, concrete, and air temperature (after 86)

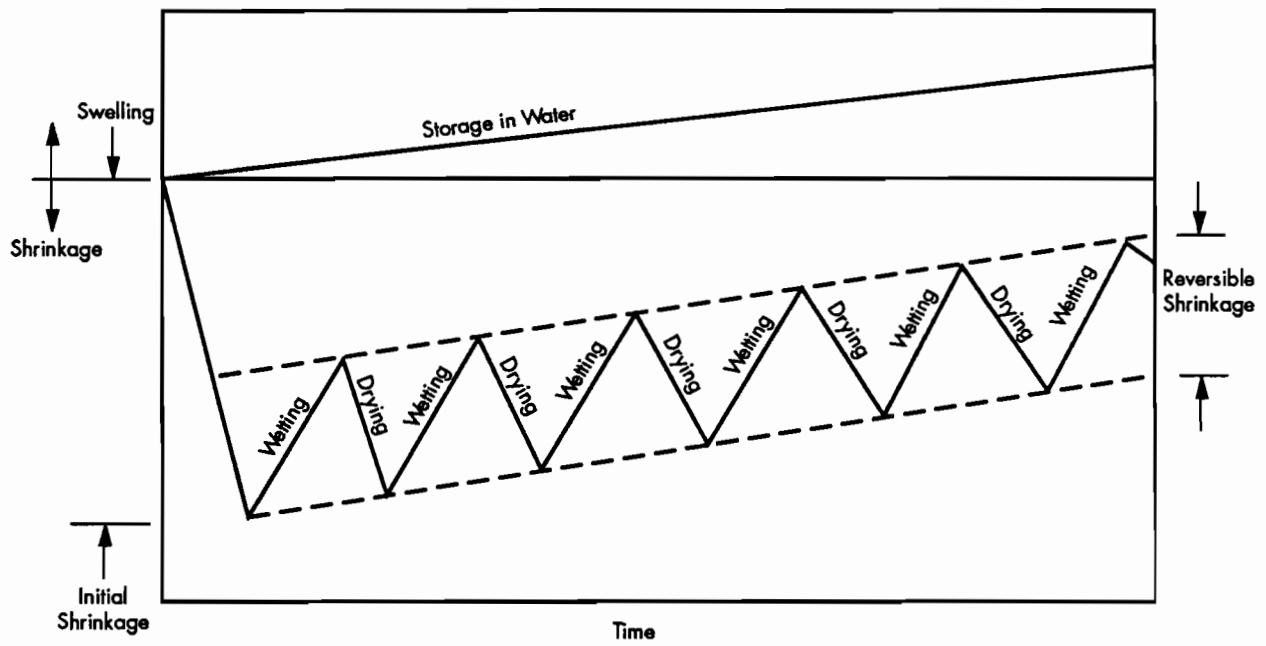


**Figure 3.17** Schematic description of volume changes in cement paste due to alternate cycles of drying and wetting (88)

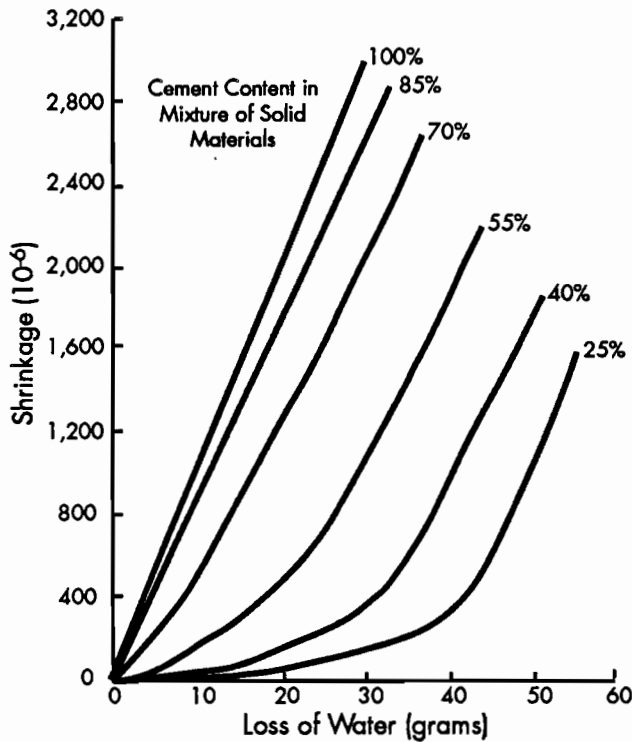


**Figure 3.18** Relationship between shrinkage and loss of water from specimens of cement-pulverized silica cured for 7 days at 21°C (70°F) and then dried (89)

aggregate on the shrinkage is clearly shown. Data from concrete made with single-sized aggregates of various types are shown in Table 3.4. Here, sandstone had the highest shrinkage while the glass spheres had the lowest shrinkage.

The same trends are evident when normal gradations of aggregate are used, as shown in Figure

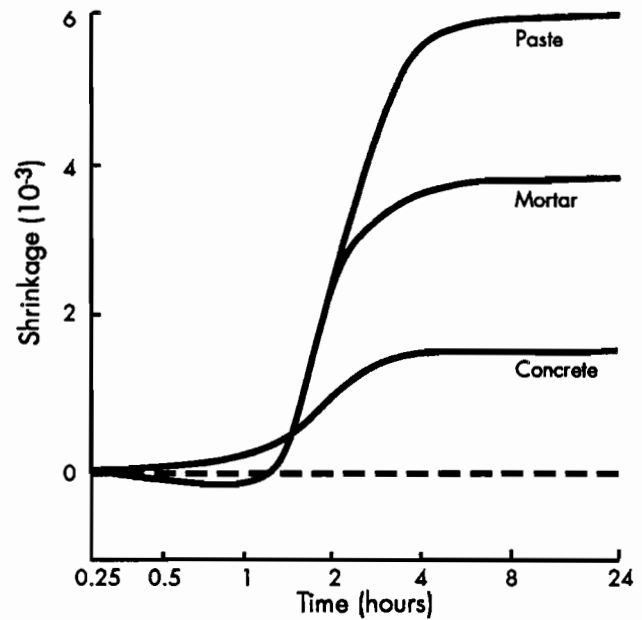


**Figure 3.19** Effect of aggregate on plastic shrinkage (after 90)

**Table 3.4 Effect of type of aggregate of a single size on the shrinkage of concrete (after 91)**

Aggregate	% Absorption	1-Year Shrinkage in Air at 50% Relative Humidity ( $10^{-6}$ )
A. Mixed Gravel	1.0	560
B. Slate, from A	1.3	680
C. Granite, from A	0.8	470
D. Quartz, from A	0.3	320
E. Sandstone	5.0	1,160
F. Solid Glass Spheres	0	250
G. Limestone	0.2	410

3.20. These data clearly show limestone and quartz to have the lowest shrinkage of the aggregates tested; however, as noted previously, limestone has a high variability in modulus, depending on the source of the material. These results should therefore be considered only as an indicator of trends.

In addition to aggregate type, other properties of the mix and its components have varying degrees of influence on the ultimate shrinkage. Neville states that entrained air and properties of the cement have little effect on the volume change characteristics of the concrete (72). Clay coatings on the aggregates, however, have been shown to increase shrinkage by as much as 70 percent (89). Normal concrete aggregate quality control testing will limit the problem of clay coating. Most other factors have only a minor effect on the ultimate shrinkage, provided construction controls are followed and normal pavement mixes are used. While the ultimate shrinkage is of

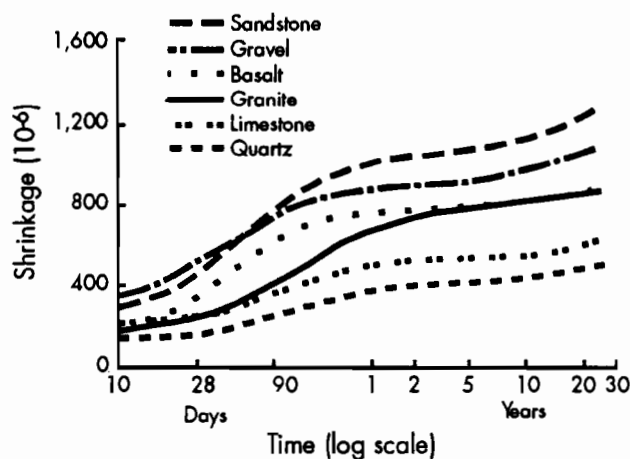


**Figure 3.20 Shrinkage of concretes of fixed mix proportion but made with different aggregates and stored in air at 21°C (70°F) and a relative humidity of 50 percent (78)**

concern when the long-term performance of bonded overlays is considered, the rate at which shrinkage occurs is also of concern in this investigation.

Troxell et al (78) have shown that although shrinkage may occur even after 28 years, the rate of shrinkage decreases rapidly with time. Figure 3.21 shows that about 20 percent of the 20-year shrinkage occurs in the first 14 days and 60 percent occurs during the first 90 days. While prolonged moist curing will delay the advent of shrinkage, the effect of moist curing on the magnitude of the ultimate shrinkage is small (72). The decreasing rate of shrinkage with time is corroborated by data collected from field and laboratory cured samples made from Texas aggregates (83). In this study high-strength

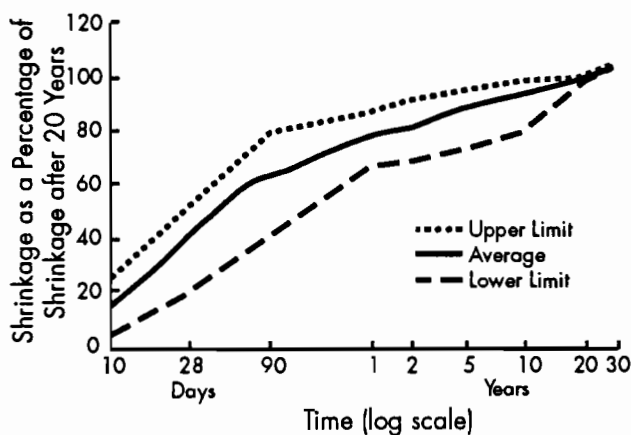


**Figure 3.21 Range of shrinkage-time curves for different concretes stored at relative humidities of 50 and 70 percent (78)**

concrete using crushed limestone and siliceous river gravel were used to cast test specimens. Details of the experiment can be found in Reference 83. Shrinkage data were collected for about 500 days, and hyperbolic regression equations were developed for each series of tests, as shown in Table 3.5.

The work of Ingram and Furr (83) in this area shown in Table 3.5, corroborates the work of other researchers. Most of the measured shrinkage occurred in the first few weeks. The values in the denominators of the regression equations shown in Table 3.5 indicate that the time, in days, for one-half the shrinkage to occur is between 10 and 25 days. The average for all the mixes tested was about 3 weeks. The mixtures used by Ingram and Furr had different cement factors, but research by the U. S. Bureau of Reclamation has indicated that cement content has only a minor influence on shrinkage (84). However, these data have been disputed by the work of Haller (85), as shown in Figure 3.22. Haller shows an effect of water-cement ratio, but the

**Table 3.5 Total shrinkage at 500 days and estimated shrinkage-time functions for field cured specimens (after 83)**

Aggregates		Shrinkage ( $10^{-6}$ in./in.)	Function
Size	Type		
Fine	Limestone and Siliceous Sand	300	\F(315T, 20+T)
Coarse	Crushed Limestone		
Fine	Limestone and Siliceous Sand	510	\F(525T, 10+T)
Coarse	Siliceous and Limestone Gravel		
Fine	70% Limestone Sand/30% Siliceous Sand	360	\F(380T, 25+T)
Coarse	Limestone Gravel		
Fine	Siliceous Sand	280	\F(290T, 25+T)
Coarse	Crushed Limestone		

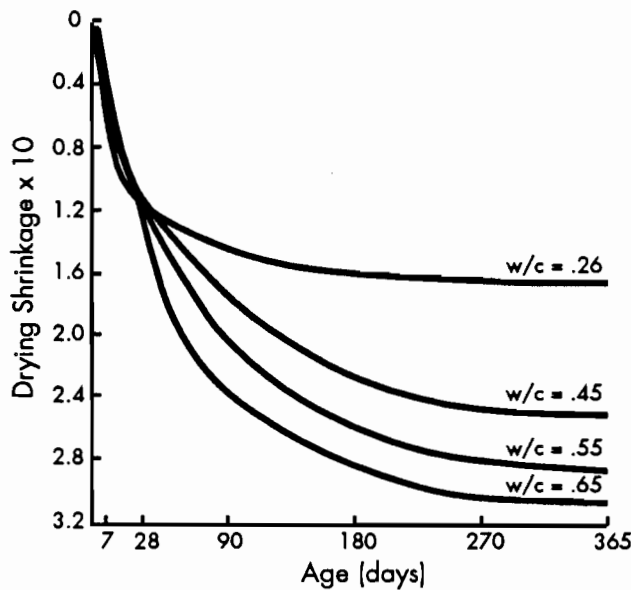


**Figure 3.22 Effect of water-cement ratio on the rate of and ultimate shrinkage of cement pastes (85)**

effect does not appear until after 28 days. It can therefore be said that for purposes of this study the water-cement ratio will not affect the shrinkage.

Additional information on the rate of shrinkage development in concrete is available from work by Jones and Hirsch (92). In their study, several concrete mixtures containing limestone or siliceous gravels were tested at early ages. Shrinkage measurements were included in the testing program. Shrinkage data from several mixtures are shown in Figures 3.23 and 3.24 for gravel and limestone aggregate concretes, respectively. Regression analysis, using the hyperbolic relationship shown previously, yields these two equations:

$$\text{Gravel: } \epsilon_s = 240T / (12+T) \quad (11)$$

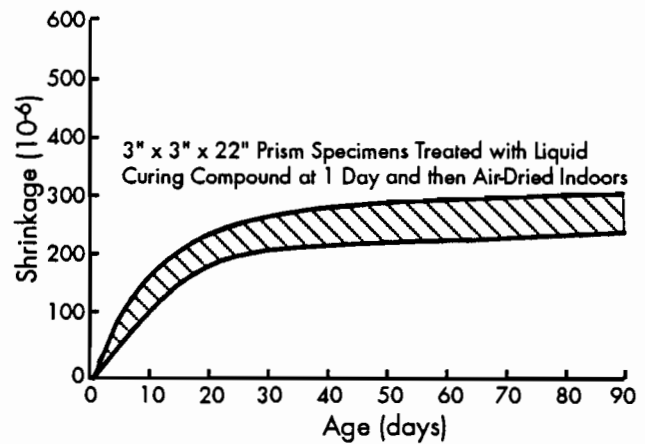


**Figure 3.23 Shrinkage of siliceous-calcerous sand and gravel concrete (92)**

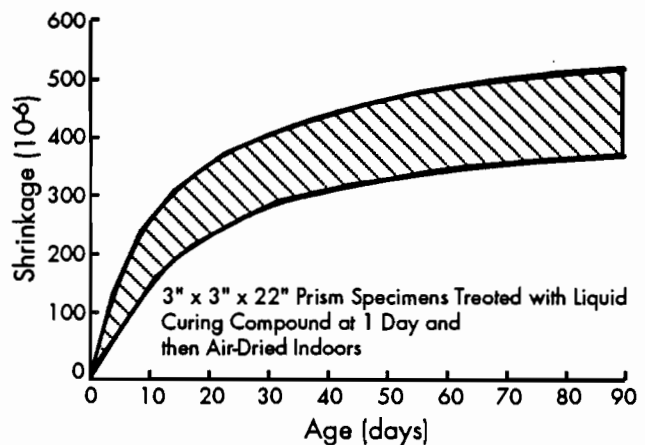


**Figure 3.24 Shrinkage of crushed limestone aggregate concrete (92)**

$$\text{Limestone: } \epsilon_s = 440T / (14+T) \quad (12)$$

where

$\epsilon_s$  = shrinkage strain, ( $10^{-6}$  in./in.), and  
 T = time since placement, days.

The equations developed above show shrinkage developed more quickly (50 percent of the ultimate shrinkage in 2 weeks) than it did in the concretes used by Ingram and Furr. The ultimate values were approximately equal. For the first seven days following placement, the estimated shrinkages for limestone and gravel concretes are shown in Table 3.6.

The data from Jones and Hirsch agree favorably with field data collected from bonded overlay con-

structed with limestone aggregate. Strains were collected with embeddable strain devices at the Loop IH 610 South site described in Chapter 2. Details of the data collection may be found elsewhere (94). The results from two sites for the first 60 days following placement, after thermal movements were accounted for, are shown in Figure 3.25. It should be noted that the shrinkage values for the limestone aggregate concrete after 60 days agree with the values obtained by Jones and Hirsch and are in reasonable agreement with those obtained by other researchers.

The average shrinkage strains for all strain gauges are shown in Figure 3.26 for the first 7 days after placement. These results indicate a slower rate of shrinkage than that estimated by Hirsch and Jones. This slower rate of shrinkage is corroborated by researchers at The University of Texas at Austin (75). Shrinkage data were collected for concretes made using limestone and siliceous river gravel aggregates. Regression equations were developed which allow the shrinkage to be estimated as a function of time. This equation was used to prepare Table 3.7. These shrinkage strains agree with the results from the strain gauges placed in the bonded overlay in Houston.

All discussion thus far has assumed that the moisture losses and the associated shrinkage strains are uniformly distributed with depth through the pavement. Intuitively, it seems that the region closest to the surface will lose moisture more rapidly than the underlying areas. This implies that a

**Table 3.6 Shrinkage estimated for the first week after placement using regression analyses of data from Jones and Hirsch (92) for limestone and gravel concrete**

Time (days)	Shrinkage ( $10^{-6}$ in./in.)	
	Limestone	Gravel
0.5	15	10
1	29	18
2	55	34
3	78	48
4	98	60
5	116	71
6	132	80
7	147	88

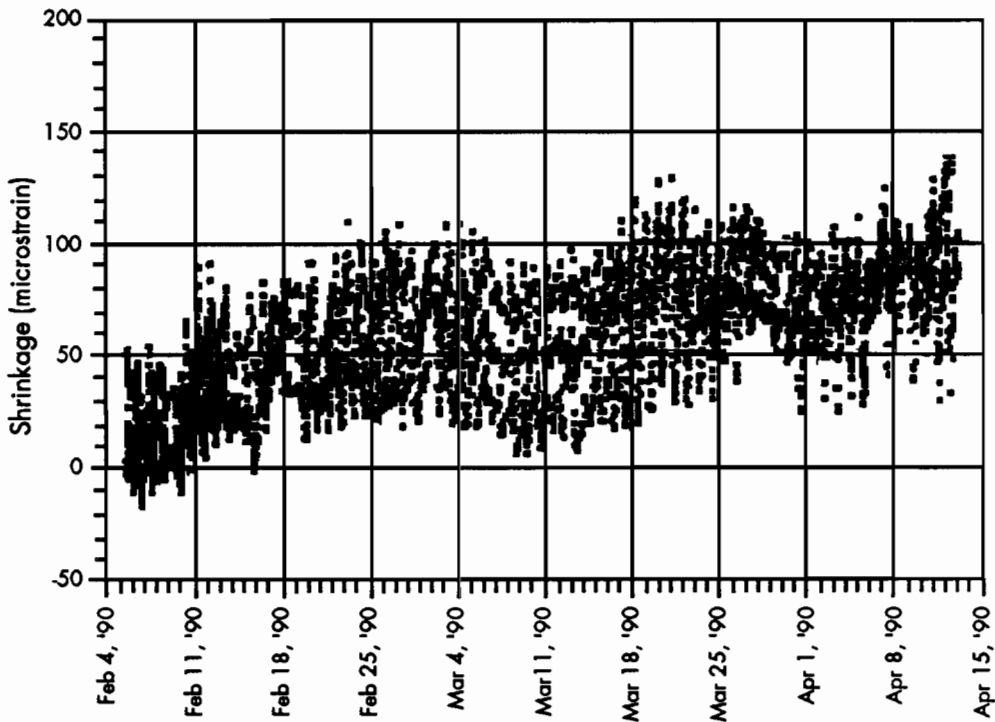


**Figure 3.25 Shrinkage strains from bonded overlay placed in Houston, Texas**

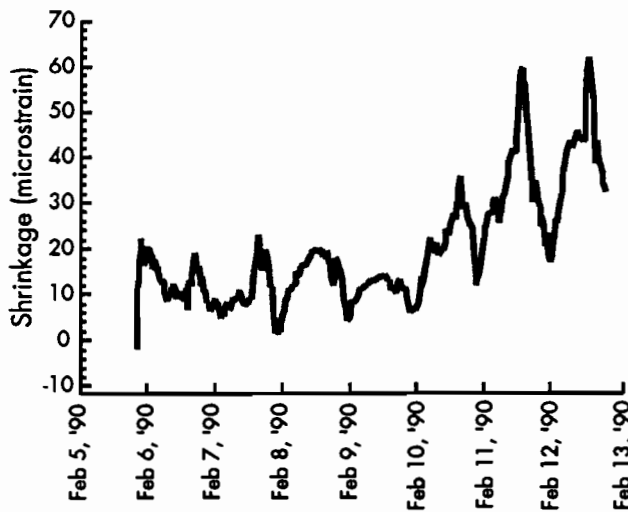


**Figure 3.26** Average shrinkage during the first 7 days following a winter placement of a 4-inch bonded overlay in Houston, Texas

**Table 3.7** Estimated shrinkage strains at early ages in concrete prepared from limestone and siliceous aggregates (75)

Time (days)	Limestone Aggregate	Siliceous Aggregate
0.5	5	6
1	11	13
2	21	25
28	197	189

moisture gradient exists in the pavement. The existence of this gradient was confirmed by the work of L'Hermite (90). L'Hermite charted the progression of shrinkage with time and distance from the surface, as shown in Figure 3.27. For the time period under consideration here, i.e., less than one week, only about the top 1 inch shrinks, while the remainder of the specimen expands slightly.

### 3.2.2 Environmental Conditions

Beyond the effect of the environment on the rate of change of each of the material properties discussed above, the environment determines the temperature of the pavement which, in turn, determines the thermal stress in the pavement. The purpose of this section is to describe the diurnal and seasonal temperature variations that might be expected and model the temperature distribution within the overlay and existing-slab system. Because corroborating data are available from bonded overlays in Texas, special attention is given to the

environmental conditions in Texas. It is believed that, except for very special conditions, the conditions in Texas are representative of the most adverse conditions that might be expected during or subsequent to any overlay placement. Before proceeding to describe the environmental variation that might be expected, it must be shown how these conditions affect the problem under consideration.

Environmental conditions affect the bonded overlay stress in several ways. The season of placement determines curing temperature, rate of strength and modulus gain, and maximum and minimum temperatures the overlay is subjected to in the first few days. The maximum and minimum temperatures to which the overlay or existing pavement is exposed will determine the thermal stresses developed at the interface. These interfacial stresses at early ages are particularly critical because the interfacial bond strengths are lowest at early ages. It is therefore important to know the temperature distribution in the pavement to determine the stress at the interface.

The technique chosen for estimating the temperature distribution assumes adiabatic conditions and is adapted from Fintel and Khan (95). Following the lead of Fintel and Khan, the surface temperature is assumed to follow the sinusoidal variation with time shown schematically in Figure 3.28. The time at which the actual maximum and minimum

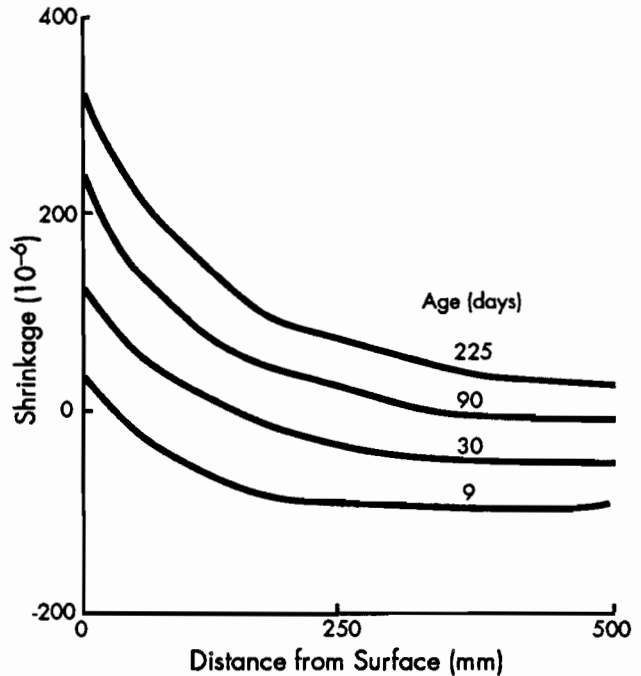


**Figure 3.27** Progress of shrinkage with time as a function of distance from drying surface (no drying possible in other directions), corrected for temperature variations (90)

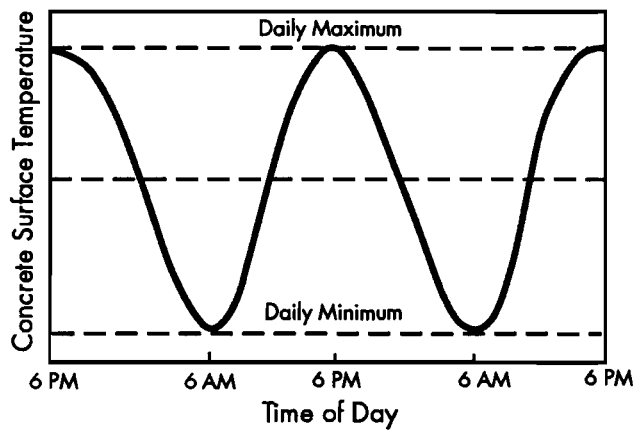


**Figure 3.28 Assumed sinusoidal diurnal temperature fluctuation used to derive the temperature with depth function**

temperatures may vary  $\pm 1$  hour from the times shown in the figure (96). Field data suggest the surface temperature is approximately  $13^{\circ}\text{F}$  warmer than the air temperature under normal conditions (97). Using the procedure from Fintel and Khan the following equation was developed for the temperature at some depth,  $z$ , at some time,  $t$ :

$$T(z, t) = T_{\text{avg}} + T_o e^{-kz} \sin \left[ \frac{2\pi t}{t_o} - kz \right] \quad (13)$$

where

$$\begin{aligned} T(z, t) &= \text{temperature at depth, } z, \text{ and time, } t; \\ T_{\text{avg}} &= \text{average surface temperature, } ^{\circ}\text{F}; \\ &= -1.2 + 1.136T_{\text{air}}; \end{aligned}$$

$$\begin{aligned} T_{\text{air}} &= \text{temperature of the air, } ^{\circ}\text{F}; \\ T_o &= \text{amplitude of surface temperature function, } ^{\circ}\text{F}; \\ k &= \sqrt{\pi / t_o h^2}; \\ t_o &= 2 \text{ (cycle period), hours}; \\ h &= \text{thermal diffusivity, ft}^2/\text{hr}; \\ t &= \text{time, hours}; \text{ and} \\ z &= \text{depth to the point in question.} \end{aligned}$$

An examination of Equation 13 shows that the temperature at any given depth depends on a number of material properties and the minimum and maximum temperatures of the pavement surface.

Weather records for the 30-year period from 1951 to 1980 were reviewed and the minimum and maximum air temperatures for each of three cities in Texas were recorded (98). From these data, the differentials for each month in Houston, El Paso, and Dallas were computed (see Table 3.8). The calculated differentials assume that the maximum and minimum temperatures occur on successive days. While this is possible, it is highly unlikely and therefore these differentials overestimate the true average differential. Therefore, the extreme value of  $30^{\circ}\text{F}$  is used for subsequent analysis.

It should also be noted that these differentials represent the difference in air temperature, not in the pavement surface temperature. However, as noted before, the surface temperature is approximately 13 percent higher than the air temperature, which results in the same differential. The average temperature of the pavement surface,  $T_{\text{avg}}$ , is 13

**Table 3.8 Thirty-year average maximum and minimum temperatures for selected cities in Texas (98)**

		Jan	Feb	Mar	Apr	May	Jun	Jul	Aug	Sep	Oct	Nov	Dec
Houston	Max	62	66	72	79	85	91	94	93	89	82	72	65
	Min	41	43	50	58	65	70	72	72	68	58	49	43
	Diff	21	23	22	21	20	21	22	21	21	24	23	23
El Paso	Max	58	63	70	79	87	96	95	93	88	79	66	58
	Min	30	34	40	48	57	66	70	68	61	49	37	31
	Diff	28	29	30	31	30	30	25	25	27	30	29	27
Dallas	Max	54	59	67	77	84	93	98	97	90	80	66	58
	Min	34	38	45	55	63	71	75	74	68	56	45	37
	Diff	20	21	22	22	21	22	23	23	22	24	21	21

percent higher than the average of the minimum and maximum air temperatures.

Having defined the temperature to which the pavement will be exposed, the material properties of the concrete must be determined. The term,  $k$ , in Equation 13 includes material properties of the concrete which represent the ability of the concrete to dissipate heat. Diffusivity, as defined by Troxell (73), is the facility with which concrete will undergo temperature change upon being heated or cooled. The diffusivity,  $h$ , is a function of the conductivity, specific heat, and density of the concrete. The diffusivity is

$$h = K / (s d)$$

where

- $K$  = thermal conductivity, Btu/ft<sup>2</sup>/hr/°F;
- $s$  = specific heat, Btu/lb/°F; and
- $d$  = density, lb/ft<sup>3</sup>.

Diffusivity varies from 0.02 to 0.08 ft<sup>2</sup>/hr according to Troxell, changing mainly with aggregate type. Values for limestone and siliceous gravels range from 0.03 to 0.07 ft<sup>2</sup>/hr. The effect of changing diffusivity within this range on the pavement temperature is relatively minor, as seen in Table 3.9. Therefore, a diffusivity value of 0.05 ft<sup>2</sup>/hr was chosen for subsequent analysis. It can also be seen from the data in Table 3.9 that no change in temperature occurs below a depth of approximately 4 inches when the distribution is calculated using Equation 13.

**Table 3.9 Effect of diffusivity variation on calculated temperature in 12-inch pavement**

Depth Below Surface (in.)	Winter Morning <sup>1</sup> Diffusivity			Summer Afternoon <sup>1</sup> Diffusivity		
	0.03	0.05	0.07	0.03	0.05	0.07
0	22	22	22	112	112	112
1	36	32	29	98	102	104
2	40	38	35	95	96	99
3	39	40	38	95	94	97
4	39	40	39	95	94	94
5	39	39	40	95	95	94
6	39	39	40	95	95	95
7	39	39	39	95	95	95
8	39	39	39	95	95	95
9	39	39	39	95	95	95
10	39	39	39	95	95	95
11	39	39	39	95	95	95
12	39	39	39	95	95	95

<sup>1</sup>Assumed difference between maximum and minimum temperature equals 30°F

Equation 13 was used to determine the temperature distribution with depth in an 8-inch existing pavement, assuming a diurnal temperature differential of 30 degrees. Figures 3.29 and 3.30 show the distributions for morning and afternoon conditions in the summer and winter seasons, respectively.

Temperature distributions with depth taken from existing concrete pavements show fair agreement

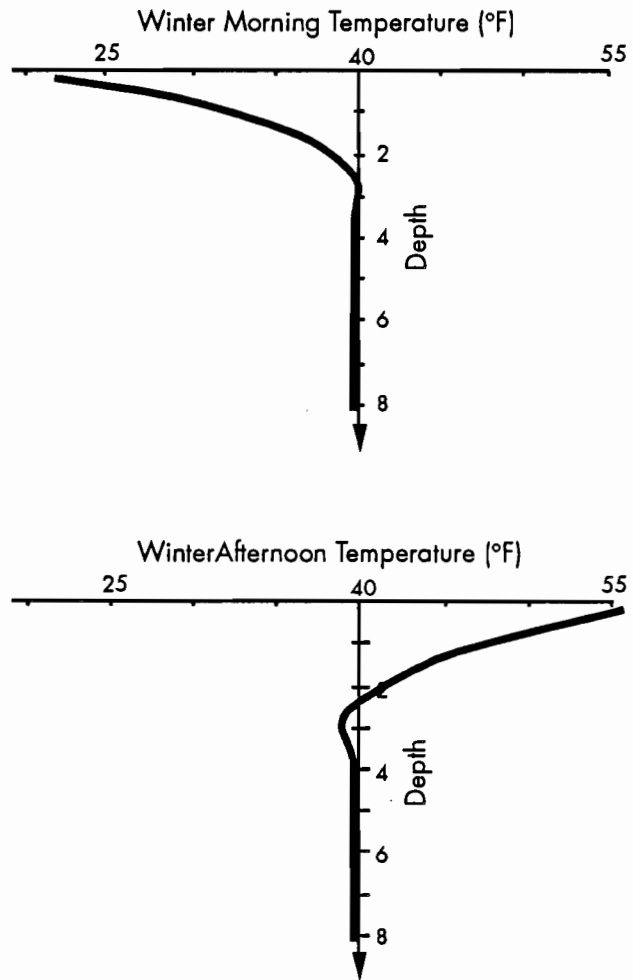


**Figure 3.29 Morning and afternoon winter temperature distribution in an 8-inch concrete pavement calculated using Equation 13**

with the calculated distribution. Figure 3.31 shows the temperature distribution in an 8-inch CRC pavement which was overlaid with 4 inches of limestone aggregate concrete. The original concrete has siliceous river gravel aggregate. The maximum and minimum daily air temperatures remained relatively constant for a period of about five days prior to the collection of these data. The maximum

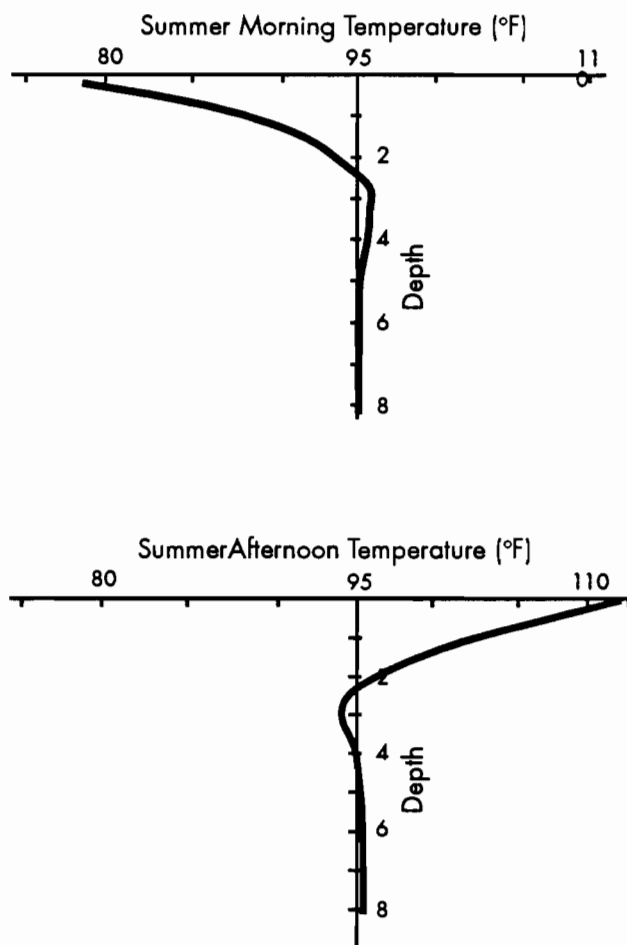


**Figure 3.30** Morning and afternoon summer temperature distribution in an 8-inch concrete pavement calculated using Equation 13

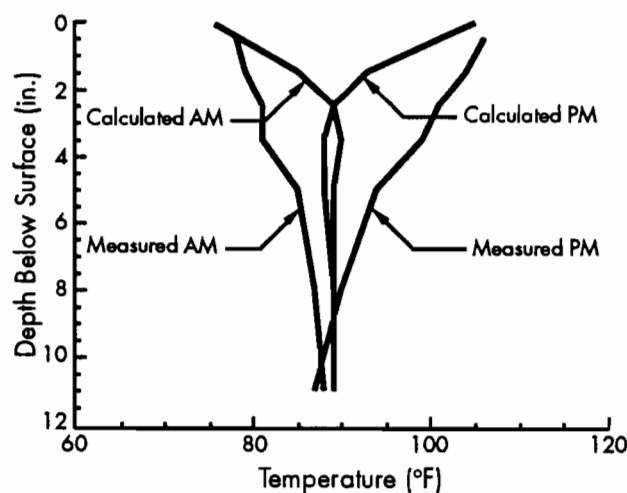


**Figure 3.31** Comparison of actual and measured temperature distributions from a 12-inch pavement in Houston, Texas

and minimum temperatures in the slab were approximated well, using the procedure by Fintel and Khan (95). The actual temperature distribution is less severe than that calculated, that is, there is a smaller temperature change per inch of concrete. Thus, the use of the calculated temperature will overestimate the thermally induced stresses in the critical region near the interface between the overlay and the existing slab.

When an overlay is placed on an existing pavement, the temperature distribution in the existing pavement will change. The nature of this change will depend on the time and season of placement and the temperature of the fresh concrete. Eventually, the resulting composite pavement will again follow a temperature distribution similar to that described by Equation 13. Temperature data from bonded overlays placed in the summer and winter seasons in Houston, Texas, indicate that the composite pavement begins to follow the temperature distribution within 24 to 48 hours after placement.

All the discussion thus far has centered on the parameters that affect the development of stress in the pavement. Obviously, there must be some mechanism that resists this stress. It is now necessary to undertake to determine the nature of the development of interfacial bond strength between the existing slab and the overlay.

### 3.2.3 Interface Bond Strength

Stresses are induced in the overlay-existing slab system as a result of the temperature and material property differences between the layers and restrained shrinkage of the overlay. All of these stress "inducers" must be resisted by the interface bond strength if the overlay is to remain bonded. The bond strength is commonly divided into shear and tensile strength components and various test methods are available to assess this strength. Many of the test methods are conducted on core or cylinder specimens some time after the overlay is placed. Therefore, as was the case for early-age modulus and strength values, early-age bond strength results rely on extrapolation from tests conducted at ages later than those of interest in this study. However, unlike the concrete material properties discussed previously, the interface strength tests assess the strength of bond between two dissimilar materials, that is, the overlay and the existing pavement.

It is well to briefly discuss the development of strength in concrete as measured by more common test procedures before discussing the interface strength. Test results are available from compression and indirect tension tests at ages of less than 12 hours (87). Typical results are shown in Figure 3.32. These results show the characteristic hyperbolic functional form of strength gain similar to that seen for

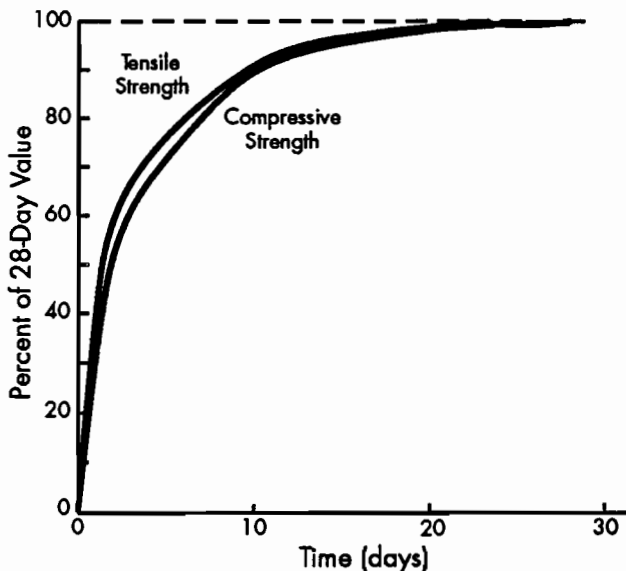


**Figure 3.32** Compression and tension test results at early ages (87)

modulus gain. When expressed as a percentage of the 28-day strength, strength percentages at early ages are similar to those shown in Table 3.2.

Researchers testing the tensile strength of concrete at very early ages found that for ordinary portland cement concrete the development of strength followed the logistic growth form shown in Figure 3.33 (99). Tests were conducted on several different blends of cementitious materials, including high early strength cement, furnace slag cement, and

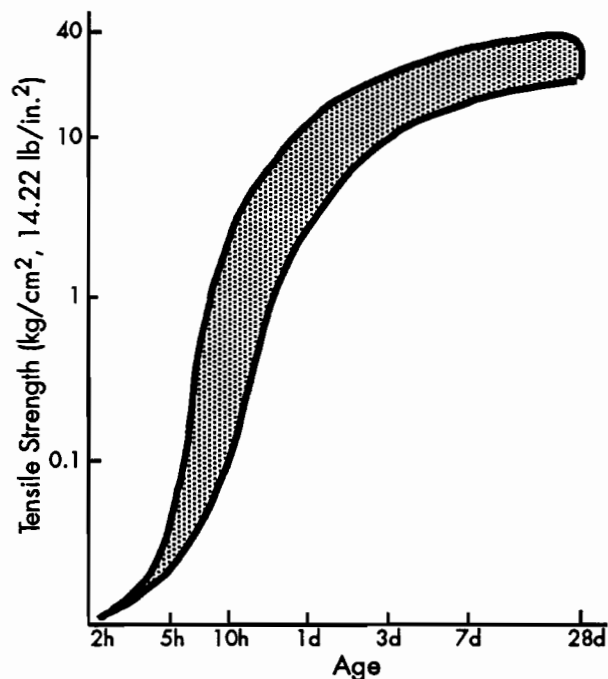


**Figure 3.33** Development of tensile strength at very early ages (99)

fly ash cement, at different water/cement ratios. All tests demonstrated the characteristic slow strength gain initially, followed by a period of rapid gain, eventually slowing to some asymptotic value. These results have not been corroborated by other researchers.

However, this form of strength gain in concrete does not necessarily apply to the interface. Furthermore, strong concrete as measured by test method ASTM C31 (81) does not necessarily indicate that the interface strength will be adequate. In fact it is quite probable that the concrete strength of the overlay is not statistically different between debonded and fully bonded areas and this was the case on a bonded overlay in the Houston area (49). Obviously, normal measures of strength cannot be taken as being indicative of overlay interface strength. For this reason, other tests have been developed.

At least five test methods have been used to measure interface strength. Two tests assess the shear strength at the interface and two other tests measure the tensile strength. These tests are typically conducted on cores or cylinders at ages greater than 3 days. A fifth test, developed at The University of Texas at Austin, attempts to assess the torsional strength at early ages. The advantages, disadvantages, and applicability to field conditions of each of these test methods are discussed below.

#### Shear Tests

Two shear tests, the slant shear and direct shear, have been used extensively to determine the interface shear strength of bonded overlays. Both tests are run in the laboratory according to standard procedures. The slant shear test relies on compression testing on a specimen in which the interface between the two materials lies at an angle of 30 degrees to the applied load, as shown in Figure 3.34. These specimens are virtually impossible to obtain from pavements and therefore most tests are run on laboratory prepared samples. Obviously, it is very difficult to apply surface preparation and bonding agents to this slanted face inside a standard compression cylinder. Coefficients of variation for these tests typically range from 30 to 50 percent (94).

Direct shear tests use a force applied parallel to and, theoretically, coplanar with the interface to induce failure as shown in Figure 3.35. Although the applied load is intended to be coplanar with the interface, practical limitations prevent this. As a result, a degree of eccentricity exists in virtually all tests and the failure is not in pure shear as intended. Also, the orientation of the core affects the results, particularly in the case of coldmilled slabs which have definite striations associated with the direction of milling. These features of the test method tend to produce coefficients of variation ranging from 25 to nearly 50

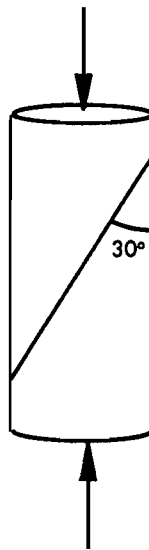


**Figure 3.34 Schematic of slant shear test specimen**

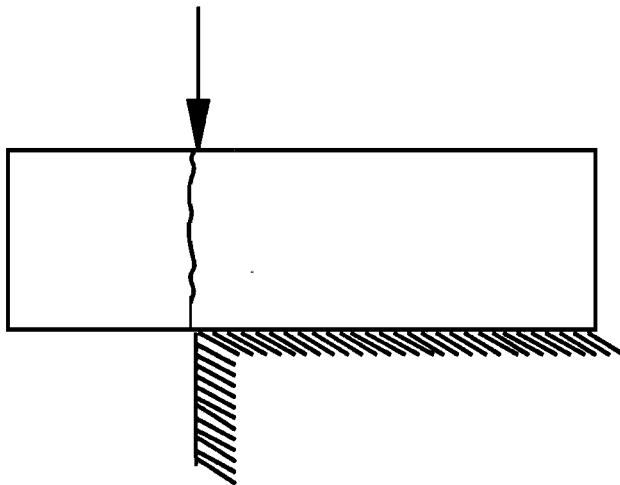


**Figure 3.35 Schematic of direct shear test**

percent. Some researchers (100) report low coefficients of variation (less than 20 percent) when testing is conducted by professional laboratories. Typical coefficients of variation on test series conducted at The University of Texas at Austin were 35 percent (94).

#### *Tension Tests*

Two forms of direct tension tests have been used by researchers to determine tensile strength of bonded overlay interfaces. The direct tensile test is a laboratory test run on either cores or cylinders, although most results are from field cores. Theoretically, tensile stress to failure is applied uniaxially through endcaps bonded to the specimen. As with the direct tension test, alignment is critical if

eccentric loadings are to be avoided. Results from testing at The University of Texas at Austin indicate relatively low coefficients of variation (less than 20 percent) are possible with this procedure (94).

A second form of tension test, the ACI 503 pull-out test (93), can be used in the laboratory or in the field. In this test, a partial depth core is cut to be below the interface and a bonding cap is applied with epoxy, as shown in Figure 3.36. This test is run using a 2- or 4-inch-diameter core barrel. Field tests can be run at relatively early ages provided the coring operation does not damage the interface. Test results to date indicate a higher coefficient of variation for the pullout test than the coefficient of variation of the direct tension test.

The final test method to be described is the torsion test. This procedure, developed at The University of Texas at Austin, was conceived as a means for determining the early-age interface strength of bonded overlays. In this procedure a cylinder of concrete the thickness of the overlay is failed in torsion, as shown in Figure 3.37. Only limited testing has been completed using this equipment. To date, results have been very erratic, with a high coefficient of variation (greater than 50 percent) (94). As with the direct tension and shear tests, eccentricity and a resulting moment are likely without extreme care on the part of the operator. These tests can be run at very early ages, less than 3 hours. However, because of the limited capacity of the torque wrench (200 ft-lb) and the operator, only a short time-window is available for testing (i.e., less than 6 hours). These early test results have not been correlated to the other, more common bond strength evaluation methods. Field application of this method requires that the paving-train pass and the apparatus shown in Figure 3.37 be inserted through the overlay. Substantial disturbance of the overlay is necessary, and the impact of this operation is not known. Thus far, this procedure has not yielded useful information on the rate of interface strength gain.

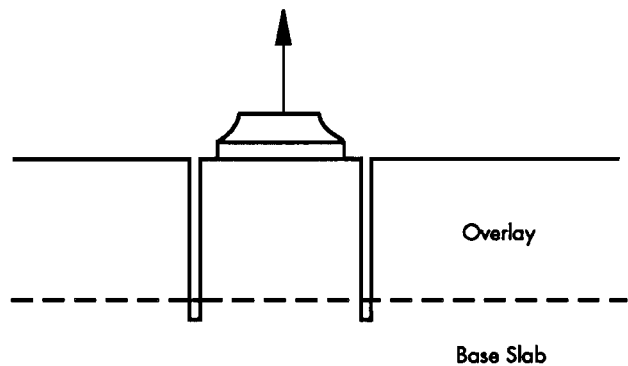


**Figure 3.36 Schematic of pull-out test**

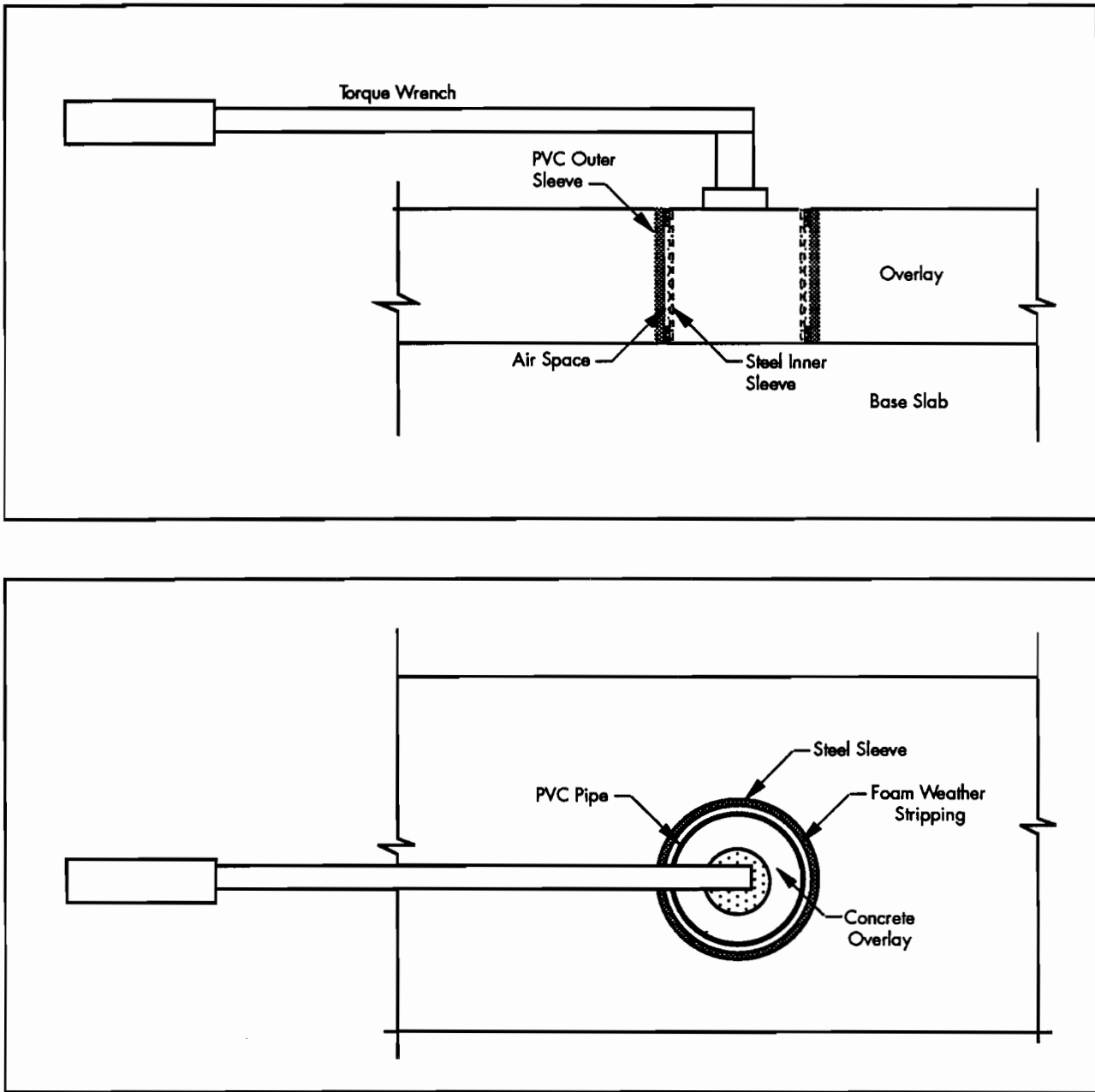


**Figure 3.37 Torsion equipment showing complete assembly (after 94)**

Beyond the effects of the strength testing procedures themselves and the obvious influence of time, the interaction of the overlay and the existing slab play a significant role in the resulting interface strength. The type of surface preparation, bonding agent, and reinforcement affect the strength. Results from laboratory tests on samples prepared using the factors shown in Tables 3.10 and 3.11 are described in Reference 94. Interface strengths were obtained using three of the five methods described above (excluding torsion and slant shear testing). All tests were conducted at 7 days following placement of the overlay. The procedures and the statistical analysis are described elsewhere (94).

It is interesting to note that the tensile strength is approximately one-half the shear strength at the interface for the results shown in Tables 3.10 and 3.11. It is not possible to measure pure shear in concrete directly because, in the presence of "pure shear" in the normal hollow cylinder test specimens, a principal tensile stress equal to the shear stress develops at a 45-degree angle to the shear. Failure occurs because of this tension rather than because of the shear. A reliable estimate of shear strength can be obtained through combined stress testing, as represented by the Mohr rupture diagram shown in Figure 3.38. The strength of concrete in pure shear,  $\tau_0$ , is represented by intersection of the failure

**Table 3.10 Average interface strength results<sup>1</sup> for various test procedures and bonded overlay types (94)**

Bonded Overlay Type		Direct Shear (4 in. Cores)		Direct Tension (4 in. Cores)		Pull-Out Tension (2 in. Cores)	
Surface Preparation	Bonding Agent	Avg	Standard Deviation	Avg	Standard Deviation	Avg	Standard Deviation
Light Shot Blast	Latex	638	228	171	68	190	99
	Epoxy	661	252	335	12	224	76
	PCC	471	269	175	48	169	55
Heavy Shot Blast	Latex	605	103	278	17	203	56
	Epoxy	608	255	289	25	199	44
	PCC	746	282	283	45	220	70
Cold Milled	Latex	679	172	239	39	202	55
	Epoxy	654	276	313	62	172	89
	PCC	530	227	210	55	172	70

**Table 3.11 Average interface strength results for various test procedures for bonded overlays placed without grout (94)**

Bonded Overlay Type		Direct Shear		Direct Tension		Pull-Out Tension	
Surface Preparation	Surface Moisture	Avg	Std Dev	Avg	Std Dev	Avg	Std Dev
Light Shot Blast	Dry	488	204	200	58	142	68
	Wet	430	193	263	55	194	20
Heavy Shot Blast	Dry	695	105	188	74	214	54
	Wet	527	156	231	42	182	60
Cold Milled	Dry	460	245	163	48	132	95
	Wet	476	170	215	36	158	45

envelope with the vertical axis. The shearing strength determined in this way was found to be approximately 20 percent of the compressive strength (76). Tensile strength of concrete is commonly assumed to be about 12 percent of the compressive strength (73). Thus, the ratio of one-half noted above is reasonable. Discrepancies may be attributed to the eccentricities introduced in the shear and tension testing.

Unfortunately, very little data are available documenting the rate of interface strength gain. Felt (13) tested an overlay cast on a 25-year-old base slab using the direct shear technique. Tests were performed at 3, 5, 7, and 28 days after placement. The results, shown in Figure 3.39, indicate a function similar to that assumed for modulus gain with time may be appropriate for interface strength. Owing to the lack of data available for the rate of increase in interface strength and the need for early strength

data, the following assumptions were made: (1) the rate of increase of interface strength can be modeled using the hyperbolic function; (2) the 28-day direct shear test results represent 100 percent of the interface strength attainable; and (3) the rate of strength gain is such that 50 percent of the 28-day strength will be obtained in 2 days. The assumptions result in the normalized equation for strength gain shown below:

$$s_T = 100T / (2+T)$$

where

$$s_T = \text{percentage of the 28-day interface strength at time } T, \text{ psi, and}$$

$$T = \text{time of placement, days.}$$

The percentages of the 28-day strengths are shown in Table 3.12. These assumptions allow the early-age strengths to be estimated for a variety of overlay

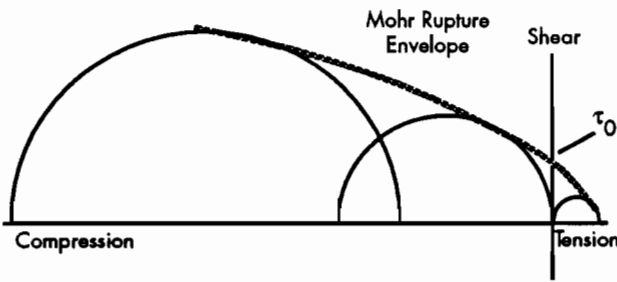


**Figure 3.38** Typical Mohr rupture diagram for concrete (76)

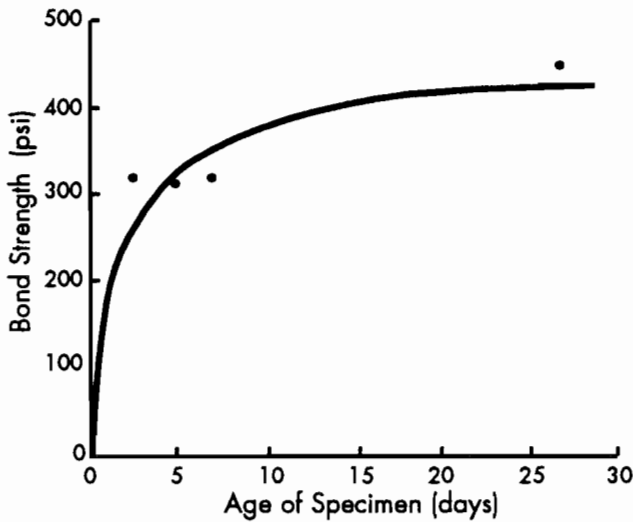


**Figure 3.39** Early-age direct shear test results (after 13)

types. The technique used herein is crude, because it does not account for the environmental conditions during curing. However, the percentages shown agree well with the rate of strength and modulus gain given for normal concrete (72, 73, 76).

### 3.3 SUMMARY

Several closed-form solution techniques available for the analysis of thermally induced stresses in dissimilar materials is discussed. All have limitations which preclude their use for an accurate analysis of the delamination of bonded concrete overlays. Finite-element analysis is identified as the most appropriate method for use in the investigation of debonding at early ages. Background information on several important variables is described, particularly with regard to the time dependent characteristics of the problem. The modulus, curing temperature, and plastic and drying shrinkages of the overlay and existing slab were identified. The influence of the environmental conditions at the time of and immediately after placement is discussed. A technique is presented to describe the temperature distribution in the pavement for a given sinusoidal air temperature. Various measures of interface bond strength are discussed.

**Table 3.12** Estimated percentage of 28-day strength attained in the first week following placement

Time (days)	Percent of 28-Day Strength
0.5	20
1	33
2	50
3	60
4	67
5	71
6	75
7	78

## CHAPTER 4. METHOD OF SOLUTION

Ideally, the evaluation of the delamination in bonded overlays at early ages would involve the analysis of the overlay and existing-slab system continuously, from the placement of the overlay to the time the overlay is first trafficked. However, the methodology for combining the models of the temperature changes in hydrating cement, the support of the existing slab, moisture and temperature changes in the existing and overlay concrete, and the development of interface strength over time does not exist. Therefore, it is necessary to combine individual models with the finite-element analysis tool to allow critical times to be investigated. This section describes the method used to arrive at a solution to the problem of delamination in bonded overlays.

The finite-element method (FEM) program to be used in the analysis of the bonded overlay-existing pavement system has been described previously. Before proceeding with the evaluation of bonded overlays, results from this program must be compared to closed-form solutions. This comparison is the first task in the evaluation of the phenomenon. Second, an analysis factorial which will efficiently address the problem of delamination of bonded overlays must be developed. Obviously, from the discussion in the previous sections, the analysis of the bonded overlay-existing pavement system is complex, with many different parameters influencing the development of early-age stress. The approach undertaken herein relies on an examination of the extremes in the environment and material characteristics which, when taken in combination, may cause delamination. When compared with the attainable interface strengths, a determination of the conditions under which overlays may be safely placed can be made. Some of the parameters or levels of parameters will be eliminated or combined by means of selective analyses, resulting in a more compact analysis factorial. Before proceeding with these analyses, it is necessary to demonstrate both the robustness and the limitations of the finite-element program NSLIP.

### 4.1 EVALUATION OF NSLIP

The effectiveness of any FEM program must be judged on one criterion, namely, whether or not the program determines the stress, strain, and deflection of interest within an acceptable tolerance at a reasonable cost. The acceptance of the stress, strain, and deflection calculated by the program is based, when possible, on a comparison of stress, strain, and deflection determined by a closed-form solution for some representative, albeit, simpler system. Once the accuracy of the program is determined, the economics of the program can be established. When using the finite-element method, increasingly accurate results are normally obtained by reducing the size of the elements. However, the cost of the analysis is inversely proportional to the size of the elements. Thus, increasing accuracy comes at an increased cost. Very small elements were used by Al-Negheimish (66) to analyze thermal stresses in bonded polymer concrete overlays. Although not directly related to this investigation, the work of Al-Negheimish provides a basis for an analysis of the effect of element size on accuracy.

#### 4.1.1 Closed-Form Solution Comparison

The results of two closed-form solution techniques are compared to the results of a finite-element analysis for similar conditions. Timoshenko developed a closed-form solution for two-dimensional analysis of dissimilar materials subjected to a uniform temperature change (54), and it will be used to compare results. The simply-supported beam shown in Figure 4.1 was analyzed using the NSLIP computer program. Figure 4.2 shows the stresses along a vertical cross section at the midpoint of the beam computed using the Timoshenko technique and the finite-element program. The derivation by Timoshenko precluded the application of the result to the zones near each end of the beam. These results demonstrate good agreement between

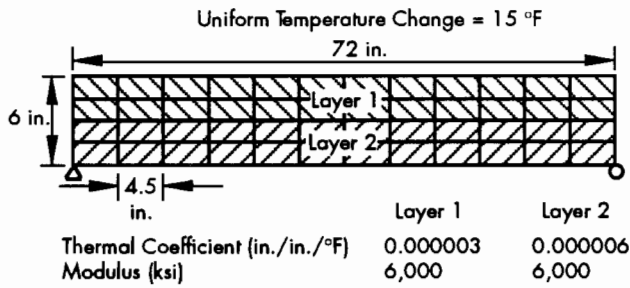


**Figure 4.1** Simply-supported beam analyzed to compare the closed form solution of Timoshenko and the finite-element program, NSLIP

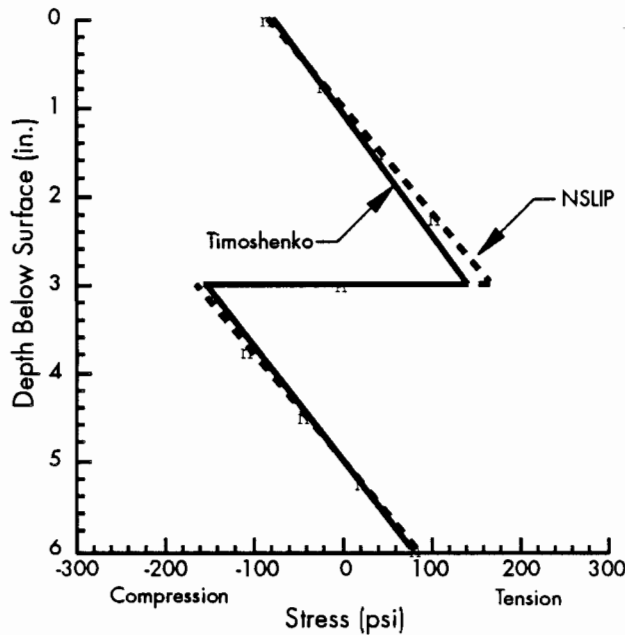


**Figure 4.2** Comparison of the distribution of stresses along a vertical cross section taken at the midpoint of a composite beam as calculated using the Timoshenko derivation and NSLIP

the stresses calculated by NSLIP and those calculated using the Timoshenko derivation.

Temperature-induced stresses and deflections in pavements were analyzed by Westergaard (65). The Westergaard solution assumed that the temperature at the mid-plane of the pavement remains constant and that the temperature varies linearly between the top and bottom of the pavement, as shown in Figure 4.3.

A temperature difference of 30 degrees was used for this analysis. The pavement system shown in Figure 4.4 was analyzed using the Westergaard and NSLIP procedures. Material properties of the layers are shown in Table 4.1. The material properties of Layers 2 and 3 were combined into a composite k-

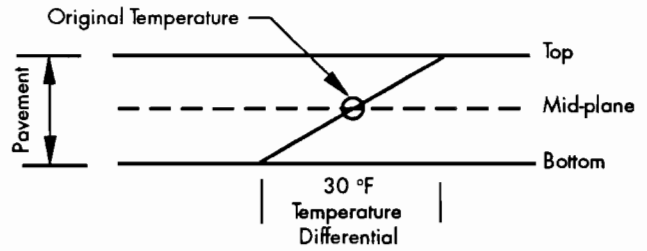


**Figure 4.3** Temperature distribution assumed by Westergaard to calculate the thermally induced stresses (65)

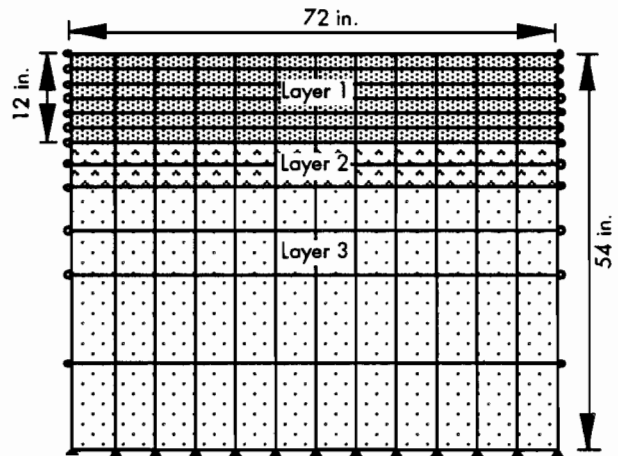


**Figure 4.4** Pavement system analyzed using the Westergaard solution and finite-element analysis

value for use in the Westergaard analysis using techniques described in the AASHTO Design Guide (101). The maximum deflection and stress calculated using the Westergaard technique were 0.022 inch and 500 psi, respectively, while those determined by the FEM program were 0.016 inch and 312 psi. The lower deflection calculated by the FEM program results from the restraint provided by the interface.

**Table 4.1** Material properties used in the FEM program to compare NSLIP to the Westergaard solution

Material Properties	Layer 1	Layer 2	Layer 3
Modulus (psi)	6,000,000	500,000	50,000
Thermal Coeff	0.000006	-	-
Poisson's Ratio	0.2	0.2	0.4
Thickness (in.)	12	6	36

### 4.1.2 Finite-Element Comparison

Work by Al-Negheimish (66) evaluated bonded polymer concrete overlays of existing concrete materials using the finite-element method. The nature of the materials and configuration of the system analyzed by Al-Negheimish necessitated the use of a fine mesh in order to assess the stresses due to temperature changes. Figure 4.5 shows one of the meshes used by Al-Negheimish (66). A comparable mesh, shown in Figure 4.6, was used to assess the results provided by NSLIP.

Having assessed the accuracy of the program in the analysis of temperature-induced stresses in continuous media, it is necessary to develop an analysis factorial which will efficiently address the chief factors thought to cause delamination in bonded overlays. Several of the important factors have been identified previously. It remains to select the levels of each factor and, where appropriate, minimize the size of the factorial through selective analyses without reducing the effectiveness of the investigation.

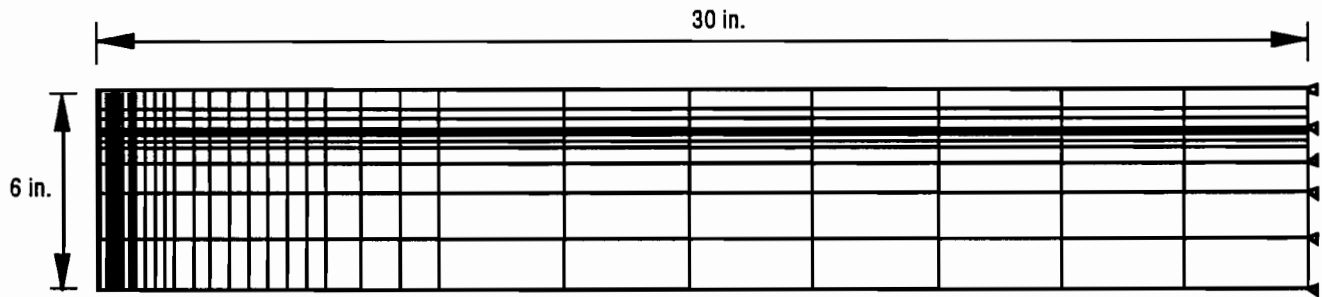


Figure 4.5 Finite-element mesh used for thermal stresses analysis by Al-Negheimish (66)

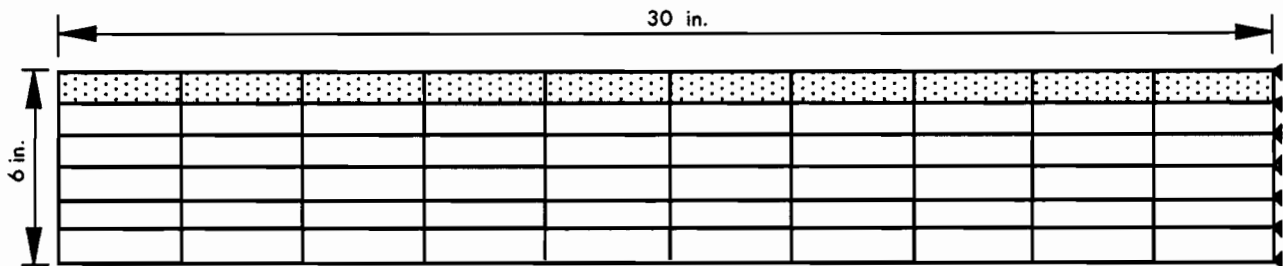


Figure 4.6 Mesh used in NSLIP to compare thermal stresses to those obtained using the finer mesh of Al-Negheimish

As shown in Figures 4.7 and 4.8, the two analyses yield similar results. The chief differences are near the pavement edge. This difference is understandable since the maximum stress from the theoretical calculations occurs at the pavement edge. Therefore, a small mesh size would more accurately reflect the increase in stress near the edge of the pavement. The greater accuracy provided by the finer mesh comes at a higher computing cost. Given the inaccuracy of many of the other finite-element inputs; e.g., shear strength gain, temperature distribution in the pavement, and early-age material properties, it was decided that the coarser mesh available in NSLIP would provide the necessary results with sufficient accuracy.

It can be seen that the finite-element program used herein yields results which compare favorably with closed-form solutions of simpler systems.

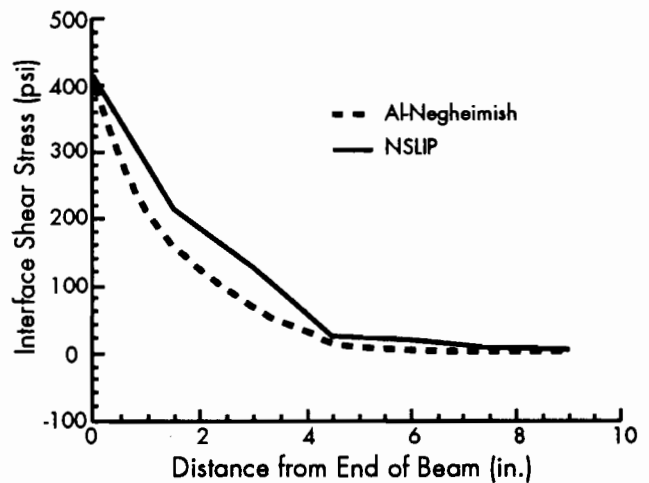
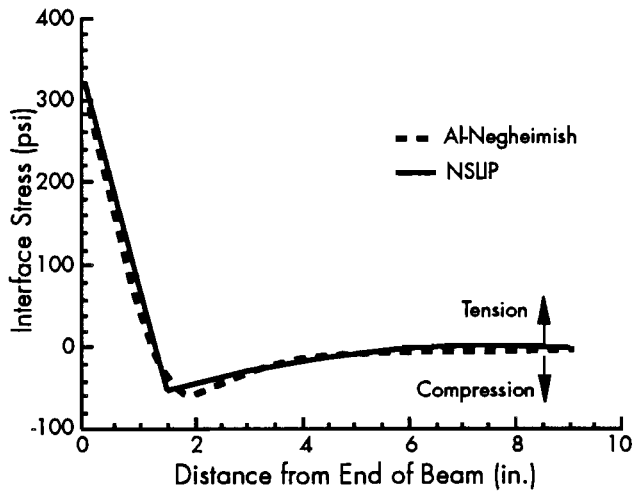


Figure 4.7 Comparison of shear stress calculated using different numbers of elements



**Figure 4.8 Comparison of normal stress calculated using different numbers of elements**

## 4.2 DEVELOPMENT OF THE ANALYSIS FACTORIAL

The efficient analysis of the stresses at the interface between an existing concrete pavement and a recently placed overlay involves a variety of factors. The factors that specifically influence the early-age stress development are shown in Table 4.2. Each of these parameters influences the development of stress at the interface between the overlay and the existing concrete pavement.

**Table 4.2 Factors considered important in the analysis of interfacial stresses in recently placed bonded overlays**

Categories	Factor
General	Time of Analysis
	2-D Representation of Problem
Environmental Conditions	Season of Placement
	Daily Temperature Change
	Time of Placement
Bonded Overlay Properties	Curing Temperature
	Thermal Coefficient
	Elastic Modulus
	Shrinkage Coefficient
	Interface Strength
	Thickness
	Location of Steel Reinforcement
	Amount of Steel Reinforcement
Existing Slab Properties	Thickness
	Elastic Modulus
	Thermal Coefficient
	Location of Steel Reinforcement
	Amount of Steel Reinforcement
Curing Temperature	

An evaluation including all these factors, with each at only two levels, would require over 500,000 computer runs, an onerous task. The importance of many of these features has been discussed in the previous chapter and, as noted earlier, this analysis will focus on the extremes of various parameters which may cause debonding. The intent of this section is to select levels of each factor and, where possible, combine or eliminate factors. The discussion of the general factors, the time of analysis, and the 2-D representation, will be deferred.

### 4.2.1 Environmental Conditions

The environment at the time of placement is extremely important to the development of stresses at the overlay and existing-slab interface. The environment can have a direct or indirect influence on the development of stresses. Direct influences determine the temperature and moisture distribution and therefore the distribution of stress within the pavement. Indirect effects include the determination of the curing temperature and the rate of interface strength gain. Both direct and indirect effects can be characterized, within the limits of current knowledge, if the temperature distribution of the pavement is known.

Extremes in seasonal temperature variation were chosen for evaluation because the extremes represent the conditions under which delamination is most likely. Seasonal extremes, hereinafter for summer and winter, were chosen to represent the time of the year when the temperature of the existing slab was highest or lowest. These extremes may or may not occur during the traditional summer and winter season depending on where the overlay is placed. Maximum air temperatures of 100°F and 50°F were selected from Table 3.8 for the summer and winter seasons, respectively. The determination of the temperature variation in the slab requires that the diurnal temperature fluctuation be known.

A diurnal temperature variation of 30°F was selected after consideration of several factors. First, Table 3.8 shows that over the last thirty years the differences between the maximum and minimum average monthly temperatures are between 20 and 30 degrees, assuming the extremes occur on successive days. Second, evaluation of paving records and construction data from two bonded overlay jobs in the Houston, Texas, area shows that the average air temperature differential between the temperature at the time of placement and the minimum the following morning was about 15°F. However, values as high as 30°F were recorded. Finally, using an air temperature differential higher than the actual differential, coupled with the distributions calculated with the Fintel and Khan equation gives a very high gradient in the top 4 inches. This feature was shown in Figure 3.31. It is

the temperature differential and the associated strains that induce stresses in the pavement. Thus by forcing the high differential to the top 4 inches, account can be made of the shrinkage differentials described in Chapter 3.

Two additional environmental factors of interest are the time of placement of the overlay and the time of the analysis. The time of placement was chosen to coincide with the minimum and maximum air temperatures to expose the overlay to the greatest temperature differential possible. An examination of weather records shows that the minimum temperature occurs at approximately 6 a.m., while the maximum occurs at about 5 p.m. (98). The maximum was shifted to 6 p.m. to allow the use of the pavement temperature distribution modeling scheme discussed earlier. This temperature model allowed the temperature distribution of the existing slab before placement and the temperature distribution of the overlay-existing slab some time after placement to be estimated.

Ideally, the overlay-pavement system stresses should be analyzed continuously from placement; however, this exceeds the capacity of the current analysis tools. Therefore, times of analysis were selected to represent critical times in the early life of the overlay and existing-slab system. Given that debonding has sometimes been discovered less than 24 hours after placement and temperature within the slab begins to cycle with the air temperature at approximately 48 hours, analysis was planned for 12 and 24 hours after placement. The lower limit of 12 hours was chosen because at less than 12 hours, material properties are highly variable and poorly defined. Selected analyses will be performed on the system 48 hours after placement to confirm that the critical times for the formation of delaminated zones are less than 48 hours.

Having selected the times for analysis, the next step is to determine the temperature distribution within the pavement at each of these times. Temperature distributions within the pavement system at times equal to 0, 12, 24, and 48 hours after placement of a composite 12-inch pavement are shown in Figures 4.9 through 4.12 for all combinations of season and time of placement. These distributions were developed from consideration of the initial slab temperature, time of placement, and the assumption that the resulting slab would begin to cycle normally after 48 hours. It is the stresses that result from these temperature distributions relative to the cure temperature that will be analyzed for this investigation.

#### **4.2.2 Pavement Properties**

Properties of the pavement system, i.e., the overlay and existing slab, may be divided into two categories. First the physical attributes of the system

must be considered, specifically layer thickness and reinforcement location and type. Second, materials properties have a major impact on the development of interfacial stresses and are discussed in detail below. The level, or levels, of each factor necessary to effectively model the overlay-existing slab system are discussed.

#### *Physical System*

The thickness of the overlay is particularly important to the development of stresses at the interface. This can be seen by examining Figures 4.9 to 4.12, where it is readily apparent that the majority of the daily temperature fluctuation occurs in the top 4 inches of the pavement. Bonded overlays range in thickness from approximately 0.5 to 6 inches. Overlays placed at thicknesses of less than 2 inches are normally specialized materials, i.e., polymer concrete or proprietary products, which have specialized needs that are not within the scope of this investigation. A notable exception to this are thin-bonded overlays of bridge decks. Portland cement concrete in thin sections of 1 to 2 inches have been used successfully for some time in rehabilitation of bridge surfaces. However in these cases, special care can be taken in surface preparation and specialized curing is practical due to the relatively small area of most bridges. Under normal circumstances, these measures are not practical for use on long highway sections. Bonded overlays of pavements are commonly placed in thicknesses of 2 to 4 inches. Four inches represents the upper limit under most circumstances because when thicker overlays are used more cost is incurred raising overhead signs and structures and guardrails. Thus, only overlay thickness of 2 and 4 inches are considered.

The thicknesses of most existing highway CRC pavements range from 8 to 12 inches. However, because of the limited temperature fluctuation below a depth of about 4 inches, only 8-inch slabs are considered herein. When a 2-inch bonded overlay is placed on an existing slab, temperature distributions different from those described for a 4-inch overlay (Figures 4.9 through 4.12) will develop because less heat of hydration results from the thinner overlay and the heat is lost more quickly. Curves similar to those shown for the 4-inch overlays were developed for a 2-inch overlay on an 8-inch existing CRC pavement.

The remaining physical characteristic of the system to be considered is reinforcement. Reinforcement in the existing slab is axiomatic, but bonded overlays of CRC pavements have been placed successfully without reinforcement, with steel fibers, and with steel mesh reinforcement. Prior to cracking, the amount or location of steel has very little effect on the pavement stress distribution, based on analysis

Winter Morning Placement  
Air Temperature Differential = 30°F

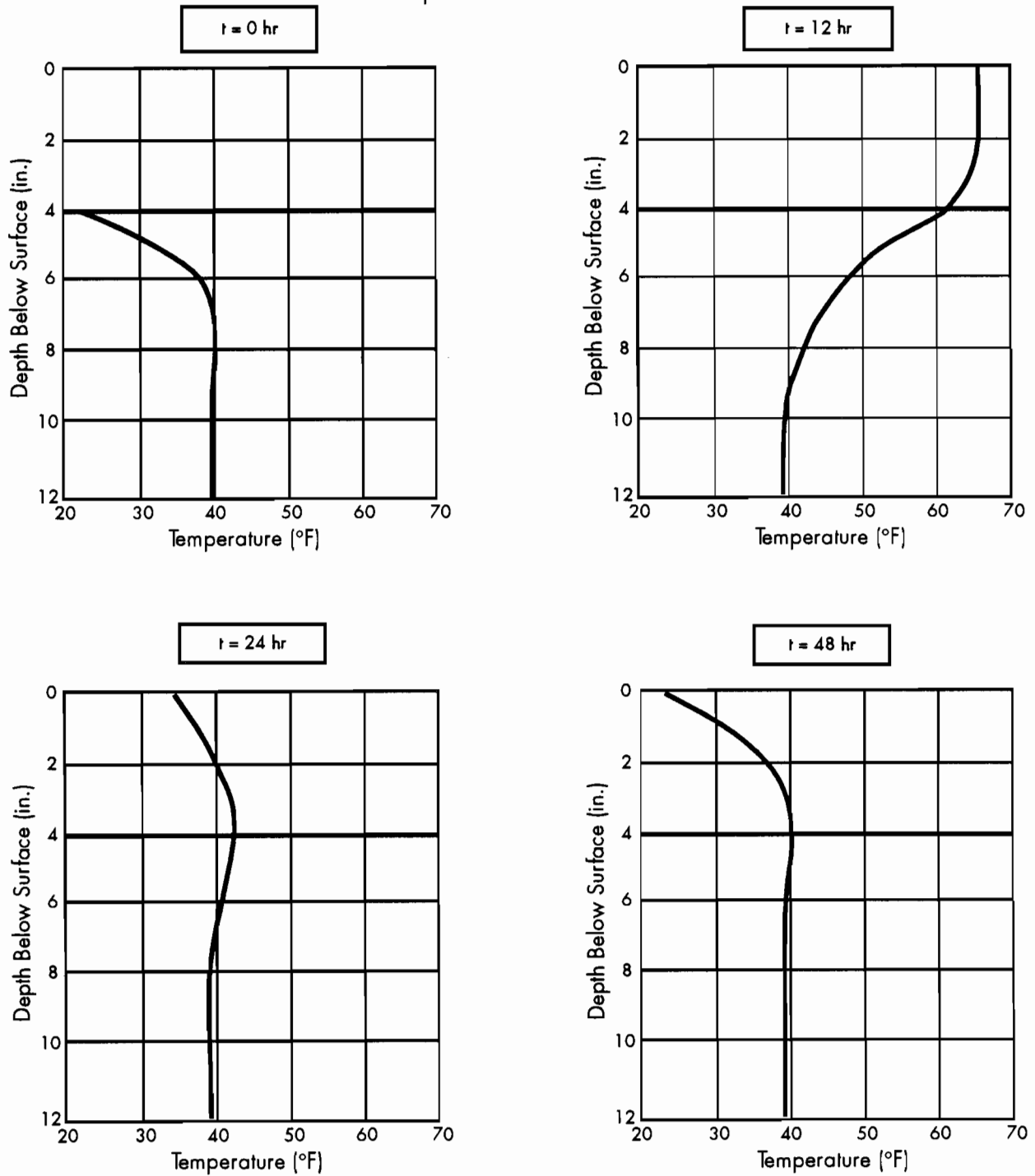
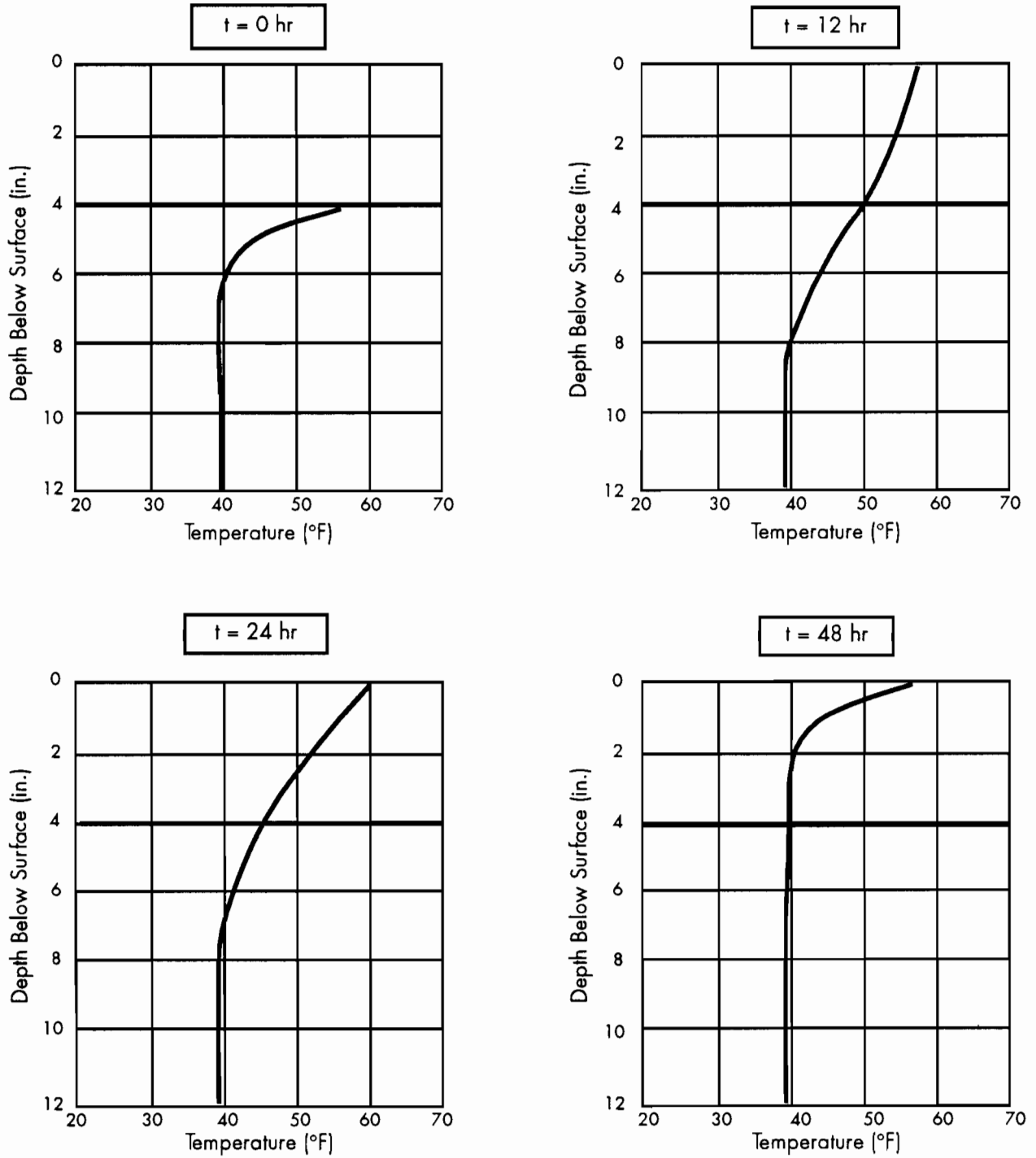


Figure 4.9 Temperature distribution in the pavement for a winter morning placement at 0, 12, 24, 48 hours after placement of the overlay

Winter Afternoon Placement  
 Air Temperature Differential = 30°F



**Figure 4.10** Temperature distribution in the pavement for a winter afternoon placement at 0, 12, 24, 48 hours after placement of the overlay

Summer Morning Placement  
 Air Temperature Differential =  
 30°F

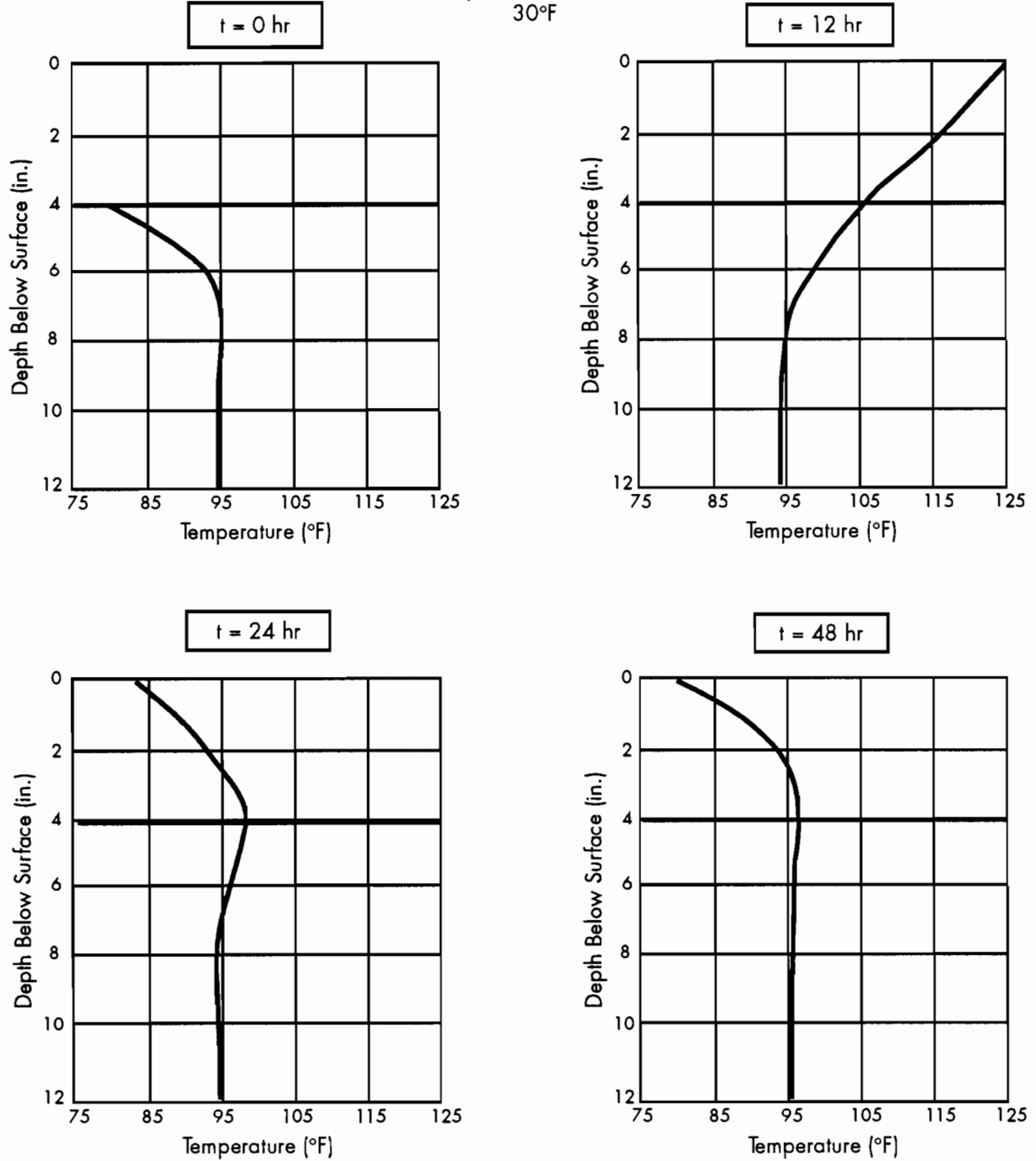


**Figure 4.11** Temperature distribution in the pavement for a summer morning placement at 0, 12, 24, 48 hours after placement of the overlay

Summer Afternoon Placement  
Air Temperature Differential = 30°F

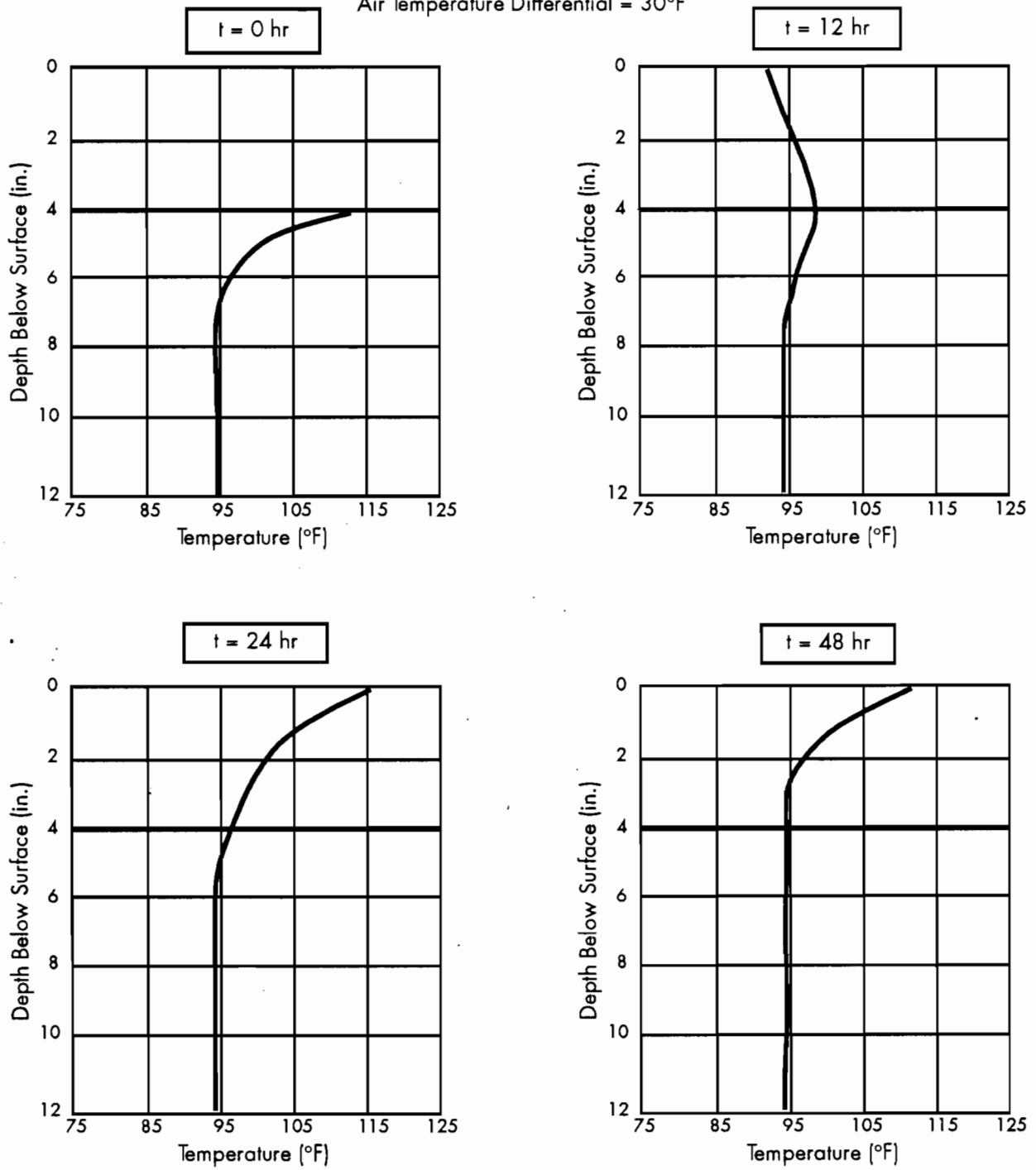


Figure 4.12 Temperature distribution in the pavement for a summer afternoon placement at 0, 12, 24, 48 hours after placement of the overlay

using the FEM program NSLIP. This was shown by analyzing the pavement system shown in Figure 4.4 with steel reinforcement located at three levels. Steel bar elements were located 2 inches below the surface for one run, 8 inches below the surface for a second run, and at 2 and 8 inches for a third run. As can be seen in Table 4.3, the presence of steel had very little effect on the maximum deflection or stress in the pavement system. These results confirm the common pavement design philosophy that the presence of steel reinforcement does not add measurably to the structural integrity of the pavement prior to cracking.

**Table 4.3 Effect of steel reinforcement at various depths in an uncracked 12-inch pavement**

<b>Pavement System</b>	<b>Maximum Tensile Stress (psi)</b>	<b>Maximum Deflection (in.)</b>
No Steel	312	.0008
Steel 2 in. Below Surface	318	.0008
Steel 8 in. Below Surface	313	.0008
Steel 2 in. and 8 in. Below Surface	319	.0008

However, after the formation of a crack, both the amount and the location of the steel influence the distribution of stress in the overlay. The systems described above were analyzed after a crack was introduced 6 inches from the pavement edge. The analysis results are shown in Table 4.4. Obviously the presence of steel reinforcement in a cracked pavement has a substantial influence on the development of stresses.

**Table 4.4 Effect of steel reinforcement at various depths in a cracked 12-inch pavement**

<b>Pavement System</b>	<b>Maximum Stress (psi)</b>	<b>Maximum Deflection (in.)</b>
No Steel	262	0.016
Steel 2 in. Below Surface	366	0.001
Steel 8 in. Below Surface	250	0.002
Steel 2 in. and 8 in. Below Surface	375	0.001

This analysis is based on pavements with fully developed strengths and moduli and, therefore, assumes fully developed stress transfer between the steel and the concrete. Neville (72) points out that the development of bond stress in concrete is proportional to the compressive strength of the

concrete. Lower compressive strengths result in lower bond stress. At the early ages under investigation in this study (less than 48 hours), concrete strengths range from 15 to 50 percent of the 28-day values. Price (102) concluded that, for 4,000-psi concrete, a bond stress of approximately 800 psi could be attained at 0.01 inch slip. However, for 1,000-psi concrete, only about a 200-psi bond stress could be developed. These results are not directly applicable to the bonded overlay problem, but they indicate the level of reduction in the attainable bond stress transfer for concrete at early ages. An additional reduction in the bond stress will result from the low concrete modulus at early ages, which will allow greater deformation in the concrete at lower stress and therefore less stress transfer to the steel reinforcement. The modeling technique used to incorporate reinforcement in the FEM program introduces another problem in the analysis of the effect of steel on interface stresses.

This problem is associated with the transfer of stress from concrete to steel. Several researchers (103, 104) have developed models describing the nature of stress transfer between steel and concrete in pavements. All indicate a zone of slippage between the steel and concrete exists in the vicinity of the crack. The FEM program used herein does not attempt to account directly for this slippage. The inclusion of local, low moduli elements adjacent to the steel in an attempt to model this zone of slippage is not possible in the analyses, if the interface delamination potential is to be considered. This is due to the relatively limited number of total elements allowed by the program. In addition to the limit on the total number of elements, it is not possible to place steel along a line that is adjacent to slip elements. This limitation precludes a thorough analysis of the influence of the steel on the interface stress, since in most bonded concrete overlays in Texas the overlay steel reinforcement is placed directly on the existing pavement. This limitation is not considered critical because the low concrete strength and modulus values at early ages investigated in this study limit the transfer of stress from the concrete to the steel.

Therefore, steel is included in the analyses only when cracks are present or the formation of cracks is anticipated. This has particular significance for both of the two-dimensional systems originally identified for analysis (see Figures 3.3 and 3.4). When analyzing the edge condition, it is assumed that no longitudinal cracking is present in the existing slab or, if longitudinal cracking was present, that it was repaired prior to the placement of the overlay. Furthermore, it is assumed that no

longitudinal cracking forms in the overlay during the first 48 hours following placement. Thus, reinforcement is included in neither the overlay nor the existing slab for the analysis of the edge condition.

Although the edge condition can be successfully analyzed without including reinforcement, this is not the case for the perpendicular cross section. The two-dimensional cross section shown in Figure 3.4, the interior condition, warrants additional consideration. As with the edge condition, longitudinal cracks need not be considered since the cross section is taken parallel to and some distance from any longitudinal cracking that might be present. However, all transverse cracks are included in the cross section and in order for the impact of these cracks, in conjunction with the reinforcement, to be assessed the pavement systems shown in Figures 4.13 and 4.14 are analyzed. These systems represent the two types of cracking found in bonded overlays, namely reflective and non-reflective cracking (49). Reinforcing steel is included in the existing slab, but not in the overlay, for the reasons cited above. Figure 4.13 shows a situation in which a crack may reflect through the overlay or may form at either side of the existing crack. The second pavement system allows the influence of the non-reflective crack to be investigated. This crack may have been initiated in the overlay by shrinkage or temperature induced volume change.

#### Material Properties

Material properties of the overlay and the existing slab also play an important role in the determination of the overlay interface stresses. Properties of the existing slab are discussed first, followed by a selection of the levels of analysis for the overlay. Three major factors related to the existing slab are of

concern. These are the modulus, curing temperature, and thermal coefficient of the concrete. It is assumed that drying shrinkage of the existing slab is no longer a factor.

#### Existing Slab

Two moduli values were selected for this analysis to represent the range of values associated with normal weight concrete. The values of 4,000 and 6,000 ksi are indicative of concretes commonly used in pavements. These values are coincidentally representative of concretes constructed with the limestone and siliceous river gravel aggregates available in Texas. Thermal coefficients of 0.000004 and 0.000006 in./in./°F were also chosen, to be representative of the extremes in normal concrete. These are also the thermal coefficients representative of limestone and siliceous gravel concretes. The lower thermal coefficient would normally be associated with the limestone aggregate and the higher coefficient with the siliceous gravel aggregate; however, in order that the inference space of this study be as large as possible, all combinations of thermal coefficient and modulus were included. With the selection of modulus, thermal coefficient, and temperature distribution in the pavement, only the temperature from which the thermal movements was to be calculated remained to be determined. The selection of the curing temperature from which to calculate the temperature induced stress was more difficult than the selection of the levels of modulus and thermal coefficient.

The determination of the curing temperature is a difficult process, as discussed in the previous chapter. This problem is compounded by the fact that, for the most part, the season and time of placement of the existing slab cannot be easily determined. Even if the date and time of placement were known, the curing temperature would have to be estimated based on engineering judgment as to

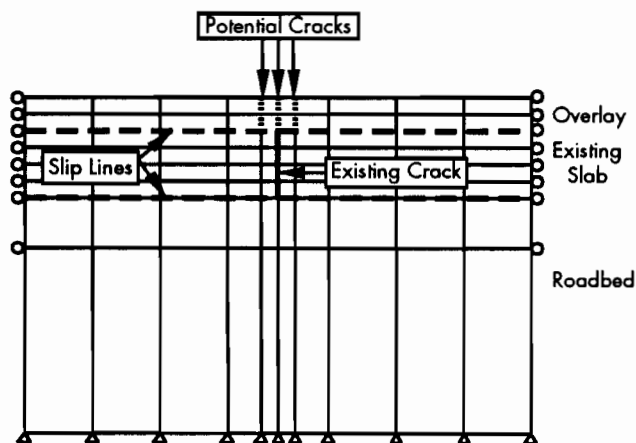


**Figure 4.13** Two-dimensional representation of interior condition used to assess the influence of reflective cracking

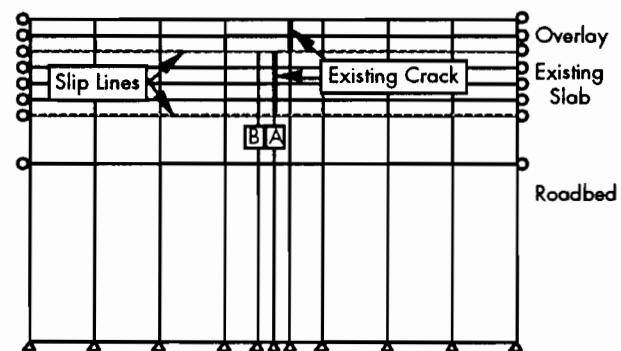


**Figure 4.14** Two-dimensional representation of interior condition used to assess the influence of non-reflective cracking

the time and associated temperature at which the concrete began to resist thermally induced movement. The curing temperature is effectively determined when the concrete begins to take stresses as a result of the imposed restraint. The magnitude of the thermally induced stress is determined from the degree of restraint present and the change in temperature from the curing temperature. It is sometimes assumed that the curing temperature is uniform with depth. However, this situation is altered substantially by the placement of an overlay.

A new restraint condition is imposed when the overlay is placed. Consider the beam shown in Figure 4.15(a), which is initially stress-free at a constant temperature equal to the cure temperature,  $t_0$ . If the unrestrained beam is subjected to a  $30^\circ\text{F}$  temperature gradient, the beam will move to the position shown in Figure 4.15(b). If the beam is now fully restrained in this new position, and then returned to the original curing temperature,  $t_0$ , the effective temperature differential is as shown in Figure 4.15(c). Under the condition shown in Figure 4.15(d), no stress would exist in the beam. However, after the restraint is imposed, even though the temperature is constant with depth and equal to the original curing temperature,  $t_0$ , there is an effective temperature differential of  $30^\circ\text{F}$  resulting from the imposition of a new cure temperature. This "new" cure temperature was defined by the temperature at the time the restraint was

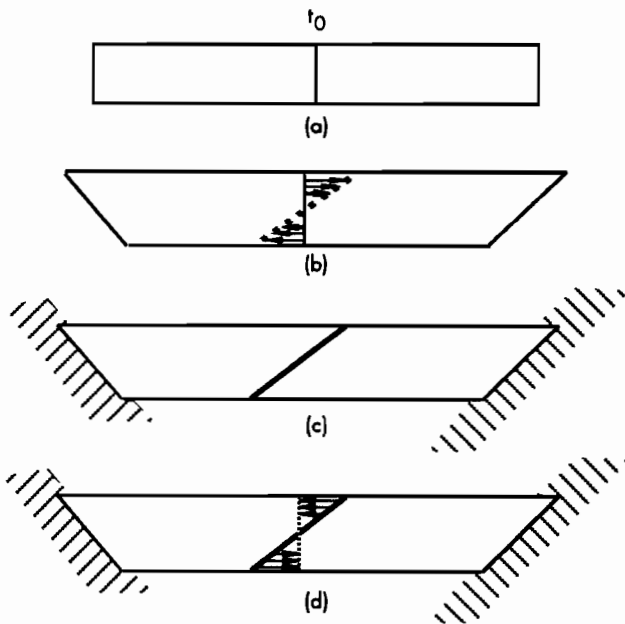


**Figure 4.15** Imposition of a new cure temperature by means of restraint

imposed. This same concept can be applied to the existing slab following the placement of an overlay.

Consider Figure 4.16 in which an 8-inch pavement serves as the base slab for a 4-inch overlay. If the base slab has the temperature distribution shown by Curve A when the overlay sets, then the imposition of the restraint by the overlay effectively describes the "new" cure temperature, against which all subsequent thermal movements are based. Thus, if the temperature distribution in the slab at some later time is as described by Curve B, then the temperature differential in the 8-inch CRC is positive rather than negative, as it would be if the original curing temperature were used.

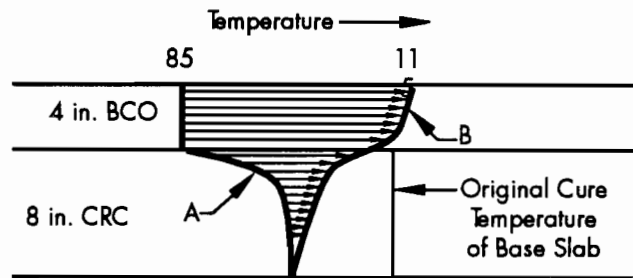


**Figure 4.16** Development of a "new" cure temperature in an existing slab based on the placement of a bonded overlay

From the discussion above it is apparent that the original cure temperature of the existing slab is not a factor in this analysis. Thus, the temperature distribution in the slab at the time the overlay begins to restrain the underlying slab must be determined. However, as discussed previously, the time at which the overlay begins to take stress cannot be determined using current technology. It is therefore assumed that the temperature distribution in the existing slab 6 hours after placement is most representative of the new curing temperature. This value was selected as representing the time when the final set occurs, as per ASTM (81). Using the temperature distributions shown in Figures 4.9 through 4.12 and the temperature distribution at 6 hours, the temperature differentials shown in Table 4.5 were determined for a 4-inch overlay at all combinations of season and time of placement to be considered. Similar techniques were used to determine the temperature differentials for 2-inch bonded overlays (Table 4.6).

Examination of these temperature distributions shows that the summer and winter morning placements induce generally more severe thermal gradients near the surface than the afternoon placements. Furthermore, the 24-hour temperature

**Table 4.5 Estimated temperature differentials with depth at 12 and 24 hours after placement in a 4-inch BCO on an 8-inch CRC**

Season	Time	Hours After Placing	Depth Below Surface (in.)												
			0	1	2	3	4	5	6	7	8	9	10	11	12
Winter	AM	12	+1	+1	0	+2	+12	+10	+8	+5	+3	+2	0	0	0
		24	-33	-28	-26	-21	-8	-4	0	+1	0	0	0	0	0
	PM	12	-5	-6	-6	-7	-10	-1	+2	+1	+1	0	0	0	0
		24	0	-5	-9	-12	-14	-4	+1	+1	0	0	0	0	0
Summer	AM	12	+15	+10	+5	0	-3	-4	0	0	0	0	0	0	0
		24	-27	-19	-16	-14	-10	-7	-2	0	0	0	0	0	0
	PM	12	-8	-6	-5	-2	-1	0	+1	0	0	0	0	0	0
		24	+16	+4	-1	-6	-6	-3	-1	0	0	0	0	0	0

**Table 4.6 Estimated temperature differentials at 12 and 24 hours after placement in a 2-inch BCO on an 8-inch CRC**

Season	Time	Hours After Placing	Depth Below Surface (in.)												
			0	1	2	3	4	5	6	7	8	9	10	11	12
Winter	AM	12	+4	+3	+2	-4	0	0	0	0	0	0	0	0	0
		24	-32	-23	-15	-6	-2	-1	0	0	0	0	0	0	0
	PM	12	-16	-12	-4	-2	-2	-1	0	0	0	0	0	0	0
		24	+12	+4	0	-2	-2	-1	-1	0	0	0	0	0	0
Summer	AM	12	+15	+6	+4	+2	+2	+1	0	0	0	0	0	0	0
		24	-22	-12	-4	+2	+2	+1	0	0	0	0	0	0	0
	PM	12	-8	-6	-2	-2	-2	0	0	0	0	0	0	0	0
		24	+18	+6	0	-4	-4	-1	0	0	0	0	0	0	0

gradient is steeper than the 12-hour distribution. This will probably result in higher stresses at 24 hours than those at 12 hours after placement. These higher stresses may be offset by the interface strength gained with the passage of the 12 hours between the two times of analysis. Having determined the temperature distribution for the slab

at the analysis times, the materials properties at the corresponding times must be determined.

#### Overlay

The material properties of the overlay included in the analysis are: (1) modulus, (2) thermal coefficient, and (3) curing temperature. Each of these

properties is discussed below. The initial drying shrinkage is taken into account through the use of a 30°F temperature differential, as previously discussed.

The modulus at a given time after placement can be determined as discussed in Chapter 3. Concrete moduli at 28 days of 4,000 and 6,000 ksi were selected to represent the range of concretes used in normal pavement construction. Using the rate of gain of modulus from Table 3.2, modulus values were estimated for 12, 24, and 48 hours. These modulus values are shown in Table 4.7.

Thermal coefficients of 0.000004 and 0.000006 in./in./°F are used in the analysis to represent the range of values common in concrete. As noted previously, thermal coefficients are not time-related functions and therefore no adjustment for the time of analysis is required (94).

Curing temperature of the overlay is assumed to be constant with depth. However, due to the increasing air temperatures to which overlays placed in the morning are exposed, the cure temperatures are normally somewhat higher, as shown in Figures 3.13 and 3.14. Therefore, the winter morning and evening overlay cure temperatures are 65 and 60°F, respectively. Those for summer morning and afternoon are 110 and 100°F, respectively. These values were selected based on field measurements of the early-age temperature distributions in 4-inch bonded overlays placed in the Houston, Texas, area in February and July.

All of the factors influencing the development of stress at the interface between an overlay and the existing CRC pavement have been identified and appropriate values selected for the analysis. The key feature remaining to be discussed is the interface strength for various combinations of surface preparation and bonding agent. The rate of gain of the interface strength must also be determined for each combination so that appropriate strengths can be selected for each time of analysis. Research conducted at The University of Texas at Austin investigated several different combinations of surface preparation methods and bonding agents (see Tables

**Table 4.7 Early-age modulus values for limestone and siliceous river gravel concretes**

Time	Modulus (ksi)	
	Limestone	Siliceous Gravel
12 hours	600	900
24 hours	1,200	1,800
48 hours	1,700	2,700
28 days	3,800	5,900

3.10 and 3.11). These results show a high degree of variability in shear and tensile strength for the bonding agent-surface preparation combinations considered.

Rather than consider directly each of the possible combinations of surface preparation and bonding agent, a 7-day interface shear strength of 200 psi is assumed. This value is approximately one-half to one-third the average of the shear strength results obtained in the laboratory (94). Field tests of cores taken from a 4-inch bonded overlay in Houston, Texas yield an average shear strength of approximately 385 psi (49). In the event that the analyses show that debonding has occurred, the analyses will be repeated using a seven-day interface shear strength of 400 psi. The strength values at 12, 24, and 48 hours were estimated for seven-day shear strengths of 200 and 400 psi using the percentages shown in Chapter 3. These values are shown in Table 4.8. Tensile strengths are assumed to be one-half the shear strength.

**Table 4.8 Estimated interface shear strength at early-ages based on the 7-day strengths**

Time (hours)	Interface Shear Strength at 7-days (psi)	
	200	400
12	50	100
24	85	170
48	130	260

All of the considerations discussed above led to the development of the analysis factorial for the edge condition shown in Figure 4.17. A similar factorial will be developed for the interior analysis; however, the system is somewhat more complex. The analysis of the interior condition also relies on the results from the edge analysis and is therefore discussed in greater detail in the next chapter.

### 4.3 SUMMARY

Results from the FEM program NSLIP compare favorably with those obtained from the closed-form solutions of Timoshenko and Westergaard based on the maximum deflection and stress. Sufficient accuracy can be obtained in the critical free-edge region with the limited number of elements allowed by NSLIP. The inclusion of steel reinforcement in the analysis of an uncracked pavement was found to be unnecessary. However, when cracks are present,



## CHAPTER 5. ANALYSIS OF BONDED OVERLAYS

An evaluation of the results of a computer analysis conducted using the program, NSLIP, is presented. Analyses were performed on perpendicular cross sections of the pavement system shown in Figure 3.2 using the combinations of environment and materials shown in Figure 4.17. The maximum interfacial shear and tensile stresses are of principal concern because it is these stresses that cause delamination. In addition to the analyses of the crack-free edge condition, the presence of cracks in the existing pavement or in the overlay is evaluated through analyses of a cross section taken parallel to the direction of vehicle travel. Before the results are discussed, a typical set of data from a single computer analysis is discussed in considerable detail. This discussion points out several important features common to each set of results. Then, the results from all the edge condition analyses are evaluated, with particular attention given to the combinations of materials and environmental conditions that are most likely to cause delamination. Next, the interior condition analysis results are presented and evaluated. These evaluations lead naturally to the discussion of the application of the results of this investigation to the design, specification, and construction of bonded overlays, which is included in the next chapter.

### 5.1 TYPICAL RESULTS

Several general features of the analysis must be discussed before the results are evaluated. The decision to present the complete results for only one combination of material properties and environmental conditions was made for two reasons. First, given the number of analyses required for this study it is not practical to present the complete results for each run. Second, as will be shown, there is considerable similarity among the results. Because of this similarity, there is no need to belabor each

computer analysis. Although the magnitude of the maximum stress changes from run to run, the nature of the stress distributions resulting from the edge condition is common to all analyses conducted. The distribution of stresses which develops in the interior of the pavement system is somewhat more complex and these analyses will be treated separately.

The cross section used to assess the distribution of stresses developed near the edge of a bonded overlay is shown in Figure 5.1. The overall dimensions of the existing CRC pavement and all layers below remain constant whether a 2- or 4-inch bonded overlay is being analyzed. Material properties and environmental conditions were changed according to the factorial set forth in the previous chapter.

Figures 5.2 through 5.4 show contour plots of the normal, transverse, and shear stresses from an edge condition analysis of a 4-inch bonded overlay placed on an 8-inch CRC pavement similar to that depicted in Figure 5.1. These figures are not drawn

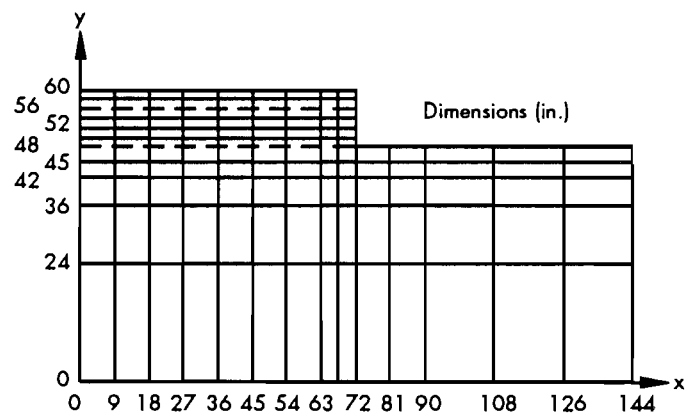


**Figure 5.1** Mesh configuration used to analyze the bonded overlay edge condition

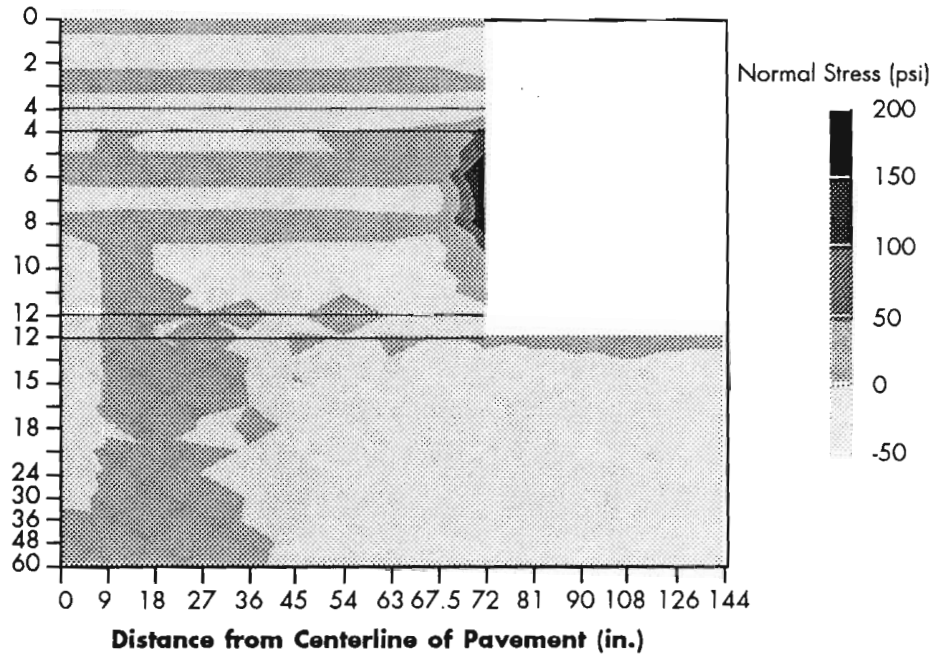


**Figure 5.2** Normal stress contour for a 4-inch BCO on an 8-inch CRC pavement 24 hours after placement

to scale. The values shown represent the stresses 24 hours after the overlay was placed. The overlay was placed on a winter morning and, at the time of analysis, the temperature distribution was as shown in Figure 5.5.

Examination of these plots shows several interesting features. First, the thermal stresses in the subbase and roadbed material are minimal. This is due, in part, to the fact that below depths of about 6 inches very little temperature change occurs in

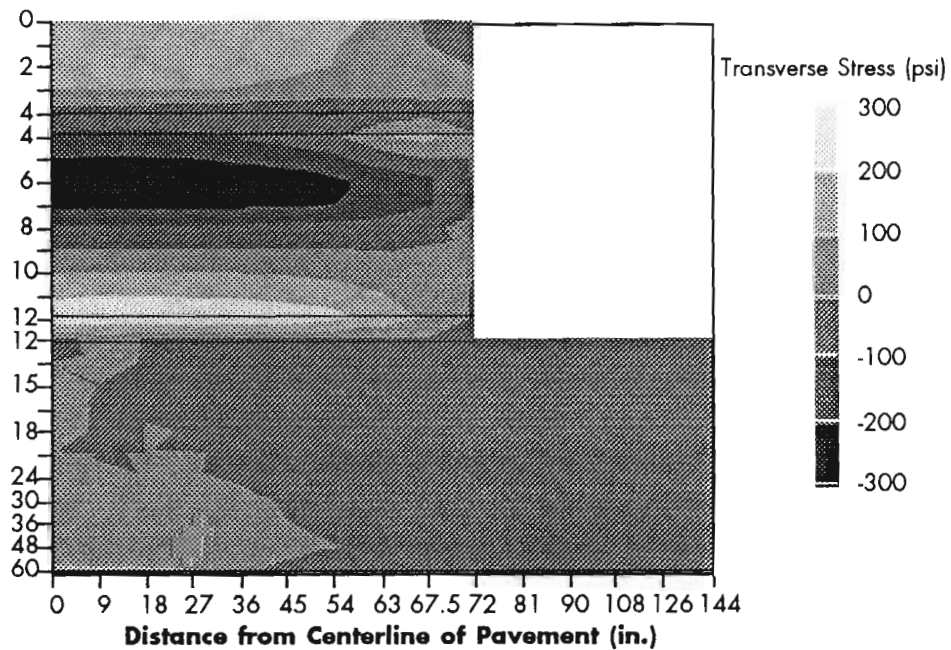


**Figure 5.3** Transverse stress contour for a 4-inch BCO on an 8-inch CRC pavement 24 hours after placement

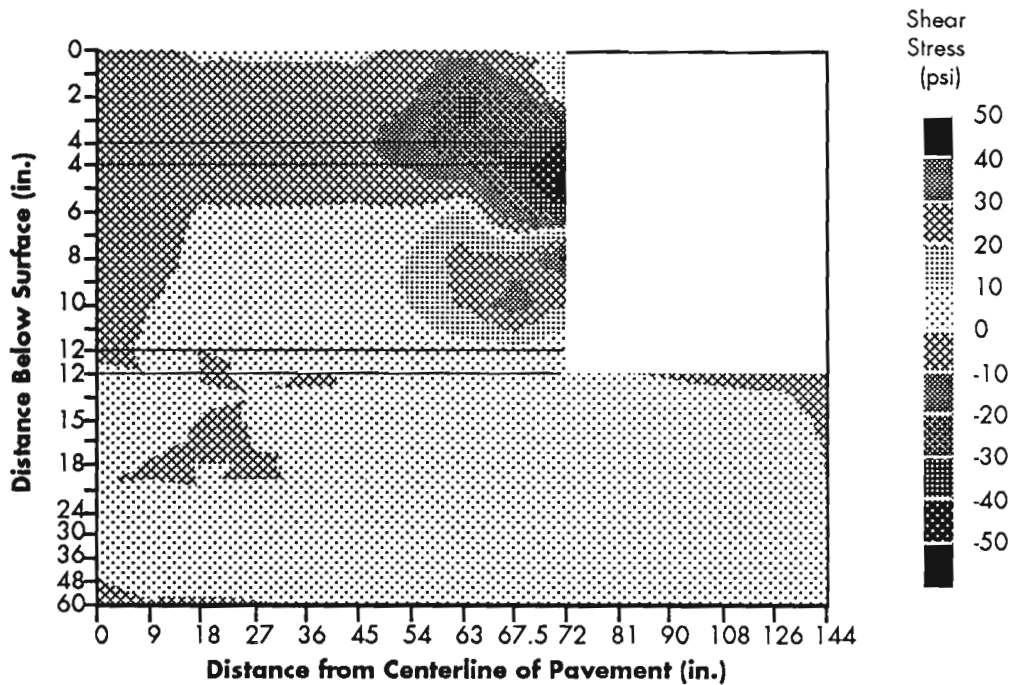


**Figure 5.4** Shear stress contour for a 4-inch BCO on an 8-inch CRC pavement 24 hours after placement.

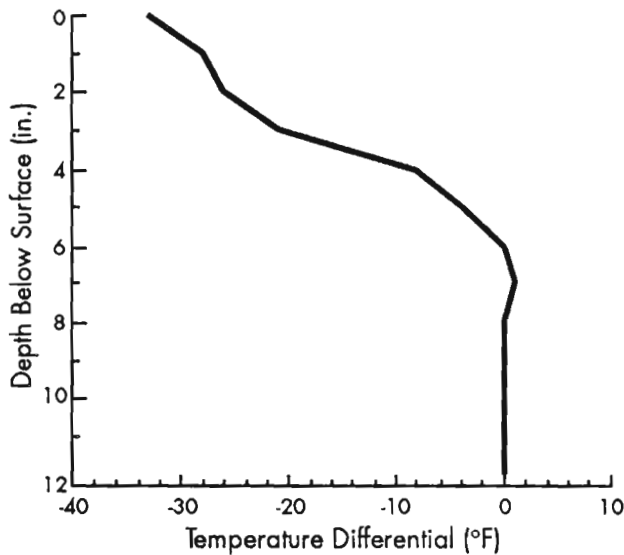


**Figure 5.5** Temperature distribution with depth 24 hours after a winter morning placement

sponse to diurnal changes. Also, very little stress is transferred through shear across the interface between the existing slab and the subbase. It is assumed that over the service life of the existing slab, much of the initial bond between the subbase and

the slab has deteriorated through water and fines infiltration and years of cyclic thermal movements. Therefore, the shear stress at the interface is low.

The width of the analysis section can have an important effect on the calculated stresses. If the section is too narrow, then the boundary conditions have an undue influence on the interface stresses. If the section is too wide, then computer time is used unnecessarily. As can be seen from the contour plots (Figures 5.2 through 5.4) there is a region of relatively constant stress for a given depth beginning some distance from the pavement edge. This indicates the pavement width selected for analysis (6 feet) is sufficient to minimize the influence of the boundary conditions.

Since the subbase and roadbed have low stresses throughout the area of interest and delamination occurs at the interface, Figures 5.2 through 5.4 were redrawn to allow the stresses in the concrete to be examined more closely. Figures 5.6, 5.7, and 5.8 show the normal, transverse, and shear stresses in the concrete layer, respectively. The normal and shear stress plots are of particular interest, since it is these stresses that initiate debonding. The plots of normal and shear stress (Figures 5.6 and 5.8) show regions of high stress concentrated near the interface at the free edge. Although the magnitude and exact location of this zone of high stress varies with the combination of environmental condition and material

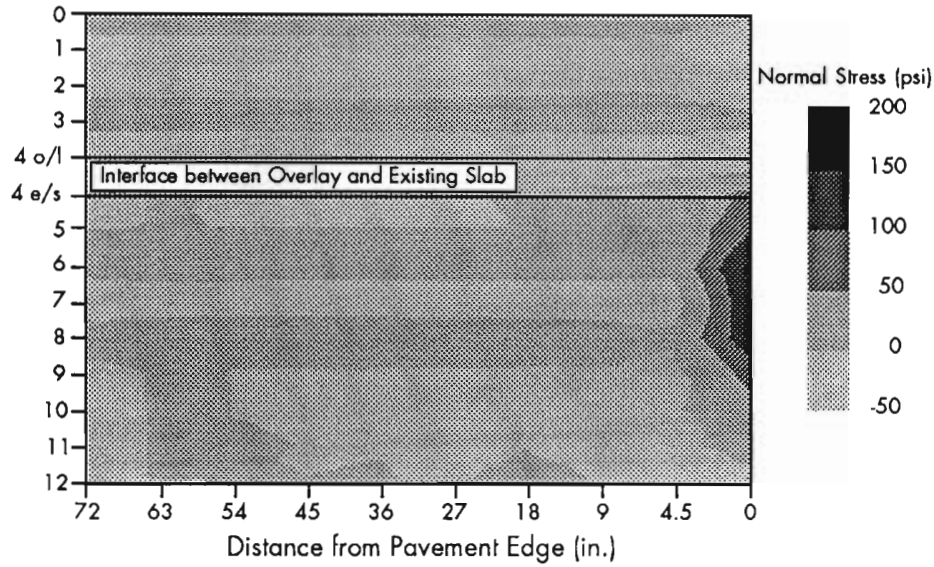


Figure 5.6 Contour plot of the normal stresses in the concrete

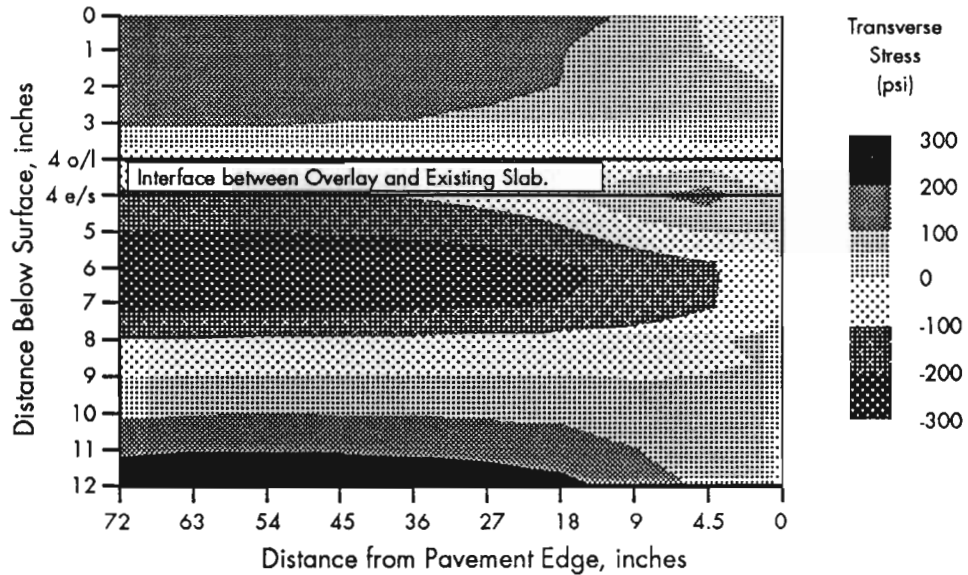


Figure 5.7 Contour plot of the transverse stresses in the concrete

considered, each analysis of the edge condition had a similar stress pattern.

Grimado (55), Al-Negheimish (66), Branson (52), and Roll (53) all reported that the stress is the highest at the free edge and will approach zero within a distance approximately equal to the combined thickness of the layers under consideration. Figures 5.6

and 5.7 demonstrate what was a consistent pattern of stress distribution along the interface for all edge analyses. This stress regime is consistent with the results from closed form solutions and other finite-element analysis. It is also consistent from an observational perspective, since all delaminated areas found in the Houston, Texas overlays were associated with

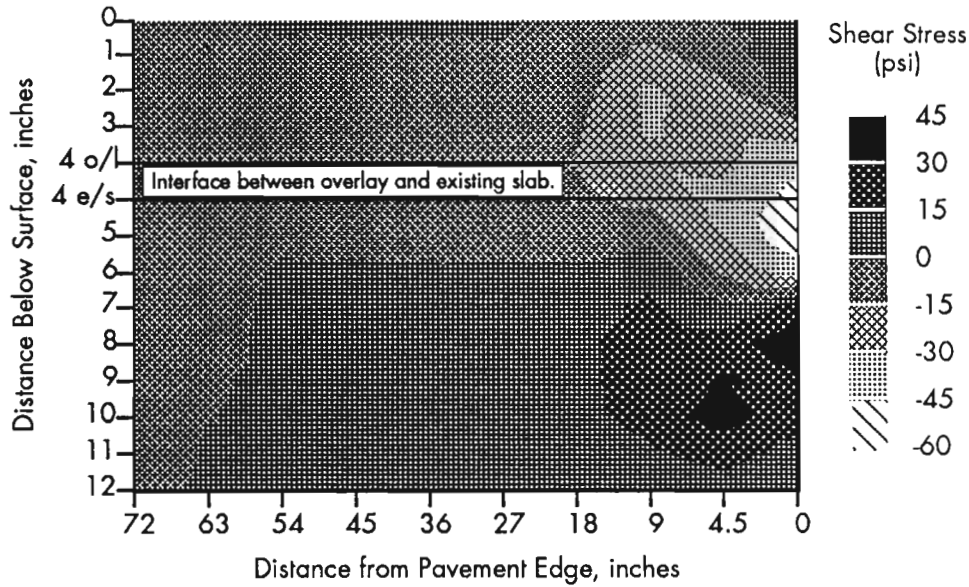


Figure 5.8 Contour plot of the shear stresses in the concrete

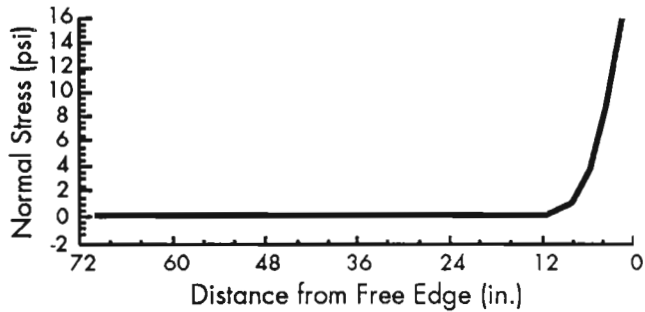


Figure 5.9 Normal stress distribution along the interface between the overlay and the existing slab

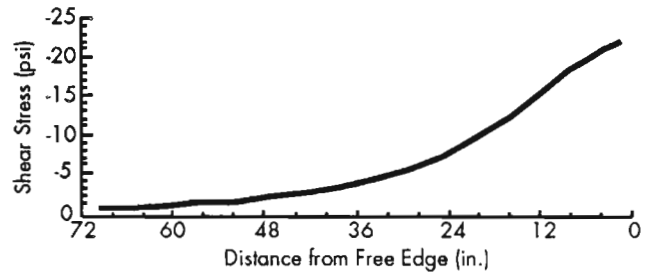


Figure 5.10 Shear stress distribution along the interface between the overlay and the existing slab

an "edge", where edge is taken to include a transverse or longitudinal crack or the actual edge of the pavement.

Figures 5.9 and 5.10 represent horizontal cross sections taken at the interface between the overlay and the existing slab. Figure 5.9 shows the shear stress on vertical cross sections taken at distances of 0 and 9 inches from the pavement edge. The influence of the slip element, which characterizes a zone of potential debonding, is clearly seen at the interface between the overlay and the existing slab (4 inches below the surface). The discontinuity is indicative of the slip at this interface.

## 5.2 EDGE CONDITION ANALYSIS

The factorial developed in Chapter 4 to investigate the stresses resulting from thermal loadings in the edge condition is repeated below in Figure 5.12. Two rows in this factorial were considered first because bonded overlays with similar combinations of material properties have been placed in Houston, Texas. The first row in the factorial represents the Loop IH 610 North overlay project in which a siliceous river gravel concrete overlay was placed on an existing siliceous gravel CRC pavement. Here, the thermal coefficients and the 28-day moduli of both layers can be assumed to be equal to each other. The assumed modulus was 6,000,000 psi and the thermal coefficient was

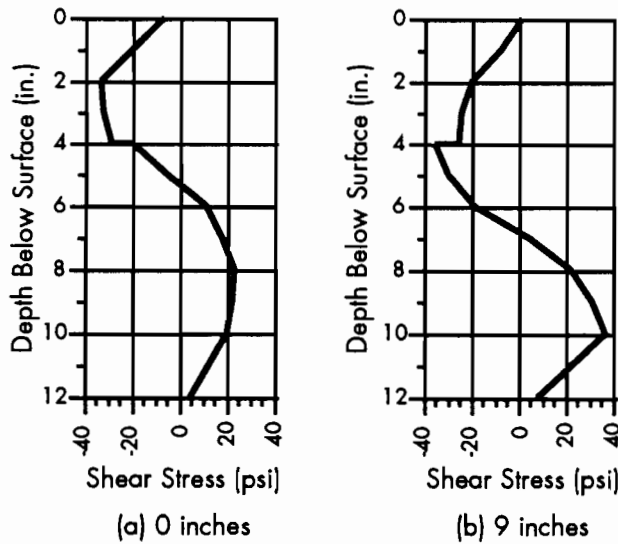


**Figure 5.11 Vertical distribution of stresses showing the influence of a horizontal slip element**

6,000,000 psi and the thermal coefficient was 0.000006 in./in./°F. A second overlay, constructed on Loop IH 610 South, placed a crushed limestone aggregate concrete over an existing siliceous river gravel CRC pavement. In this case, the modulus at 28 days and the thermal coefficient of the overlay were assumed to be equal to 4,000,000 psi and 0.000004 in./in./°F, respectively. The existing slab on the South Loop project had the same properties as the existing slab on the North Loop job. The thicknesses of both overlays were nominally 4 inches, but the two rows identified in Figure 5.12 include 2-inch overlays.

The maximum tensile and shear stresses calculated for these cases are shown in Figure 5.13. A comparison of the stresses indicates that, for all environmental combinations considered, the use of the lower modulus, lower thermal coefficient concrete on the South Loop project resulted in lower interface stresses. Overall there was an average reduction of 50 percent in tensile stress and 40 percent in shear stress as a result of using limestone aggregate. The highest stresses were found 24 hours after a summer or winter placement in a 4-inch-thick overlay. These high stresses led to the analyses of all material combinations of 2- and 4-inch overlays placed during a summer or winter morning. Maximum tensile and shear stresses for all runs are shown in Figure 5.13.

Examination of these data yields several interesting conclusions. First, the morning placements, summer or winter, result in higher stresses than the afternoon placements for both the 2- and 4-inch overlays.

This result is logical and was expected, after a review of the temperature distributions for the morning and afternoon placements (see Tables 4.5 and 4.6), in which the most severe temperature gradients in the overlay were found for the morning conditions. For example, the temperature differential between the surface and the bottom of the overlay for the winter morning placement is -25°F. The temperature differential for the winter afternoon placement is +14°F. The morning placement distribution results in maximum shear stresses of 22 psi, while the afternoon placements yield a maximum shear stress of only 6 psi.

The maximum tensile and shear stresses also are universally higher 24 hours after placement compared to those calculated 12 hours after placement. Again, an examination of the assumed temperature distributions (Tables 4.5 and 4.6) reveals the cause of the increased stress. The temperature gradient in the overlay is much more severe at 24 hours than at 12 hours. The temperature gradient 12 hours after placement for an overlay on a winter morning is only 12 degrees, while at 24 hours the gradient is 25 degrees. The interfacial stresses 24 hours after placement are therefore higher in the pavement system than the stresses at 12 hours. In and of itself, this does not indicate that the period of 24 hours after placement is the most likely time for delamination. Even though the 24-hour stresses are higher, it must be remembered that the interface strength is also higher at 24 hours.

In order to allow the interface shear and tensile stresses to be predicted for a given set of environmental conditions, multiple regression analyses were run. The analyses used overlay and existing slab moduli and thermal coefficients as the independent variables. Separate analyses were made for each of the environmental conditions where high interface stresses were noted. The results are shown in Table 5.1 for shear stress and in Table 5.2 for tensile stress. The general form of the equation is as shown below.

$$x = A_0 + A_1E_o + A_2E_e + A_3\alpha_o + A_4\alpha_e$$

where

$x$  = parameter of interest, shear stress,  $\tau$ , or normal stress,  $\sigma$ ,

$E_o$  = modulus of the overlay,

$E_e$  = modulus of the existing slab,

$\alpha_o$  = thermal coefficient of the overlay,

$\alpha_e$  = thermal coefficient of the existing slab, and

$A_i$  = regression coefficients.

From these results it is obvious that the thermal coefficient of the overlay is the most important

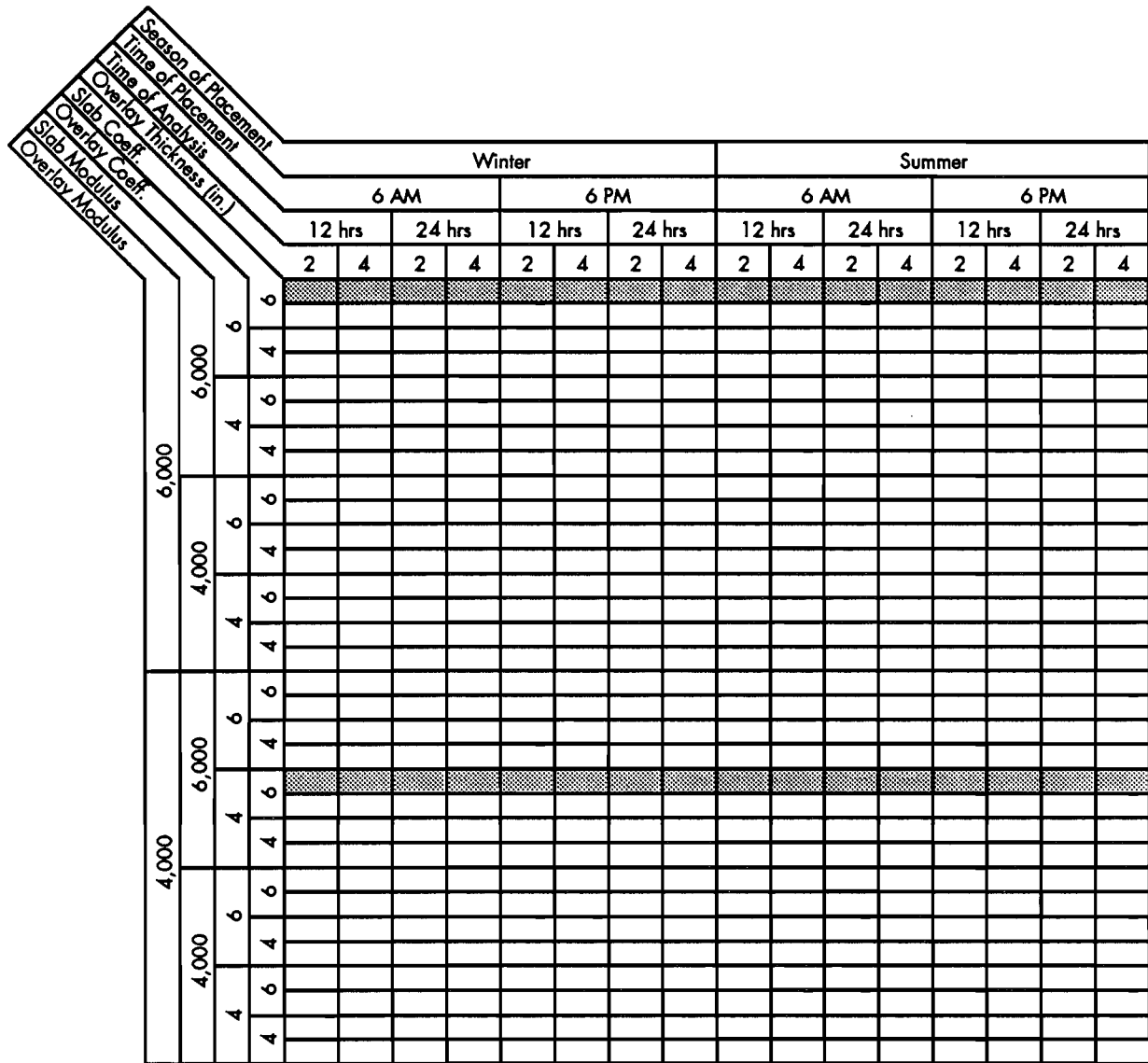


Figure 5.12 Analysis factorial developed for the edge condition

Table 5.1 Results from regression analysis of shear stress values 24 hours after placement

Regression Parameter	Winter	Winter	Summer	Summer
	Morning	Morning	Morning	Morning
	2 in. Overlay	4 in. Overlay	2 in. Overlay	4 in. Overlay
A <sub>0</sub>	-17.15	-10.45	-7.25	-3.89
A <sub>1</sub>	1.88	0.95	0.78	0.081*
A <sub>2</sub>	1.15	1.1	0.52	0.78
A <sub>3</sub>	3.55	4.11	2.05	2.5
A <sub>4</sub>	-0.88	-0.89	0.2*	-1.16
R <sup>2</sup>	0.92	0.99	0.97	0.89

\*Partial F < 1.0



element of the parameters analyzed. Given that the modulus and thermal coefficient of the existing slab are fixed in a given rehabilitation project, then the greatest reduction in the interface shear and tensile stresses will result from the use of an overlay concrete with a lower thermal coefficient. This technique will reduce the interface stress, but the ratio of the strength to stress at the time of analysis is of equal importance.

The interface strength is increasing with time after placement. Therefore, it is more appropriate to examine the ratio of strength to stress rather than the stress alone when attempting to determine the likelihood of delamination. Ratios of strength to stress were calculated for all BCO combinations investigated. These values are shown in Figure 5.14 for both tensile and shear stress. Examination of these data shows that under certain environmental

Season of Placement	Time of Placement	Time of Analysis	Overlay Thickness (in.)	Overlay Coeff.	Slab Coeff.	Overlay Modulus	Slab Modulus	Winter								Summer								
								6 AM				6 PM				6 AM				6 PM				
								12 hrs		24 hrs		12 hrs		24 hrs		12 hrs		24 hrs		12 hrs		24 hrs		
								2	4	2	4	2	4	2	4	2	4	2	4	2	4	2	4	
6,000	6	6	6	6	6	6	6	11	6	5	4	8	9	10	14	11	6	6	9	18	14	6	39	
								-	4	5	3	6	27	-	32	-	12	4	5	13	6	-	16	
										4	4							6	7			7		
										4	3							4	4			-		
											7								27					
											4								13					
	4,000	6	6	6	6	6	6	6			6	4							7	11		7		
											5	3							5	6			-	
											4	4							7	8			8	
		4	4	4	4	4	4	4	4				3							5	5		-	
													8							33				
													5							14				
6,000	6	6	6	6	6	6	6			6	4							7	10		8			
										6	3							5	6			-		
										5	4							7	8			9		
	4	4	4	4	4	4	4	4	17	8	14	8	19	19	16	-	28	9	10	11	45	26	10	33
									-	4	11	5	13	36	-	-	-	19	8	25	31	28	-	26
												7							16					
4,000	6	6	6	6	6	6	6				4								9					
										7	5							7	12			8		
										6	3							5	7			-		
	4	4	4	4	4	4	4	4			8	5							7	9		9		
											5	3							5	5			-	
												9							35					
4	4	4	4	4	4	4	4				5								16					
											7							18						
											5							10						

Notes: Shaded areas are tensile strength-to-tensile stress ratios.  
 Non-shaded areas are shear strength-to-shear stress ratios.  
 Dashes indicate ratios greater than 50.

Figure 5.14 Ratios of interface strength to shear and normal stress for various combinations of BCO materials

conditions delamination would be more likely to occur 12 hours after placement even though the interface stress is higher 24 hours after placement. This is particularly true for 4-inch overlays placed in the afternoon. However, all ratios show the interface strength to be at least 3 times the stress.

The role of material properties in determining the interfacial stress is somewhat more complicated. However, generally, when the thermal coefficient in the overlay is equal to or higher than the coefficient of the existing slab, higher stresses result. Stresses increase by as much as 100 percent when a higher thermal coefficient material is used above a lower coefficient compared to the reverse situation. Again, this result is logical since it is known that a higher thermal coefficient in the region with the highest temperature gradient will develop larger thermal movements. Furthermore, it is corroborated by the regression analyses shown in Tables 5.1 and 5.2.

Perhaps the most significant feature of the analyses conducted to ascertain the magnitude of the interfacial stresses at early ages at the free edge is that delamination did not occur under any combination of material and environmental condition. The maximum shear stress was about 25 psi and the maximum tensile stress was 17 psi. The ratios shown in Figure 5.14 demonstrate that, in all cases, the average interface strength was at least three times the calculated stress. Thus, based on the edge analyses, even under extremely harsh environmental conditions, delamination is unlikely unless the interface strength is very low.

### 5.3 INTERIOR CONDITION ANALYSIS

The analyses used to determine the influence of vertical cracks in the existing slab or overlay were collectively termed interior conditions. The presence of transverse cracks in either the existing CRC pavement or in the overlay was modeled using the two systems shown in Figures 5.15 and 5.16. The pavement systems shown are intended to address fundamental concerns regarding the design and performance of bonded overlays as they relate to cracking in the pavement.

It has been proposed that, under ideal circumstances, the overlay would develop no more cracks than the existing CRC had before the overlay was placed. Yet, studies of both recently placed overlays and those in service for a number of years indicate that many cracks develop in the overlay which are not present in the existing slab. The intent of this study is not to determine the ultimate mode of failure or the influence of these non-reflective cracks on that failure, but it can be reasoned that any increase in the number of cracks in the surface of a pavement

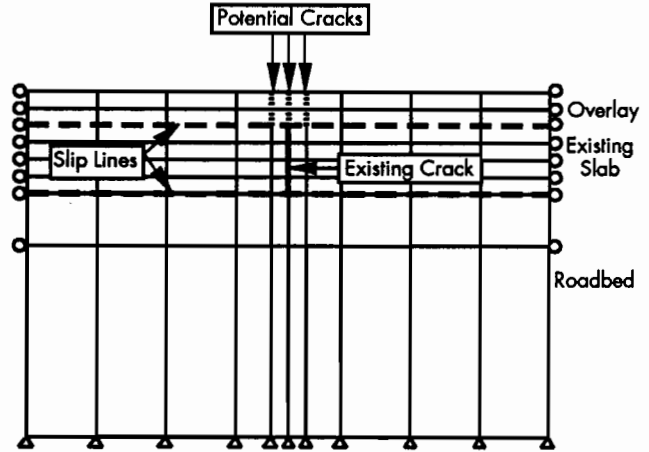


**Figure 5.15** System analyzed to determine the influence of transverse cracks in the existing slab

is detrimental to the performance of the composite structure. These cracks tend to negate some of the benefit to be derived from the placement of a bonded overlay. Each crack is a potential site of spalling and will allow the infiltration of fines or water. Also, given the location of debonded zones in the Houston, Texas overlays, any crack is a potential site of delamination. It is therefore important to understand the nature of cracks in the overlay, particularly as they affect the development of interfacial stress at early ages.

The first pavement system investigated (Figure 5.15) had cracks in the existing CRC slab. The intent of the investigation was to determine whether or not the additional cracking observed in the field resulted

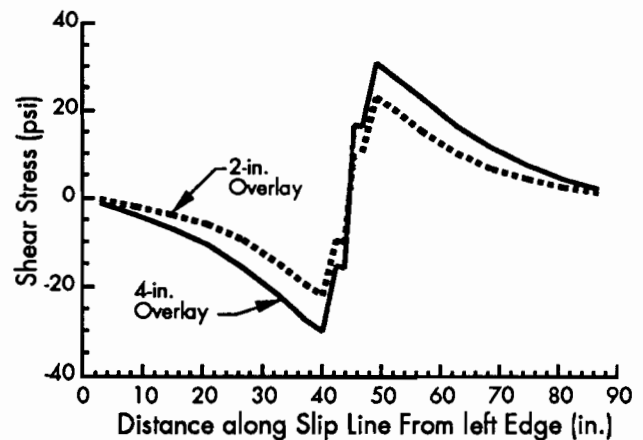


**Figure 5.16** Interfacial shear stress distribution in the vicinity of a vertical crack in the existing slab

from cracks propagating from below. This phenomenon would be possible only if the crack moved horizontally along the interface before moving upward through the overlay. This horizontal migration of the crack would effectively create a debonded zone between the existing crack and the new crack in the overlay.

The results obtained from the FEM program indicate a crack in the existing CRC slab will propagate through the overlay if a slip element is aligned with the existing crack. The aligned vertical slip element was given the same shear and tensile strength limits as the horizontal slip elements in each analysis. Therefore, there was the same opportunity for the formation of a vertical reflective cracking as for the formation of a horizontal delaminated zone. In all the cases analyzed, a reflective crack formed without any adjacent debonding. Although no delamination occurred near the crack, the shear stress in the vicinity of the crack was higher than that calculated for the free edge. The maximum shear and tensile stresses were 30 and 21 psi., respectively. The distribution of shear stress is shown in Figure 5.17. The distribution of stresses on either side of the crack is very similar to that described above for the free edge condition, i.e., high stress near the crack, which decreases to zero with distance from the crack. The maximum shear values are about 30 percent higher than for the free edge condition, but are still approximately one-half the interface strengths. Before proceeding with an analysis of this interior scenario similar to that undertaken for the edge condition, a second interior situation was investigated.

The second system analyzed assumed that a crack had formed in the new overlay some distance from a crack in the old CRC pavement. This crack would have been initiated by volume change stresses in the overlay. These volume change cracks would

initiate at the surface of the overlay propagating downward to the interface. The crack would have been initiated by plastic shrinkage cracking resulting from ineffective curing. The objective was to investigate the interfacial stresses resulting from the presence of this crack and whether or not these stresses were of sufficient magnitude to cause debonding. Two analyses were conducted. The cracks in the existing pavement and overlay were located from each other at distances of 3 and 6 inches. For both these investigations, the winter morning placement environmental conditions were used. Analyses were conducted of 2- and 4-inch overlays 24 hours after placement.

A similar distribution of stress can be seen near a non-reflective vertical crack in the overlay (see Figure 5.18). The figure shows that shear stress at the interface between the two vertical cracks is low and delamination does not occur.

The interior condition produced higher stresses than the free edge condition for the same combination of environmental conditions and materials. The two scenarios investigated yielded essentially identical maximum shear and tensile stresses. Therefore, because less computer time was required to analyze the reflective crack, an analysis factorial similar to that used in the analysis of the edge condition was investigated. As for the case with the edge condition, the material combination used on the Loop IH 610 North bonded overlay project was first investigated for combinations of environmental conditions. Selected environmental conditions which produced higher shear or tensile stresses were then studied to determine the effect of varying combination of materials. The shear and tensile stresses calculated are shown in Figure 5.19. Ratios of strength to stress are shown in Figure 5.20.

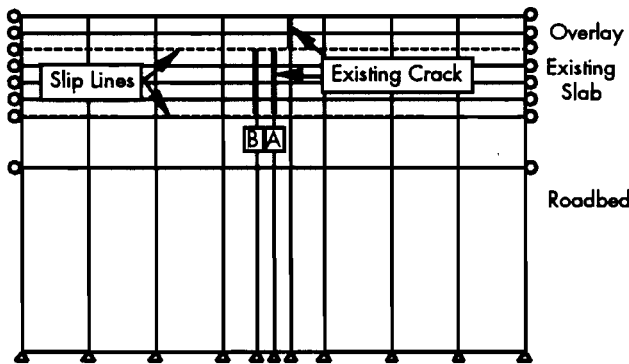


**Figure 5.17** System used to analyze the influence of non-reflective cracking in the overlay

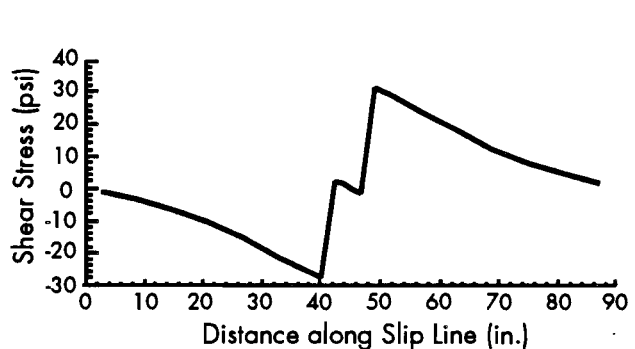


**Figure 5.18** Interfacial shear stress distribution in the vicinity of a non-reflective crack in the overlay

Season of Placement:	Time of Placement:	Overlay Thickness (in.)	Overlay Coef.	Slab Modulus	Overlay Modulus	WINTER								SUMMER										
						6AM				6PM				6AM				6PM						
						12 hrs		24 hrs		12 hrs		24 hrs		12 hrs		24 hrs		12 hrs		24 hrs				
						2	4	2	4	2	4	2	4	2	4	2	4	2	4	2	4			
6,000	6	6	6	6	6	3.6	0.1	20.7	28.7	7.2	6.7	-	-	-	-	14.9	15.3	3.1	3.8	-	-			
						0.0	0.1	11.5	21.4	5.3	1.5	-	-	-	-	11.0	12.0	2.4	4.8	-	-	-	-	
6,000	6	4	6	6	6			23.1	30.3							14.8	18.0							
								12.5	22.3							11.0	13.6							
								11.3	17.6							10.4	7.5							
								6.8	13.4							7.5	6.5							
4,000	6	4	6	6	6			13.8	19.3							10.1	10.3							
								7.6	14.3							7.4	8.0							
								20.3	27.1							14.5	14.7							
								11.3	20.7							10.8	11.8							
4,000	6	4	6	6	6			22.6	28.5							14.3	17.2							
								12.2	21.5							10.7	13.2							
								11.3	16.7							9.9	7.4							
								6.7	13.0							7.3	6.4							
6,000	6	4	6	6	6			13.5	18.1							9.7	9.9							
								7.5	13.7							7.2	7.8							
								16.7	24.5							12.3	12.9							
								9.8	19.2							9.3	10.7							
4,000	6	4	6	6	6			18.9	25.9							12.1	15.4							
								10.8	20.1							9.2	12.1							
								9.1	15.0							8.3	6.2							
								5.6	12.0							6.3	5.7							
4,000	6	4	6	6	6			11.2	16.4							8.3	8.8							
								6.5	12.8							6.2	7.1							
								16.7	23.4							11.9	12.6							
								9.4	18.6							9.1	10.5							
4,000	6	4	6	6	6			18.6	24.7							11.8	14.8							
								10.6	19.4							9.1	11.8							
								9.1	14.4							8.2	6.2							
								5.6	11.6							6.2	5.7							
4,000	6	4	6	6	6			11.0	15.7							8.0	8.5							
								6.4	12.4							6.1	6.9							

Notes: Shaded areas indicate normal stresses.  
Non-shaded areas indicate shear stresses.

Figure 5.19 Shear and tensile stresses calculated for interior condition

Analyses of the edge and interior conditions have shown that, for the combinations of materials representing normal concretes, interfacial stresses are less than the estimated strengths. The environmental conditions selected for these analyses were the harshest that realistically could be expected to occur under normal construction scenarios. While it is certainly possible to cause debonding in the computer model through the selection of either a weaker interface or a steeper thermal gradient in the overlay, these conditions are not representative of normal overlay construction. Given that the environmental

conditions and interface strengths input are appropriate, then there is still the question of what caused the observed delamination. It must be concluded that the interface strength in those areas that debonded was extremely low at early ages, on the order of 20 to 40 psi.

#### 5.4 SUMMARY

The results from the analyses of the factorial developed in the previous chapter were evaluated. This evaluation determined that higher interfacial stresses develop in winter or summer morning

Season of Placement	Time of Placement	Overlay Thickness (in.)	Slab Coeff.	Overlay Coeff.	Slab Modulus	Overlay Modulus	Winter								Summer							
							6 AM				6 PM				6 AM				6 PM			
							12 hrs		24 hrs		12 hrs		24 hrs		12 hrs		24 hrs		12 hrs		24 hrs	
							2	4	2	4	2	4	2	4	2	4	2	4	2	4	2	4
6,000	6	6	14	-	4	3	7	7					6	6	14	11						
			-	-	4	2	5	17					4	4	18	9						
		4	4	3								6	5									
			3	2								4	3									
		6	8	5								8	11									
			6	3								6	6									
	4	6	6	4							8	8										
			6	3							6	5										
		4	4	3							6	6										
			4	2							4	4										
		6	4	3							6	5										
			3	2							4	3										
4,000	6	6	8	5									9	11								
			6	3							6	7										
		4	6	5								9	9									
			6	3								6	5									
		6	5	3								7	7									
			4	2								5	4									
	4	6	4	3										7	6							
			4	2										5	3							
		6	9	6										10	14							
			8	4										7	7							
		4	8	5										10	10							
			6	3										7	6							
4,000	6	5	4									7	7									
		4	2										5	4								
	4	5	3										7	6								
		4	2										5	4								
	6	9	6										10	14								
		8	4										7	7								
4	8	5										11	10									
	7	3										7	6									

Notes: Shaded areas indicate normal strength-to-normal stress ratios.  
 Non-shaded areas indicate shear strength-to-shear stress ratios.

Figure 5.20 Strength to stress ratios for calculated stresses shown in Figure 5.19

placements compared to afternoon placements. The critical time after placement appears to be 24 hours following placement for most overlay systems analyzed. Lower interfacial stresses result when the modulus and thermal coefficient of the overlay are lower than the modulus and thermal coefficient of the existing pavement. However, even under the harshest environment and worst combination of materials, the interface stresses were only about one-third the estimated interface strength.

The interior analyses revealed that higher interfacial stresses develop in the vicinity of transverse cracks than develop at the free edge under similar environmental conditions. Although

the stresses were about 30 percent higher than for the free edge condition, the average interface strength was approximately 200 percent higher than the calculated stress. All analyses conducted indicate that delamination will not occur under normal circumstances, unless the interfacial strength is extremely low, or the rate of gain of this strength is low.

The analysis results show that the tensile and shear stresses are concentrated near the free edge of the pavement or near a crack in the overlay. The concentration of stresses in these two zones corresponds to location of delamination observed in the field.

## CHAPTER 6. DESIGN AND CONSTRUCTION OF BONDED OVERLAYS

Based on the evaluation of bonded overlays conducted in the previous chapter, the next logical step is to apply the results to the design, specification, and construction of bonded overlays. The objective of this chapter is to provide guidelines that will reduce the risk of delamination at early ages. Even though the calculated interfacial stresses were considerably less than the estimated interfacial strength for all combinations investigated, delamination has occurred on several overlay projects throughout the country. Therefore, there must be combinations of environmental conditions and materials that result in debonding. These critical combinations can be avoided and the probability of delamination reduced through a proper design and careful control of the overlay construction.

The experience gained during the computer analysis in the laboratory and from construction will be combined to assure, to the extent possible, that delamination will not occur. The calculated tensile and shear stresses are compared to the expected strength at the interface to allow the selection of appropriate material combinations, construction procedures, and specifications that minimize the chance of delamination. The development of these guidelines is divided into three categories: (1) design, (2) specification, and (3) construction. While adherence to these guidelines will not guarantee the long-term success of the overlay, experience to date has shown that if the overlay does not debond at early ages, then the rehabilitation will likely be a success. Therefore, the early-age performance, particularly with regard to the prevention of debonding, is paramount to the success of the overlay.

### 6.1 DESIGN

Many criteria are used to determine the most appropriate rehabilitation alternative for continuously reinforced concrete pavements. Among the criteria considered are the condition of the pavement, the user costs during construction, traffic handling procedures, expected traffic, and life-cycle costs of various rehabilitation options. Assuming that after consideration of these criteria a bonded overlay is deemed

the most appropriate alternative, then every effort must be made to ensure that the overlay will perform as intended. The long-term performance of the overlay depends on several factors, which are discussed in considerable detail in Reference 46. If these features are taken into account, then the success of the overlay at early ages is dependent on the two design parameters that have the greatest influence on the interface stress. These two parameters are the thickness of the overlay and the type and location of the reinforcement.

#### 6.1.1 Thickness

The selection of the thickness of the overlay must include consideration of four criteria. First, the thickness must be sufficient to carry the expected traffic. Second, the impact of the thickness on various physical aspects of the facility must be recognized. Thickness may affect the cross-slope drainage or overhead clearances. These considerations may preclude the use of thicker overlays, particularly in some urban areas. Limitations on clearances, and the increased project costs associated with raising overhead structures, would favor the use of thinner overlays. These factors are case specific and therefore will not be included in further discussions. Third, the overlay thickness may be considered an indicator of the frequency of required maintenance and the time to the next major rehabilitation, i.e., the long-term performance of the overlay. It is commonly assumed that, within limits, a thicker overlay will last longer with less maintenance than a thin overlay placed under similar circumstances. Thus, with other things equal, thicker overlays would be favored due to the lower life cycle and user costs. Finally, the early-age influence of overlay thickness must be considered. Here the role of thickness in increasing or reducing the interfacial stress is considered. Because of the case-specific nature of facility considerations and the uncertainty of the long-term performance of bonded overlays, only the early-age structural implications of overlay thickness will be considered.

The results from the FEM analysis of 2- and 4-inch bonded overlays show that, in some cases, the

interfacial shear and tensile stresses were lower for the 2-inch overlays than for the 4-inch overlays. This would lead one to think that the 2-inch overlay would be less likely to delaminate than the 4-inch overlay. However, an important feature is not the calculated stress, but the minimum ratio of the interface strength to the stress for a given combination of materials. The strength to stress ratios for the material combinations used on the North and South Loops were averaged separately for the 2- and 4-inch overlays. When this was done for all seasons and times of placement, it was found that there was no clear superiority between the two thicknesses. These data are shown in Table 6.1. Therefore, given that a shorter service life is expected from a 2-inch overlay, 4-inch overlays have an advantage.

Limited analyses were conducted on 6-inch overlays to determine the strength-to-stress ratios for thicker overlays. While there is a slight increase in the stress in the thicker overlay (about 5 percent), the difference in the strength-to-stress ratio is not significant. Overlays thicker than 4 inches have not normally been used because of the additional loss of overhead clearance.

Field experience in the Houston, Texas area has shown that 2-, 3-, and 4-inch bonded overlays can be successfully placed on existing 8-inch CRC pavements under a variety of environmental conditions. Current design practice favors the placement of 4-inch overlays. This decision is predicated on the assumption that thicker overlays will last longer than thinner overlays and that overlays thicker than 4 inches cause an unnecessary reduction in overhead clearance. However, when overhead clearances are not a limiting factor, there is no reason why a 6-inch bonded overlay could not be used, based on early-age criteria. Cost is a consideration, however; other types of rehabilitation should be considered if a 6-inch BCO is calculated.

### 6.1.2 Reinforcement

The FEM analysis of reinforcement in bonded overlays was severely limited by the implementation

of the bar elements in the program. Further limiting the analysis was the restriction on the total number of elements to be used in a given run. When considered together, these restrictions prevented locating reinforcement at the actual level of the mesh in the field. This limitation is not considered particularly damaging in the early-age analysis of overlay, due to the low bond stress transfer potential of concrete at early ages. Field experience must therefore be relied upon to develop guidelines for reinforcement.

Field experience has shown that overlays can be successfully placed using welded wire fabric, steel fibers, or no reinforcement. The current design practice in the Texas State Department of Highways and Public Transportation (SDHPT) favors the use of steel mesh reinforcement in the overlay at the same percentage as the existing CRC pavement. Steel mesh reinforcement is used for two reasons. First, should any debonding occur, the mesh will limit the safety hazard due to loss of the overlay under traffic by keeping the area in place until repairs can be effected. Second, it is felt that the use of the same percentage steel in the overlay as was used in the existing slab will result in the same crack spacing and width in the overlay as was found in the existing slab. While the first reason is most certainly sound and, in fact, has been shown to be of value in the field, the second reason requires some additional discussion.

The crack pattern in the existing CRC pavement developed as a result of the curing temperature, concrete strength, subbase friction, early-age environmental conditions, and years of traffic loading. Even if materials similar to those in the existing slab are used in the overlay, it is unlikely that a similar pattern will develop in the overlay as a result of the use of the same amount of steel. The environmental conditions, physical dimensions, and the restraint of the underlying layers are completely different. It is possible, however, that if the cracks in the existing slab reflect through the overlay the reinforcement will control the crack width in a manner similar to that of the existing slab steel. Surveys of in-place overlays in Texas have shown, however, that many non-reflective cracks form (46).

The presence of the non-reflective cracking further compounds the problem of determining the influence of the reinforcement. Texas SDHPT designs currently allow the mesh to be placed directly on the existing CRC. Examination of Figure 6.1 shows the influence of reinforcement on reflective and non-reflective cracks. The usefulness of the steel in limiting the crack width in reflective cracks is clear. If there is full coverage of the steel, two layers work together to limit the crack width. However, because of the location of the steel, little crack-width control can be gained from the steel in

**Table 6.1** Strength-to-edge-stress ratios for 2- and 4-inch thick overlays similar to those placed on the Loop IH 610 North and South Houston, Texas

Material Combination	Stress	Overlay Thickness	
		2-in.	4-in.
North Loop	Shear	9	13
	Tensile	29	13
South Loop	Shear	20	21
	Tensile	33	24

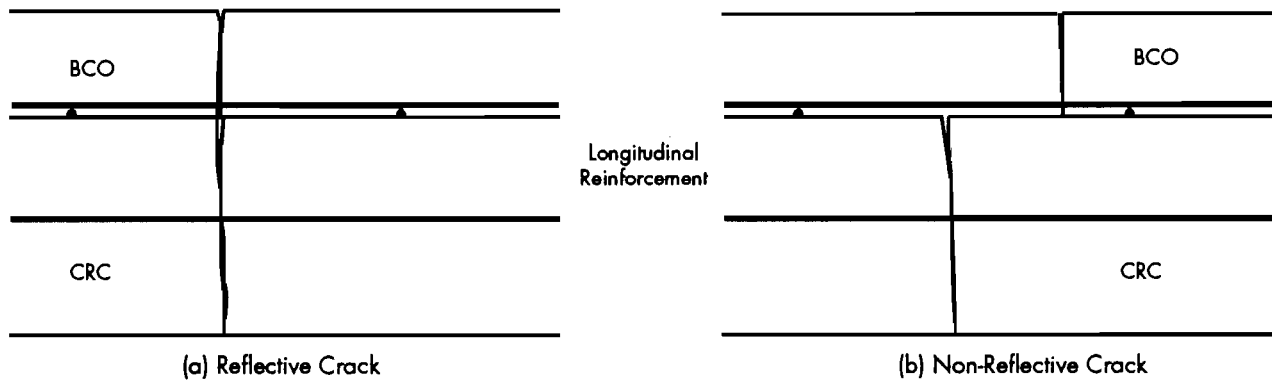


**Figure 6.1 Schematics of the influence of steel on reflective and non-reflective crack-width control**

the case of the non-reflective crack. Here, the steel is located at the bottom of the layer, in what is a compressive stress zone. Therefore, if the steel continues to be placed directly on the existing slab, the main function will remain one of delamination-loss control. It may be possible to prevent the loss of any debonded areas under traffic with a lower percentage steel than that normally required to control crack width and spacing.

The impact of the layer of steel mesh at or near the interface on the strength of the bond between the two layers is not well understood. Logically, the introduction of a layer of steel mesh at the interface would adversely affect the strength. Only limited test results are available, but, when pull-out tests were conducted in one study (105), no significant difference in shear strength could be found when the reinforcing mesh was placed on the existing slab or at mid-depth in the overlay.

Although the vast majority of the overlays placed in Texas have been placed using steel mesh reinforcement, experimental sections have been constructed using steel fibers and using no reinforcement. A 2-inch bonded overlay without any reinforcement in Houston has been in service for seven years without any performance problems. The use of steel fiber reinforcement has been tested in three separate test sections placed over the course of six years. The test sections were placed under a variety of conditions. All are performing well, with little or no delamination.

## 6.2 SPECIFICATION

The specification and construction of bonded overlays are very important to the early-age success of bonded overlay. Since successful overlays have been placed using a variety of thicknesses and materials and several different types of reinforcement, it is likely that the specification of the overlay and the

control of construction are paramount to the success of the overlay. There is no one item that is most important to the successful construction of bonded overlays and, therefore, the discussion that follows covers the construction of a bonded overlay from the selection of materials to the curing of the overlay.

### 6.2.1 Materials

After the decision has been made to construct a bonded overlay, the first step is to select the materials for use in the overlay. The FEM analyses discussed previously showed that the use of aggregates for the overlay concrete that produce moduli and thermal coefficients lower than those found in the existing slab results in lower interfacial stresses regardless of the time or season of placement. This concept was expanded in the last chapter through regression analysis, which showed that the interfacial stresses can be predicted for a given environment with a high degree of accuracy for a combination of overlay and existing slab material properties. This is important because the aggregate type has the major influence on the thermal coefficient and modulus of the concrete. A reduction in the elastic modulus of the aggregate normally results in a reduction of the concrete modulus and the thermal coefficient. This may not be the case with certain types of manufactured aggregates; however, within the limits of the regression analysis, these special cases can be accommodated.

Other materials of interest to the early-age development of stress in bonded overlays are the cement and admixtures used in concrete. In the past, Type I cement has been used successfully and, given the magnitude of the stresses developed at the interface, there does not appear to be a need to use high-early-strength cements. Petrographic analyses of cores taken from delaminated areas on Loop IH 610 North showed the early formation of the products commonly associated with alkali-aggregate reactions

(106). The cause of these formations is not known, but the importance of maintaining the normal specification limit on alkali content should be emphasized.

The use of admixtures of various types is common in concrete pavement construction today. Retarders are used to allow adequate time for transporting and finishing the low slump concretes commonly used with slip form pavers. The influence of these retarders, and other admixtures, on the rate of gain of interface strength is not known. It can be reasoned, however, that if the rate of strength gain in the concrete is substantially reduced, then the rate of interface strength gain will also be reduced. These lower strengths make debonding more likely for a given set of environmental conditions.

### 6.2.2 Surface Preparation

The next step in the specification of bonded overlays is to assure that the existing slab is adequately prepared to receive the overlay. Adequate preparation must include a thorough cleaning of the surface. Bonded overlays have been placed successfully on surfaces prepared using shot blasting, sand blasting, or coldmilling. The texture is much more angular after milling, compared to the rounded aggregate surfaces exposed after shot or sand blasting (see Figure 6.2). From the standpoint of mechanical interlock, the milled surface would be more appealing. However, milling relies on a fracturing of the surface, which may cause microfractures in the remaining material. The importance of this feature is not known, but it may account for the similar interface shear strengths

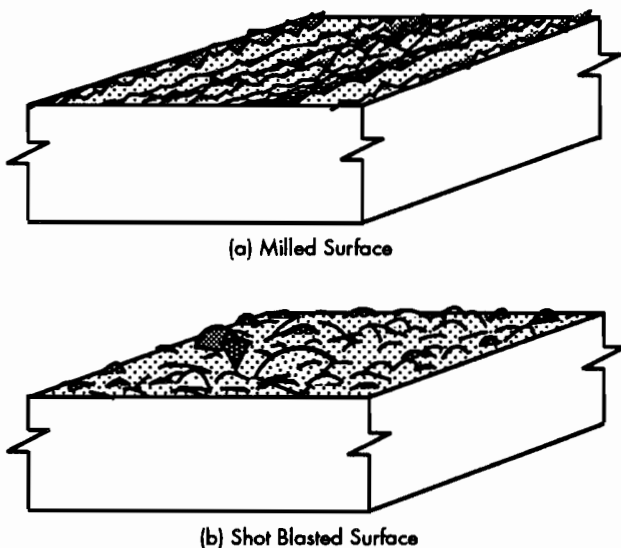


**Figure 6.2** Schematics of milled and shot blast surfaces with equal texture measurements

found in milled and blasted surfaces (see Tables 3.10 and 3.11). Therefore, based on strength alone, there is no reason to specify the method of surface preparation.

Consideration should be given to the cost, rate of production, and environmental desirability of the various alternatives. Cost figures from the Houston area overlay projects indicate that the cost of shot blasting is about one-half the cost of milling. These costs and the rate of production are controlled to some extent through the specification of the depth of removal or required texture. Shot blasting results in less environmental impact from the dust through the shot and dust recovery system included in the newer, self-contained equipment. These factors will change from project to project, but the shot blast technique appears to be the most desirable.

If the method of surface preparation need not be specified to insure adequate bond strength, then the surface preparation must be specified in terms of the depth of surface removal or some standardized texture test method, such as the Texas Sand Patch Test, or a combination of the two. Both methods have advantages and disadvantages. Texture test methods have been standardized and therefore have some known repeatability and error. However, they have the disadvantage that tests can produce precisely the same value of texture for two completely different surface preparation techniques that have markedly different surface characteristics. These tests do not characterize the surface angularity or contour; only the average depth of the surface is determined. Laboratory and field testing have shown that adequate strengths can be obtained using either blasting or milling, and therefore this disadvantage is not significant.

The specification of a particular depth of removal has the advantage that it assures that all surface contaminants are removed and that, if significant carbonation has occurred, this material will be removed. Also, in areas where salts are used to control ice, the specification of a depth of removal can insure that the highly sulfate-contaminated material is removed. When cold milling is used, determination of the thickness removed is relatively easy. However, the depth of removal is sometimes difficult to determine when shot or sand blasting is used and must depend on the experience of the inspector.

In summary, the specification of a surface preparation method is not necessary to assure bond strength. However, to insure that all contaminants are removed from the existing slab, a depth of removal should be specified. The removal of 1/4 inch of material is suggested, but a greater depth may be necessary in areas where sulfate contamination is common. The texture should be checked using the Sand Patch Test or an equivalent.

Until other information is available, an average texture depth of 0.08 inch is suggested.

There are other controls which will be used in the construction of the overlay. These features will be included in the project specifications, but they will be discussed in conjunction with the construction of the overlay.

### 6.3 CONSTRUCTION

The control of the construction of the overlay is important if the probability of delamination is to be reduced. Beyond the normal construction controls that are used for any concrete paving job, certain controls are required that are specific to bonded overlay placement. These construction controls fall into three categories. First, there is a need for environmental controls that provide limits on the time and season of placement so that interfacial stresses can be minimized. Second, limitations on the bonding agent used, and on the condition of the interface at the time the overlay concrete is placed, are necessary. Finally, special precautions are necessary to insure adequate curing of the overlay.

#### 6.3.1 Environmental Controls

The environmental conditions during and immediately after placement of the overlay play a very important role in the development of the interfacial stresses. It has already been shown that for a given combination of materials in the overlay and existing slab, the interfacial shear stress may be increased more than 500 percent, simply by placing the overlay in the early morning instead of the late afternoon. It is therefore prudent to include certain environmental controls during construction.

The analyses indicate that, even under the extreme conditions of time and season of placement, debonding will not occur. Initially, this would tend to indicate that environmental controls are not necessary to the success of overlays. However, the interface strengths used at the analysis times of 12 and 24 hours were based on a seven-day interface strength value of 200 psi. The results of laboratory testing of many different bonded overlay types constructed using a variety of surface preparation techniques and bonding agents show that in all cases the mean interface shear strength was in excess of 200 psi (see Tables 3.10 and 3.11). Theoretically, there should be no debonding.

There is delamination, however, and an examination of the standard deviations of the means shown in Tables 3.10 and 3.11 indicates one possible reason for the occurrence of debonding. The one-tailed confidence intervals for  $\alpha$ -levels of 1, 5, and 10 percent are shown for the shear strengths in Table 6.2. It can be clearly seen that, with the large

standard deviation associated with the shear strength, a large percentage of the total population of any given type of BCO will fall below the suggested limit of 200 psi. Although it cannot be said with certainty, it is likely that the failures that have occurred on the North Loop came about as the result of low strengths combined with severe environmental conditions. This concept can best be illustrated by consideration of the example discussed below.

Assume that a 4-inch overlay was placed on the North Loop under environmental conditions which produced a shear stress at the interface 24 hours after placement of 25 psi. This stress would develop in an overlay placed during a winter morning. If the interface shear strength throughout the placement is 200 psi at seven days, then the estimated strength of 85 psi at 24 hours is adequate and no delamination will occur. However, as with other physical quantities, the interface strength has variability. In fact, in the case of the interface strength, that variability is quite high.

For example, the average shear strength of 25 cores taken from the North Loop overlay project six months after placement was 387 psi. The standard deviation was 155 psi. Assuming the 7-day strength is 75 percent of the 6-month strength, then the strength at seven days was 290 psi. From Table 3.12, the 24-hour strength is one-third of the 7-day strength, or in this case 96 psi. If the magnitude of the coefficient of variation at 24 hours is assumed to be equal to the magnitude of the coefficient at 6 months, then the standard deviation at 24 hours is 38 psi. Now assuming that the interface strength is normally distributed, the  $\alpha$ -level associated with the expected stress of 25 psi is 3 percent. Thus, about 3 percent of the overlay placed under these conditions would have an interface strength less than the stress, and debonding would result. The computed value is reasonable when compared with the extent of delamination on the North Loop. The percentage on Loop IH 610 North was approximately 1.1 percent. The overlay on the North Loop was placed under a variety of conditions, which could account for the differences.

The occurrence of debonding can be accounted for based on the variability of interfacial strength even though the average strength is well above the calculated stress. This would naturally lead to the desire to increase the interface strength through the use of different surface preparation techniques or bonding agents. However, research conducted at The University of Texas at Austin (94) has shown there is no statistical difference among the various surface preparation methods or bonding agents commonly used today. Therefore, if the average interface strength cannot be increased, then the variability

**Table 6.2 One-tailed confidence limits for seven-day laboratory shear strength data**

Surface Preparation	Bonding Agent	Mean Shear Strength (psi)	Confidence Interval		
			90%	95%	99%
Light Shot Blasting	Latex	638	346	263	108
	Epoxy	661	338	264	75
	PCC	471	126	28	-
	None-Dry	488	226	152	13
	None-Wet	430	183	112	-
Heavy Shot Blasting	Latex	605	473	436	365
	Epoxy	608	281	188	15
	PCC	746	385	282	90
	None-Dry	695	560	522	450
	None-Wet	527	327	270	164
Cold Milling	Latex	679	459	396	279
	Epoxy	654	300	200	12
	PCC	530	239	157	2
	None-Dry	460	146	57	-
	None-Wet	476	258	196	80

the strength must be reduced or the induced stress must be lowered.

The means by which the variability of the strength can be reduced are not known. Research conducted at The University of Texas at Austin (94) investigated modifying the rate of application of the bonding agent and the time from the application of the agent to the placement of the overlay. These factors did not have a significant effect on the average strength or the variability of that strength. Until information can be found on ways of reducing the variability of the strength, other means of decreasing the occurrence of delamination must be found. These other measures rely on reducing the induced stresses.

Environmental controls on the time of construction of bonded overlays provide a means of reducing the chance of debonding. Limits must be placed on the time of placement of the overlay, which will insure that stresses will remain below the expected strengths. The technique for implementation of these controls is described below. In summary, this technique relies on an expected 7-day shear strength for the project, as determined by the direct shear test method described above. An acceptable level of debonding is selected, say one-half of 1 percent, and the maximum allowable interface shear stress is determined. The allowable shear stress is then compared to the stress calculated by the FEM program for the materials in the existing slab and those selected for use in the overlay. By comparing the allowable stress for certain key environmental conditions, those seasons and times of placement that

would cause failure are identified and can be avoided. Details of the method are described below.

The first step is to select a reasonable range of interface strengths. Seven-day interface shear strengths from 100 to 1,000 psi were chosen. Then, using the relationship between the 7-day strength and 24-hour strength shown in Table 3.12, Figure 6.3 was developed. This figure shows the maximum allowable interfacial shear stress for the 24-hour time of analysis. Levels of reliability between 90 and 99.5 percent are shown. It should be noted that levels of reliability greater than 99.5 percent are not possible

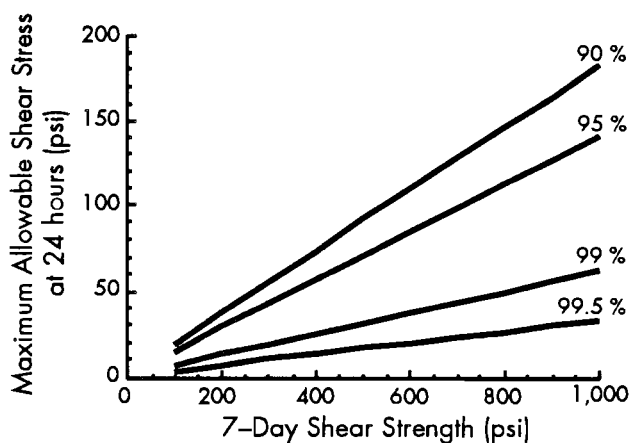


**Figure 6.3 Maximum allowable interface shear stress 24 hours after placement for various levels of reliability**

because of the high variability of the strengths. The allowable shear strength and the associated tensile strength would then be compared to the expected stress resulting from a given environmental condition to determine if an overlay should be placed. This procedure is described below. The equation relating 7-day shear strength and the maximum allowable shear stress is shown below.

$$\tau_{\text{allow.}} = x (S_{7\text{-day}} - \sigma Z_{1-a})$$

where

- $\tau_{\text{allow.}}$  = allowable shear stress,
- $S_{7\text{-day}}$  = seven-day shear strength,
- $\sigma$  = standard deviation of the shear strength,
- $Z_{1-a}$  = Z-score associated with the desired reliability, and
- $x$  = 0.256 for 12-hour analyses,  
0.423 for 24-hour analyses, and  
0.641 for 48-hour analyses.

The steps for determining if an overlay should be placed during a given season and time are as follows:

- (1) Determine the modulus and thermal coefficient of the existing pavement.
- (2) Select the thickness, modulus, and thermal coefficient of the overlay.
- (3) From laboratory testing or experience estimate the 7-day interface shear strength.
- (4) Using Figure 6.3, determine the maximum allowable interface shear stress for the desired level of reliability. The maximum allowable tensile stress is one-half the allowable shear stress.
- (5) Compare the maximum allowable stresses from Step 4 to the maximum expected stress for the combination of existing slab and overlay material properties shown in Table 6.3.
- (6) If the allowable stress is greater than the expected stress for all combinations of environment, debonding will not occur, within the limits of the reliability selected.

An example is given below to further clarify the procedure.

If the existing CRC pavement was constructed from siliceous river gravel concrete, then the modulus and the thermal coefficient can be estimated to be 6,000,000 psi and 0.000006 in./in./°F, respectively. If a 4-inch overlay is planned using the same aggregate type, then the modulus and thermal coefficient of the overlay will equal those of the existing slab. Laboratory test results show the direct shear strength to be 600 psi at seven days for the combination of surface preparation, bonding agent, and overlay concrete to be used. If one-half of 1 percent delamination can be tolerated, then the maximum allowable shear stress at 24 hours after placement is about 20

psi and the corresponding allowable tensile stress is 10 psi. Comparison of these values with the expected stresses, developed in Chapter 5 and summarized in Table 6.3, shows that this overlay should not be placed during winter or summer mornings. However by changing the overlay aggregate to limestone (4,000,000 psi and 0.000004 in./in./°F), this overlay could be placed throughout the year.

When materials used have properties that are not directly addressed in Table 6.3, stresses can be calculated using the regression analyses shown in Tables 5.1 and 5.2. This will allow new materials to be considered when overlays are designed. The inferential space is limited to concrete moduli of between 4 and 6 million psi and thermal coefficients of between 0.000004 and 0.000006 in./in./°F.

### 6.3.2 Bonding Agents

The use of bonding agents with overlays is common for many agencies. The laboratory data for latex-modified cement grout, epoxy bonding agent, and portland cement grout and for overlays placed without grout are shown in Tables 3.10 and 3.11. Given the magnitude of the standard deviations for all combinations, there is no statistical difference in the mean shear strengths. Therefore, based on the laboratory shear strength data, there is no reason to favor one type of bonding agent over another.

There are differences in the tensile strengths shown in Tables 3.10 and 3.11. The tensile strengths as characterized by the direct tension test are statistically different; however, when the pull-out test was used, no statistical difference was found between various bond agents. Thus, there is no reason to favor one bonding agent over the others, based on laboratory test results (101).

Field experience has demonstrated that overlays can be placed successfully with or without bonding agents. The vast majority of the overlays placed in the Houston area have been placed using portland cement grout. The application of grout results in a slight increase in construction cost, but when properly applied, it appears to work well. There is the potential for a problem associated with the application of grout, particularly on hot, dry, or windy days. The grout may dry before the concrete can be placed, effectively creating a layer that prevents, or retards, the development of the interface bond. This problem can be avoided by specifying that the contractor apply grout immediately before placement of the concrete and by maintaining vigilant inspection to assure the requirement is being met. This specification increases the job inspection duties for the owner. The problem could be avoided, and the cost per square yard reduced, if the need for any bonding agent could be eliminated.

**Table 6.3** Calculated stresses for winter and summer mornings for various combinations of BCO materials

Slab Modulus	Overlay Thermal Coeff.	Overlay Modulus	Overlay Thermal Coeff.	Overlay Thickness (in.)	Type of Stress	Winter Morning				Summer Morning							
						2		4		2		4					
						Shear	Tensile	Shear	Tensile	Shear	Tensile	Shear	Tensile				
4	4	4	4	4	4	4	11	6	16	12	8	6	9	7			
						6	19	11	25	19	12	9	15	12			
		6	4	4	4	4	4	14	8	18	14	10	7	10	8		
							6	23	12	28	21	14	11	17	13		
	6	4	4	4	4	4	4	9	6	14	12	8	6	6	6		
							6	17	9	23	19	12	9	13	11		
		6	4	4	4	4	4	4	11	7	17	13	10	7	7	6	
								6	20	11	27	21	14	11	15	12	
	6	4	4	4	4	4	4	11	6	16	13	8	6	9	7		
							6	19	11	26	20	12	9	15	12		
			6	4	4	4	4	4	4	14	8	19	14	10	7	10	8
									6	23	13	30	22	15	11	18	14
6		4	4	4	4	4	4	9	6	15	12	8	6	6	6		
							6	17	10	24	19	12	9	13	11		
		6	4	4	4	4	4	4	11	7	18	13	10	8	8	7	
								6	21	12	29	21	15	11	15	12	

The experimental sections placed without grout in Houston are performing well. With the exception of the latex-modified grout, laboratory data indicate that no statistical difference exists between shear strengths for grout and no-grout specimens. Therefore, it appears that bonded overlays could be placed without grout, at a lower cost, without an increased risk of delamination.

### 6.3.3 Curing

Effective curing of concrete is particularly important to the success of bonded overlays. Early and effective application of the curing compound is important for two reasons. First, the curing measures will reduce the early-age moisture losses that result in increased volume changes, thereby decreasing the early-age interfacial stresses. Second, the use of curing measures will reduce the likelihood of the formation of plastic shrinkage cracks. The formation of these cracks is particularly detrimental to the bonded overlay because a 1-inch-deep shrinkage crack in the overlay may constitute 25 percent of the total thickness. A crack constituting 25 percent of the depth of the concrete is similar to the proportion of the concrete thickness sawn when longitudinal and transverse joints are formed in new construction.

The development of some of the non-reflective cracks in the overlay may result from these plastic shrinkage cracks. Because FEM analysis showed that the stresses in the vicinity of a non-reflective crack are similar in magnitude to those near the free edge, measures must be taken to avoid the development of these cracks at early ages.

One method for avoiding these cracks is to limit the rate of water loss from the fresh concrete. The American Concrete Institute presents a nomograph (shown in Figure 3.16) to be used to estimate the evaporation rate from fresh concrete using the air and concrete temperatures, relative humidity, and wind speed. The allowable upper limit recommended by ACI is 0.2 lb/sq ft/hour. Unless special measures over and above those for the normal double application of curing compound (120 sq ft/gallon) are taken, overlay placement should not be allowed when the evaporation rate is above 0.2 lb/sq ft/hour. These special measures would include wet blankets or fog curing.

### 6.4 SUMMARY

The evaluation of the previous chapter is applied to the design, specification, and construction of

bonded overlays. Based on the early-age analysis and field performance, overlays could be constructed at thicknesses of 2, 4, or 6 inches using steel mesh. Field performance of plain and fiber reinforced experimental sections indicates that these combinations could be used successfully. The modulus and thermal coefficient of the overlay should be less than the modulus and thermal coefficient of the existing slab. No significant difference in interface strength can be found as the result of the use of shot blasting or cold milling surface preparation techniques, and therefore either could be used successfully. A depth of removal and an average texture depth should be specified.

The season and time of placement construction control that relies on the expected 7-day strength for a given combination of surface preparation, bonding agent, and concrete mixture is presented. This technique utilizes the stresses calculated by the FEM program for a specific set of environmental conditions and an acceptable level of delamination to isolate feasible times and seasons of placement. A bonding agent does not appear to be necessary for the success of bonded overlays at early ages. Curing measures are required to reduce the chance of delamination and the ACI evaporation rate limit of 0.2 lb/sq ft/hour is recommended for use during the construction of bonded overlays.

## CHAPTER 7. CONCLUSIONS AND RECOMMENDATIONS

The objective of this study was to insure that bonded concrete overlays remain a viable option for the rehabilitation of continuously reinforced concrete pavements. One means of insuring that bonded overlays remain in the repertoire of pavement designers is to reduce the chance of delamination. The main task of this study was to develop a procedure that would reduce the risk of bonded overlay delamination. To that end, recommendations for the design, specification, and construction of bonded overlays that limit the likelihood of debonding were prepared. Specific conclusions and recommendations resulting from the development of the procedure are discussed below.

### 7.1 CONCLUSIONS

The recommendations for procedures to prevent early-age delamination of bonded overlays were developed based on several conclusions regarding the characteristics of the pavement system at early ages. These conclusions are summarized below.

#### 7.1.1 Case Studies

After a review of several bonded overlay projects placed over the last 30 years, the following conclusions were reached.

- (1) Debonding of overlays is an early-age phenomenon. When a specific effort is made, debonding can be found less than 24 hours after placement.
- (2) All debonding can be found adjacent to either a longitudinal or a transverse crack or the free edge.
- (3) Although not the only cause, some early-age cracking in the overlay can be attributed to excessive loss of moisture and the associated volume change.
- (4) Most researchers agree that long-term traffic loadings do not cause the propagation of delamination.
- (5) Any zone of delamination represents a significant departure from the design assumptions of bonded overlays. Debonding increases the stresses and there is a substantial reduction in the life of the overlay.

The case studies led to a review of available modeling techniques.

#### 7.1.2 Modeling Techniques

Modeling techniques were examined for both the pavement system and the environmental conditions at or near the time of overlay placement. Study of these modeling techniques led to the following conclusions.

- (1) Currently available closed-form solutions are not capable of assessing the overlay-existing-system with sufficient accuracy.
- (2) Two-dimensional plane strain analyses are appropriate for the analysis of thermal stress problems of the type presented herein.
- (3) Two cross sections, one parallel and one perpendicular to the flow of traffic, are adequate for evaluation of the critical free edge and interior cracks.
- (4) The placement of an overlay effectively redefines the curing temperature of existing CRC pavement through the imposition of restraint at the surface. This new curing temperature is equal to the temperature in the base slab at the time the overlay begins to resist stress.
- (5) By assuming adiabatic conditions, the temperature throughout the pavement can be estimated for a given time and diurnal temperature change.

These modeling techniques require the selection of a variety of inputs. The inputs are described below.

#### 7.1.3 Analysis Inputs

The review of literature and laboratory results led to the following conclusions regarding the use of material properties and environmental conditions at early ages.

- (1) Shrinkage does not play an important role in the development of interfacial stresses at early ages. This conclusion is predicated on the assumption that normal curing measures are used soon after placement of the overlay.
- (2) When overlays were placed using epoxy, latex-modified grout, portland cement grout, or no grout as the bonding agent, there was no

statistical difference found in interface shear strength between light and heavy shot blasting and cold milling .

- (3) Interface strength is highly variable, as evidenced by coefficients of variation in excess of 30 percent for all interface test methods used in the laboratory study.
- (4) The rate of interface strength gain is assumed to be equal to the rate of strength gain in concrete.
- (5) The interfacial tensile strength can be assumed to be equal to one-half the shear strength at any given time.
- (6) Higher temperature gradients result when overlays are placed in the morning than result when overlays are placed in the afternoon.

Based on the conclusions reached regarding the inputs, the analysis and evaluation of bonded overlays at early ages proceeded and the following conclusions were reached.

#### **7.1.4 Analysis Results**

- (1) Tensile and shear stresses are concentrated at or near the interface in the vicinity of cracks or a free edge.
- (2) Extremes in seasonal and diurnal temperature variations result in thermal stresses of less than 40 psi in the most severe cases examined.
- (3) The average interface tensile and shear strengths are at least two times the calculated interfacial stresses.
- (4) Cracks in the existing CRC pavement will propagate through the overlay unless cracking initiated at the surface of the overlay relieves the stress. This surface-based cracking could result from plastic shrinkage.
- (5) Interface shear and tensile stresses are higher in the vicinity of reflective and non-reflective cracks than at the free edge.
- (6) Regression analyses can be used to estimate the interface stresses for overlay material combinations within the designated inferential space that were not directly considered in the analysis.

When considered in total, conclusions resulting from the analysis led to the development of the recommendations described below.

## **7.2 RECOMMENDATIONS**

The recommendations presented herein are case specific, in that they result from an examination of the early-age characteristics of bonded overlays. Before proceeding with the design or construction of a bonded overlay, the long-term performance characteristics of this rehabilitation option must be considered.

### **7.2.1 Design, Specification, and Construction of Bonded Overlays**

Based on the early-age analysis conducted in this study, the following recommendations related to the design, specification, and construction of bonded overlays are provided.

- (1) Overlays of 2, 4, or 6 inches can be constructed. There is no more likelihood of delamination in any one thickness than another.
- (2) Overlay reinforcement may consist of steel fiber or steel mesh, and overlays may be placed without reinforcement. However, steel mesh is superior in the retention of debonded areas should that need arise.
- (3) Type I cements may be used, but adherence to specified alkali limits is considered important to successful overlays.
- (4) Overlays may be placed using concretes containing retarders; however, care must be taken to avoid any admixtures that cause unnecessary reduction in the rate of strength gain.
- (5) Overlay concrete aggregates should be selected which will result in the overlay thermal coefficient being less than the existing slab thermal coefficient.
- (6) Adequate surface preparation will result from the use of shot blasting equipment provided a depth of removal of 0.25 inch is specified and the resulting average texture depth is 0.08 inch.
- (7) Adequate interfacial strengths result from the use of any of the bonding agents examined in this study. If bonding agents are used, then care must be taken to insure that the agent does not dry prior to the placement of the overlay.
- (8) Curing measures should insure that plastic shrinkage cracking does not occur. A double application of curing compound at the combined rate of 120 sq ft per gallon is recommended. If the ACI evaporation rate exceeds 0.2 lb/hr/ft<sup>2</sup>, then special curing measures, such as fogging or curing blankets, should be applied.
- (9) The procedure outlined herein should be used to compare the maximum allowable stress to the calculated stress for the extreme environmental conditions. If the comparison indicates delamination is likely, then alternate placement times should be selected.

### **7.2.2 Further Research**

Although the conclusions and recommendations presented above are based on sound analysis and evaluation, certain features of the analysis could be improved through additional research.

- (1) Better test procedures should be developed to characterize the interface shear and tensile strength. These methods should have lower coefficients of variation. Also, additional testing should be conducted to determine if the rate of interface strength gain can be related to the rate of strength gain of the concrete itself.
- (2) The spectral analysis of surface waves technique as applied to the characterization of the early-age modulus in concrete should be incorporated into the analysis as results become available.
- (3) The computer program NSLIP should be modified to allow the influence of steel reinforcement to be incorporated in the analysis.
- (4) Additional field data should be collected to confirm that the variation of temperature with depth in new overlays is as assumed in this analysis.

## REFERENCES

1. National Transportation Statistics-Annual Report, United States Department of Transportation, Report No. DOT-TSC-RSPA-88-2, August 1988.
2. Summary of National Transportation Statistics, United States Department of Transportation, Report No. DOT-TSC-OST 1986.
3. Oglesby, C.H., Hicks, R.G., Highway Engineering, 4th Edition, John Wiley and Sons, New York, 1982.
4. "State Department of Highways and Public Transportation," published by State Department of Highways and Public Transportation, 1988.
5. Carey, W. N., Irick, P.E., "The Pavement Serviceability-Performance Concept," Highway Research Board Bulletin 250, 1960.
6. Highway Research Board, "The AASHO Road Test: Report 5 - Pavement Research," Highway Research Board Special Report 61-E, 1962.
7. Smith, R.E., Palmieri, R.P., Darter, M.I., Lytton, R.L., "Pavement Overlay Design Procedures and Assumptions: Volume I, Analysis of Existing Pavements," United States Department of Transportation, Federal Highway Administration, Report No. FHWA/RD-85/006, August 1986.
8. Majidzadeh, K., Ilves, G.J., "Evaluation of Rigid Pavement Overlay Design Procedure: Development of the OAR Procedure," Office of Research and Development, Federal Highway Administration, Report No. FHWA/RD-83/090, December, 1983.
9. Personal communication with Mr. William V. Ward at Center for Transportation Research, The University of Texas at Austin, Austin, Texas, 1989.
10. Neal, B.F., "California's Thin Bonded PCC Overlay," United States Department of Transportation, Federal Highway Administration, Report No. FHWA/CA/TL-83/04, June 1983.
11. Gillette, R.W., "A 10-Year Report on Performance of Bonded Concrete Resurfacing," Highway Research Board, Highway Research Report No. 94, 1965.
12. Fleming, E.M., "Resurfacing with PCC", Proceedings, Highway Research Board Volume No. 12, 1932, pp 206-230.
13. Felt, E.J., "Resurfacing and Patching Concrete Pavements with Bonded Concrete," Proceedings, Highway Research Board, Volume No. 35, 1956, pp 444-469.
14. Davis, R.E., Davis, H.E., "Bonding New Concrete to Old at Horizontal Construction Joints," Proceedings, American Concrete Institute, Volume 30, May-June 1934, pp 422-436.
15. Koesno, S., Meyer, A.H., Fowler, D.W., "A Study of the Influence of the Temperature of the Substrate on the Construction of Bonded Portland Cement Concrete Overlays," The University of Texas at Austin, Center for Transportation Research, Research Report 1124-1F, November 1988.
16. Koesno, K., McCullough, B.F., "Evaluation of the Performance of the Bonded Concrete Overlay on Interstate Highway 610 North, Houston, Texas," The University of Texas at Austin, Center for Transportation Research, Research Report No. 920-2, December 1987.
17. Solanki, A.I., Fowler, D.W., McCullough, B.F., "A Study of the Effect of Construction Variable on the Bond Behavior of CRCP Overlays," The University of Texas at Austin, Center for Transportation Research, Research Report No. 457-4, October 1987.
18. Neal, B.F., "California's Thin Bonded PCC Overlay," California Department of Transportation, Report No. FHWA/CA/TL-83/04, June 1983.
19. Tayabji, S.D., Ball, C.G., "Field Evaluation of Bonded Concrete Overlays," Construction Technology Laboratories, Project HR-288, Skokie, Illinois, November 1986.

20. Voight, G.F., Carpenter, S.A., Darter, M.I., "Rehabilitation of Concrete Pavements Volume II - Overlay Rehabilitation Techniques," United States Department of Transportation, Federal Highway Administration, Report No. FHWA-RD-88-072, July 1989.
21. Knutson, M.J., "Iowa's Bonded Concrete Overlays," Proceedings, PCC Recycling Seminar, United States Department of Transportation, Federal Highway Administration, Report No. FHWA-TS-82-208.
22. Darter, M.I., Barenberg, E.J., "Bonding Concrete Overlays: Construction and Performance", Miscellaneous Paper GL 80-11, Corps of Engineers, Waterways Experiment Station, 1980.
23. Voight, G.F., Darter, M.I., Carpenter, S.H., "Field Performance of Bonded Concrete Overlays", National Research Council, Transportation Research Board, Transportation Research Record No. 1110, 1987.
24. Bagate, M., McCullough, B.F., Fowler, D.W., Muthu, M., "An Experimental Thin-Bonded Concrete Overlay Placement," The University of Texas at Austin, Center for Transportation Research, Research Report No. 357-2F, November 1985.
25. Tayabji, S.D., Okamoto, P.A., "Thickness Design of Concrete Resurfacing," Third International Conference on Concrete Pavement Design and Rehabilitation, Purdue University, West Lafayette, Indiana, April 1985.
26. Ray, G.K., "Design of Concrete Overlays for Pavements," Title No. 64-40, Journal of the American Concrete Institute, August 1967.
27. "AASHTO Guide for Design of Pavement Structures 1986," American Association of State Highway and Transportation Officials, Washington, D.C. 1986.
28. McComb, R.A., Labra, J.J., "A Review of Structural Evaluation and Overlay Design for Highway Pavements," Proceedings, Pavement Rehabilitation Workshop, Transportation Research Board, FHWA-RD-74-60, Washington, D.C., June 1974.
29. Mellinger, F.M., "Structural Design of Concrete Overlays," Journal of the American Concrete Institute, February 1963.
30. Seeds, S., McCullough, B.F., Hudson, W.R., de Velasco, M.G., "Implementation of New Overlay Design Procedure in Texas," Transportation Research Board, Transportation Research Record No. 756, 1980.
31. Sherman, G.B., Hannon, J.B., "Overlay Design Using Deflections," State of California, Division of Highways, Materials and Research Department, Research Report No. M & R 633128, August 1970.
32. Packard, R.G., Tayabji, S.D., "New PCA Thickness Design Procedure for Concrete Highway and Street Pavements," Third International Conference on Concrete Pavement Design and Rehabilitation, Purdue University, West Lafayette, Indiana, April 1985.
33. Barenberg, E.J., "Rehabilitation of Concrete Pavements by Using Portland Cement Concrete Overlays," Transportation Research Board, Transportation Research Record No. 814, 1981.
34. Ray, G.K., "Design of Concrete Overlays for Pavements," Journal of the American Concrete Institute, August 1967.
35. van Dam, T., Blackmon, E., Shahin, M.Y., "Effect of Concrete Overlay Debonding on Pavement Performance," Transportation Research Board, Transportation Research Record No. 1136, 1987.
36. Lall B., Lees, G., "Analysis of Stresses in Unbonded Concrete Overlay," Transportation Research Board, Transportation Research Record No. 930, 1983.
37. Korovisis, G.T., Ioannides, A.M., Discussion of "Effect of Concrete Overlay Debonding on Pavement Performance," Transportation Research Board, Transportation Research Record No. 1136, 1987.
38. Huang, Y.H., Wang, S.T., "Finite-Element Analysis of Rigid Pavements with Partial Subgrade Contact," Transportation Research Board, Transportation Research Record No. 485, 1974.
39. Chou, Y.T., "Structural Analysis Computer Programs for Rigid Multicomponent Pavement Structures with Discontinuities—WESLIQID and WESLAYER," Reports 1-3, Technical Report GL-81-6, U.S. Army Engineer Waterways Experiment Station, Vicksburg, Mississippi, May 1981.
40. Vesic, A.S., Saxena, S.K., "Analysis of Structural Behavior of Road Test Rigid Pavements," Highway Research Record No. 291, pp 156-158, 1969, Highway Research Board, National Academy of Sciences—National Research Council, Washington, D.C.

41. Taute, A., McCullough, B.F., Hudson, W.R., "Improvements to the Materials Characterization and Fatigue Life Prediction Methods of the Texas Rigid Pavement Overlay Design Procedure," The University of Texas at Austin, Center for Transportation Research, Research Report No. 249-1, November 1981.
42. Treybig, H.J., McCullough, B.F., Smith, P., Von Quintus, H., "Overlay Design and Reflection Cracking Analysis for Rigid Pavements, Volume 1 - Development of New Design Criteria," Research Report No. FHWA-RD-77-66, Federal Highway Administration, Washington, D.C., August 1977.
43. Treybig, H.J., McCullough, B.F., Smith, P., Von Quintus, H., "Overlay Design and Reflection Cracking Analysis for Rigid Pavements, Volume 2 - Design Procedures," Research Report No. FHWA-RD-77-67, Federal Highway Administration, Washington, D.C., August 1977.
44. Hicks, R.G., "Use of Layered Theory in the Design and Evaluation of Pavement Systems," State of Alaska, Department of Transportation and Public Facilities, Report No. FHWA-AK-RD-83-8, July 1982.
46. van Metzinger, W.A., "An Empirical-Mechanistic Design Method Using Bonded Concrete Overlays for the Rehabilitation of Pavements," Ph.D. Dissertation, The University of Texas at Austin, August 1990.
45. "Design Analysis for Rehabilitation of the CRCP on Southeast Quadrant of Houston Loop 610," The University of Texas at Austin, Center for Transportation Research, Research Report No. 920-1, October 1986.
47. McCullough, B.F., Lundy, J.R., "The Performance of Bonded Concrete Overlays in Texas," Proceedings, Eighth Quinquennial Convention SAICE/ATC, Republic of South Africa, July 1988.
48. Lundy, J.R., McCullough, B.F., "Delamination in Bonded Concrete Overlays of Continuously Reinforced Concrete Pavements," Proceedings, Fourth International Conference on Concrete Pavement Design and Rehabilitation, Purdue University, April 1989.
49. Teo, A., Fowler, D.W., McCullough, B.F., "Monitoring and Testing of Bonded Concrete Overlay on Interstate Highway 610 North in Houston, Texas," The University of Texas at Austin, Center for Transportation Research, Research Report No. 920-3, November 1990.
50. "Hot Weather Concreting," American Concrete Institute Committee 305, American Concrete Institute, ACI 305R-89, April 1989.
51. Hess, M.S., "The End Problem for a Laminated Elastic Strip-II. Differential Expansion Stresses," Journal of Composite Materials, Volume 3, October 1969, pp 630-641.
52. Branson, D.E., Deformation of Concrete Structures, McGraw Hill Company, New York, New York, 1977, pp 85-110.
53. Roll, F., "Effects of Differential Shrinkage and Creep in Composite-Concrete Structures," Designing for Effects of Creep, Shrinkage and Temperature in Concrete Structures, ACI Special Publications SP-27, American Concrete Institute, Detroit, MI, 1971, pp. 187-214.
54. Timoshenko, S., "Analysis of Bi-metal Thermostats," Journal of the Optical Society of America, Volume 11, 1925, pp 233 -255.
55. Grimado, P.B., "Interlaminar Thermoelastic Stresses in Layered Beams," Journal of Thermal Stresses, Vol. 1, No. 1, 1978, pp. 75-86.
56. Chen, D., Cheng, S., Gerhardt, T.D., "Thermal Stresses in Laminated Beams," Journal of Thermal Stresses, Volume 5, 1982.
57. Delale, F., Erdogan, F., Aydinoglu, M.N., "Stresses in Adhesively Bonded Joints: A Closed-Form Solution," Journal of Composite Materials, Volume 15, May 1981.
58. Hart-Smith, L.J., "Further Developments in the Design and Analysis of Adhesive-Bonded Structural Joints," Joining of Composite Materials, ASTM STP 749, K.T. Kedward, Ed., American Society of Testing and Materials, 1981.
59. Yuceoglu, U., Dean, U., "Bending and Shear Deformation Effects in Lap Joints," Journal of Engineering Mechanics, Proceedings, ASCE, Volume 106, No. EM1, February 1980.
60. Birkland, H.W., "Differential Shrinkage in Composite Beams," ACI Journal Proceedings, Vol. 56, No. 11, May 1960, pp. 1123-1136.
61. Wang, S.S., Choi, I., "Boundary-Layer Effects in Composite Laminates: Part I - Free- Edge Stress Singularities," ASME Journal of Applied Mechanics, Volume 49 1982.
62. Kim, R.Y., Soni, S.R., "Experimental and Analytical Studies on the Onset of Delamination in Laminated Composites," Journal of Composite Materials, Volume 18, January 1984.

63. Reddy, A.D., Rehfield, L.W., Haag, R.S., "Influence of Prescribed Delaminations on Stiffness-Controlled Behavior of Composite Laminates," Effects of Defects in Composite Materials, ASTM STP 836, American Society of Testing and Materials, 1984.
64. Rusch, H., Jungwirth, D., Hilsdorf, H., "Creep and Shrinkage – Their Effect on the Behavior of Concrete Structures," Springer – Verlag, New York, New York, 1983.
65. Westergaard, H.M., "Analysis of Stresses in Concrete Pavements due to Variations of Temperature", Highway Research Board, Volume 6, 1926, PP 201-215.
66. Al-Negheimish, A.I., "Bond Strength, Long-Term Performance and Temperature Induced Stresses in Polymer Concrete-Portland Cement Concrete Composite Members," Ph.D. Dissertation, The University of Texas at Austin, December 1988.
67. Majidzadeh, K., Suckarieh, G.G., "Analytical Modeling and Field Verification of Thermal Stresses in Overlay," Transportation Research Board, Transportation Research Record No. 632, 1977.
68. Cook, R.D., Concepts and Applications of Finite Element Analysis, Second Edition, John Wiley and Sons, Inc., 1981.
69. Zienkiewicz, O.C., The Finite Element Method, Third Edition, McGraw-Hill Book Company, Inc. 1977.
70. Desai, C.S., Abel, J.F., Introduction to the Finite-element Method. A Numerical Method for Engineering Analysis, Van Nostrand Reinhold Company, New York, New York, 1972.
71. Vallabhan, C.V.G., Asik, M., Rahman, K., "A Finite Element Program for Analysis of Bonded Concrete Overlays," Texas Tech University, Center for Applied Research and Engineering, Research Report 1205-3, July 1990.
72. Neville, A.M., Properties of Concrete, Third Edition, Longham Scientific and Technical, Essex, England, 1981.
73. Troxell, G.E., Davis, H.E., Kelly, J.W., Composition and Properties of Concrete, Second Edition, McGraw-Hill Book Company, New York, New York, 1968.
74. Noble, P.M., "The Effect of Aggregate and Other Variables on the Elastic Properties of Concrete," Proceedings, ASTM, Volume 31, Part 1, 1931, pp. 399-426.
75. Aslam, M.F., Saraf, C., Carrasquillo, R.L., McCullough, B.F., "Design Recommendations for Steel Reinforcement of CRCP," The University of Texas at Austin, Center for Transportation Research, Research Report 422-2, November 1987.
76. Mindess, S., Young, J.F., Concrete, Prentice-Hall, Inc., New Jersey, 1981.
77. Rix, G.J., Bay, J.A., Stokoe, K.H., "Assessing In-Situ Stiffness of Curing Portland Cement Concrete with Seismic Tests," Preprint of Paper presented at 69th Annual Transportation Research Board Meeting, Washington, D.C., January 1990.
78. Troxell, G.E. Raphael, J.M., Davis, R.E. "Long-term Creep and Shrinkage Test of Plain and Reinforced Concrete," Proceedings ASTM, Volume 58, pp. 1101-1120, 1958.
79. Powers, T.C., Brownyard, T.L., "Studies of the Physical Properties of Hardened Portland Cement Paste," Journal of the American Concrete Institute, Volume 43, April 1947.
80. Meyers, S.L., "How Temperature and Moisture Changes May Effect the Durability of Concrete," Rock Products, Chicago, August, 1951, pp. 153-157.
81. 1985 Test Methods, American Society for Testing and Materials.
82. van Metzinger, W.A., Lundy, J.R., Suh, Y.C., McCullough, B.F., "The Influence of Curing Temperature on the Design and Performance of Concrete Pavement," Advance copy of paper prepared for ATC Conference, August, 1990.
83. Ingram, L.L., Furr, H.L., "Creep and Shrinkage of Concrete Based on Major Variables Encountered in the State of Texas," Texas Transportation Institute, Texas A&M University, Research Report 170 - 1F, August 1973.
84. Concrete Manual, 7th Edition, U.S. Bureau of Reclamation, Denver, Colorado, 1963.
85. Haller, P., "Shrinkage and Creep of Mortar and Concrete," Zurich EMPA, 1940, Diskussionbericht, No. 124.
86. Engineering Bulletin, 11th Edition, Portland Cement Association, Skokie, Illinois, 1968.
87. Olulkun, F.A., Burdette, E.G., Deatherage, J.H., "Rates of Development of Physical Properties of Concrete at Early Ages," Preprint of Presentation, Transportation Research Board Meeting, January, 1990.

88. Soroka, I., Portland Cement Paste and Concrete, London, McMillan, 1979.
89. Powers, T.C., "Causes and Control of Volume Change," Journal of Portland Cement Association Research and Development Laboratories, Volume 1, No. 1, pp. 29-39, January 1959.
90. L'Hermite, R.G., "Volume Change of Concrete," Proceedings 4th International Symposium on the Chemistry of Cement, Washington, D.C., 1960, pp. 659-694.
91. Carlson, R.W., "Drying Shrinkage of Concrete as Affected by Many Factors," Proceedings ASTM, Volume 38, Part II, 1938, pp. 419-437.
92. Jones, T.R., Hirsh, T.J., "The Physical Properties of Concrete at Early Ages," Texas Transportation Institute, Texas A&M University, Research Paper 19, August 1961.
93. "Test Method ACI 503 Pullout-Tests," Committee Recommendation, American Concrete Institute Committee 503R, 1985.
94. Whitney, D., Fowler, D.W., Isis, P., "An Investigation of Various Factors Affecting Bonding in Bonded Concrete Overlays," The University of Texas at Austin, Center for Transportation Research, Draft Copy of Research Report No. 920-4, August 1990.
95. Fintel, M., Khan, F.R., "Effects of Column Exposure in Tall Structures," Portland Cement Association, Engineering Bulletin 018.01D, 1968.
96. Hourly Climatological Data Summary, Houston Intercontinental Airport, Texas Water Commission, 1981-1987, May 1988.
97. Unpublished field data collected at The University of Texas at Austin pavement test facility, 1990.
98. The Weather Source, 4th Edition, Edited by J.A. Ruffner, F.E. Bair, Gale Research Company, Detroit, Michigan, 1984.
99. Kasai, Y, Yokoyama, K., Matsui, I., "Tensile Properties of Early Age Concrete," Mechanical Behavior of Materials, Proceedings, International Conference on Mechanical Behavior, Volume IV, The Society of Material Science, Japan, 1971.
100. "Thin Bonded Concrete Overlay at Lingco Drive," Public Service Department, City of Richardson, Texas, February 1988.
101. AASHTO Guide for Design of Pavement Structures 1986, American Association of State Highway and Transportation Officials, 1986.
102. Price, W.H., "Factors Influencing Concrete Strength," Journal of the American Concrete Institute, Volume 47, February 1951, pp. 417-432.
103. Won, M., "Mechanistic Analysis of CRCP Considering Material Characteristics, Variability, and Fatigue," PhD Dissertation, The University of Texas at Austin, May 1989.
104. Jaing, J.H., Shah, S.P., Andone, A.T., "Study of the Transfer of Tensile Force by Bond," Proceedings, ACI Journal, July-August 1988.
105. Kandiah, K., "Bond Pull Out Test," The University of Texas at Austin, Center for Transportation Research, Technical Memorandum 357-18, December 1983.
106. Patty, T.S., Letter report to the Center for Transportation Research on the results of a petrographic analysis of cores taken from I.H. 610 North Loop, Houston, Texas, May 18, 1987.
107. Pechlivandis, C., Papaleontion, C., Meyer, A.H., Fowler, D.W., "The Effectiveness of Membrane Curing Compounds for Portland Cement Concrete Pavements," Center for Transportation Research, The University of Texas at Austin, Research Report 1118-1F, November 1988.

